Quantum dynamics of multiparticle states: saturons and condensates

Giacomo Contri

München 2025

Quantum dynamics of multiparticle states: saturons and condensates

Giacomo Contri

Dissertation
der Fakultät für Physik
der Ludwig-Maximilians-Universität
München

vorgelegt von
Giacomo Contri
aus Milan

München, den 30.09.2025

Erstgutachter: Prof. Dr. Gia Dvali
Zweitgutachter: Prof. Dr. Dieter Lüst
Tag der mündlichen Prüfung: 12.11.2025

Contents

List of Figures

Zusammenfassung

Die Analyse der Quantendynamik von Mehrteilchenzuständen in Quantenfeldtheorien ist, über ihre allgemeine Relevanz hinaus, grundlegend für bestimmte Systemklassen wie schwarze Löcher und andere saturierte Zustände.

Die Erforschung der Physik schwarzer Löcher hat jüngst zur Identifizierung einer neuen Klasse von Zuständen in nicht-gravitativen Quantenfeldtheorien geführt, der sogenannten Saturonen. Diese sind durch die Sättigung der Grenze für eine maximale quantenfeldtheoretische Mikrozustandsentropie gekennzeichnet. Zahlreiche Beispiele zeigen, dass Saturonen Eigenschaften besitzen, die schwarzen Löchern vollständig analog sind.

Im ersten Teil dieser Arbeit untersuchen wir ein $1+1$-dimensionales Beispiel eines Saturons in einer renormierbaren Quantenfeldtheorie mit großer $SU(N)$-Symmetriegruppe. In diesem Rahmen erscheint das Saturon als Vakuumblase einer spontan gebrochenen $SU(N)$-Symmetrie im Symmetriegrundzustand.

Die Blase ist klassisch stabil, zerfällt jedoch quantenmechanisch bei Kopplung an masselose Fermionen. Dank der Einfachheit des modells analysieren wir den Evaporationsprozess detailliert und reproduzieren eine Hawking-artige Zerfallsrate, die umgekehrt proportional zur Blasengröße ist. Das Evaporationsspektrum bestimmen wir semiklassisch über die Analyse der Bogoliubov-Koeffizienten des fermionischen Feldes sowie quantenmechanisch, indem wir die Blase als hochbesetzten Zustand von Goldstone-Bosonen der gebrochenen Symmetrie behandeln. Damit folgt der Prozess aus der quantenmechanischen Zerfallsrate der konstituierenden Goldstones und reproduziert im geeigneten Grenzfall das semiklassische Resultat.

Im zweiten Teil analysieren wir die Quantendynamik eines homogenen Superfluids in einer relativistischen $U(1)$-Theorie. Klassische Zustände erscheinen quantenmechanisch als eingekleidete kohärente Zustände mit großer mittlerer Besetzungszahl. Üblicherweise treiben Quanteneffekte Mehrteilchensysteme durch Rückstreuungen von der Klassizität weg. Hier zeigen wir, dass geladene Superfluide – im Gegensatz zu ihren ladungslosen Gegenstücken – ihre interne Kohärenz in der Quantentheorie dauerhaft bewahren. Die Stabilität belegen wir, indem wir den passenden Zustand als Vakuum des modifizierten Hamiltonoperators $\hat{H} - \mu\hat{Q}$ konstruieren und seine Dynamik untersuchen; μ wirkt als quantenmechanisches chemisches Potential, $\hat{Q}$ als $U(1)$-Ladung. Wir erklären die Rolle der nicht-gaußschen Einkleidung, um Stabilität jenseits des Baum-Niveaus zu gewährleisten. Schließlich bestimmen wir das Fluktuationsspektrum von dem Superfluid und prüfen explizit die Existenz einer masselosen Goldstone-Mode bis zur ersten Loop-Ordnung.

Abstract

The analysis of the quantum dynamics of multiparticle states in quantum field theories, beyond its general relevance, is of fundamental importance for some particular systems, such as black holes and other saturated states.

The study of black hole physics has recently led to the identification of a new class of states in non-gravitational quantum field theories, the so-called saturons. Such states are characterized by the saturation of the bound for a maximal quantum field theoretic microstate entropy. It was shown in many examples that saturons exhibit properties completely analogous to black holes.

In the first part of this work, we study in depth a $1+1$ dimensional example of a saturon in a renormalizable quantum field theory with a large $SU(N)$ symmetry group. In this context, the saturon appears as a vacuum bubble of spontaneously broken $SU(N)$ symmetry within the symmetric vacuum.

The bubble is classically stable, but decays quantum mechanically if coupled to massless fermions. Thanks to the simplicity of the model, we are able to analyze the evaporation process in great detail and to reproduce a Hawking-like decay rate inversely proportional to the bubble size. We compute the evaporation spectrum semiclassically, by performing an analysis of the Bogoliubov coefficients of the fermionic field, as well as quantum mechanically. The latter approach is carried out by studying the bubble at the quantum level as a highly occupied state of Goldstone bosons of the broken symmetry. Then, the evaporation process can be understood in terms of the quantum decay rate of the constituent Goldstones and reproduces the semiclassical result in the appropriate limit.

In the second part of the thesis, we proceed to analyze in detail the quantum dynamics of a homogeneous superfluid state in a relativistic $U(1)$ theory. Classical states are resolved quantum mechanically as dressed coherent states with a large average occupation number. Generically, one expects that quantum effects drive multiparticle systems away from classicality due to rescattering of the quantum constituents. Here, we show that, contrary to their zero-charge counterparts, charged superfluids retain their internal coherence indefinitely in the quantum theory. Stability is shown by explicitly constructing the appropriate state as the vacuum of the modified Hamiltonian $\hat{H}-\mu\hat{Q}$, with μ the full-fledged quantum chemical potential and $\hat{Q}$ the $U(1)$ charge, and by studying its dynamics. We clarify the role of the non-Gaussian dressing of the state in order to guarantee its stability beyond tree level. Finally, we study the spectrum of the fluctuations on top of the superfluid, and we explicitly check the existence of a gapless Goldstone mode at one-loop order.

Publications

This thesis is based on the work conducted at the Max Planck Institut für Physik and at the Ludwig Maximilians Universität (LMU) of Munich. The thesis is based on the following publications:

- G. Contri, G. Dvali and O. Sakhelashvili, *Similarities in the evaporation of saturated solitons and black holes*, 2509.08049
- L. Berezhiani, G. Cintia and G. Contri, *Coherence and Quantum Stability of Relativistic Superfluid States*, 2509.21667

All the papers share first authorship, and the authors are listed in alphabetical order as customary in high-energy physics. A substantial part of the thesis, in particular chapters 3 and 4, is, to a large extent, an *ad verbatim* reproduction of the text, figures, and equations of the articles above, although rephrased to give context and a better understanding.

Finally, let us also mention other works in preparation, whose content have been produced during the doctoral period:

- P. Bakauov, G. Contri, G. Dvali, *in preparation*
- M. Bachmaier, G. Contri, G. Dvali, J. S. Valbuena-Bermudez, *in preparation*.

Introduction

The interplay between the quantum dynamics of field theories and their classical counterparts is a topic of great interest in its own right. Indeed, a consistent description of the world requires classicality to emerge autonomously from the more fundamental quantum field theoretic description of nature, in the appropriate regime. Generally, in quantum field theory, a classical regime is understood as a weak coupling limit for states with a large number of constituents [4–6]. For such a class of states, quantum effects are highly suppressed, while the classical nonlinear dynamics controlled by a finite collective coupling emerges as a good approximation to the behavior of the system. However, the role of quantum corrections is far from trivial, and becomes of paramount importance for certain systems.

The most striking example is probably offered by black hole physics. Classical black holes are objects of great interest in their own right. Discovered shortly after the formulation of General Relativity, they were established as a robust prediction of the theory by Penrose's singularity theorems [7]. Indeed, a black hole is formed whenever a given energy E is localized within a physical size equal to its gravitational radius EG, where G is Newton's constant. Classical black holes are characterized by a simple set of properties. Powerful no-hair theorems restrict their characterization to a handful of parameters, namely their mass, angular momentum, and gauge charges. It seems that, classically, a black hole captures a gigantic load of information, which then hides beyond a horizon whose size can never shrink [8].

Although classical black holes are remarkable objects, they become even more central in quantum gravity. In a quantum setting, black holes are not only fascinating entities, but they also play a fundamental role in the UV-completion of the theory itself. If we try to probe shorter and shorter distances, let us say by scattering two particles, the uncertainty principle tells us that we necessarily pay an energy price, which gets higher the smaller the size we are probing. On the other hand, General Relativity tells us that energy gravitates. Once we put the two together, a fundamental minimal scale, the Planck length $L_{\rm pl} = \sqrt{\hbar G}$, emerges. Whenever we try to probe smaller distances, the required energy price is so large, that we necessarily create a black hole, whose size grows larger and larger the smaller the distance we were originally trying to probe. This sets the Planck length as the minimal scale of a quantum gravitational theory. Therefore, gravitational UV physics is controlled by black hole physics [9, 10]. At this stage of the discussion, it remains to be understood the microscopic process that can lead to the formation of a large macroscopic object from

even a few energetic constituents.

At the same time, the quantum dynamics of black holes turns out to be much richer than its classical counterpart. Quantum mechanically, black holes are endowed with a huge entropy, which scales as their area in units of Planck length squared [11]. Moreover, they are not as black as they are in the classical limit. Semiclassically, Hawking discovered that black hole radiates thermally, with a temperature inversely proportional to their radius [12]. This raised many puzzles on how the information stored inside a black hole could be recovered, the so-called information paradox.

The understanding of all these very surprising aspects of quantum black holes requires a careful investigation of their quantum dynamics. Indeed, although black holes seem large macroscopic objects for which quantum corrections are naively negligible, one can argue that these apparent mysteries can be attacked only by considering them as fully quantum states within the gravitational, quantum effective field theory. In [13, 14], Gia Dvali and Cesar Gomez offered a fully quantum description of a black hole, the N-portrait, as an N-gravitons bound state held together by collective interactions at a critical point of a quantum phase transition. In such a model, one can reproduce all the key properties of quantum black holes. Classicality emerges in the limit of an infinite number N of constituents, while the quantum dynamics generates $1/N$ corrections that are paramount for the understanding of the quantum properties listed above [15]. For example, these are the corrections that allow for a consistent retrieval of the black hole information.

Shortly after, it was understood that the key properties of quantum black holes are shared by a larger class of states in non-gravitational theories, the so-called saturons [16–21]. Saturated states are multi-particle states that emerge when some theories are pushed towards their unitarity limit. Saturons can be defined as states that carry the maximal possible microstate entropy, which is bounded by the relevant inverse quantum coupling constant, evaluated at the scale of the state. It turns out that they exhibit properties completely analogous to those of black holes. Their entropy follows an area law, where the area is measured in units of the Goldstone decay constant of the broken Poincaré symmetry. Semiclassically, they exhibit an information horizon and radiate at a rate inverse to their size. Quantum mechanically, information can be retrieved in a macroscopically long time thanks to $1/S$ corrections. Most importantly, saturons clarify the role of the area law entropy. Their large degeneracy perfectly balances the generic exponential suppression for the creation of multi-particle states from a few energetic particles, leading to their unsuppressed production in scattering processes at the correct kinematic window. This, in turn, clarifies the role of black hole entropy in unitarizing the gravitational scattering amplitudes [17].

Given the discussion above, it is clear that for a generic saturon, as for black holes, even if they are multiparticle states in a seemingly classical regime, the quantum aspects of their dynamics are of fundamental importance.

In the first original part of this work, following [2], we study a specific instance of a saturon in a renormalizable $1+1$ dinemsional theory. In this controlled setting, we are able to precisely demonstrate all the relevant properties of saturation, such as the area law for the microstate entropy. In particular, we reproduce the typical saturon radiation rate

both with semiclassical and quantum mechanical methods, and we estimate the relevant quantum corrections, thereby confirming in our setting the universality of the physics of saturated states. Moreover, this allows us to clarify how the semiclassical dynamics emerges from quantum mechanical processes, which in turn supports the black hole quantum N-portrait.

The relevance of quantum corrections to classical dynamics, first considered for gravitational systems as black holes and de Sitter [22, 23], was also underlined in many other physical systems in a classical regime. It was argued on general grounds that quantum dynamics deviates from its classical trajectory at a quantum timescale named quantum break-time [23, 24]. This phenomenon can be understood as originating from the internal rescattering of the quantum constituents of a multi-particle "classical" state, which causes a loss of coherence. For black holes, it was argued that the cumulative effect of such quantum corrections leads to a complete departure from classicality at Page's time, and the onset of the so-called memory burden effect [25–27].

A rigorous understanding of these important phenomena also led to the analysis of such quantum effects in prototypical systems, initiated in [28,29]. There, Berezhiani, Cintia, and Zantedeschi resolved a homogeneous real condensate in a relativistic theory of a real scalar field with quartic interactions as a quantum coherent state of zero momentum particles. The authors applied the systematic approach of the background field method [30] to confirm the emergence of a quantum deviation from the classical evolution due to the rescattering of the constituent particles. There and in subsequent works, they also clarified the importance of appropriate non-Gaussian dressing in defining a state with physical properties, such as finiteness of the energy [31].

In the second part of this work, we extend the analysis to a complex $U(1)$ superfluid [3]. We show how the special symmetry properties of a homogeneous superfluid allow for the definition of a state that is fully stable quantum mechanically. We clarify the role of non-Gaussianities in preserving coherence, and we discuss the spectrum of fluctuations at one loop in a consistent approach.

To conclude, we give a quick outline of the thesis.

- In the first chapter, we utilize the kink, the Gross-Neveu model [32] at large-N, and Q-balls [33, 34] to review some fundamental concepts of nonperturbative quantum field theory and of large-N physics, which shall set the basis for the following discussions.

- In chapter two, we introduce the phenomenon of saturation. First, we give an extensive review of black hole physics, both classically and quantum mechanically. Then, we discuss the quantum N-portrait, as a quantum mechanical description of black holes [13]. We proceed to introduce the concept of saturation, highlighting the role of black holes as prototypical examples of saturated states. Finally, we discuss two examples of saturons in non-gravitational quantum field theories, as bound states in the aforementioned Gross-Neveu model and baryons in large-N QCD [16, 19].

- The third and fourth chapters are the core of the thesis. In the third chapter,

following [2], we discuss in great depth a model of a saturon as a vacuum bubble in a $1+1$ dimensional theory with a large global $SU(N)$ symmetry group. We derive all the characterizing features of saturation. Then, we focus on its radiation properties, and in the semiclassical large-N limit we reproduce a Hawking-like decay rate, in full analogy with black holes. We conclude by discussing the quantum timescale of information retrieval to complete the picture of the bubble as a saturated state.

- In the fourth and last chapter, we move to the rigorous study of the quantum dynamics of a homogeneous superfluid in a $U(1)$ theory with quartic interactions [3]. After a short review of the background field method as a systematic expansion for the dynamics of multiparticle states, we apply it to the theory under consideration. We give a fully quantum definition of the superfluid state; then we proceed to prove its stability and the finiteness of all its parameters under quantum corrections. We move on to discuss alternative choices, and we clarify the importance of our specific choice to ensure stability. Finally, we analyze the one-loop spectrum of fluctuations, confirming the existence of a gapless Goldstone mode.

Chapter 1

Non-perturbative configurations in quantum field theories

In this chapter, we introduce many of the basic ingredients that we are going to need in the rest of the thesis. Namely, we are going to discuss some instances of non-perturbative classical configurations in various relativistic field theories, and their quantization. On one hand, states of this kind are prototypical examples of bound-states kept together by self-interactions in a regime where strong classical nonlinearities are important. On the other hand, such configurations exist at weak quantum coupling, and hence are amenable to a perturbative quantum description in terms of a large number of weakly coupled quantum constituents.

First, we will focus on the theories that admit topological solitons, namely solitonic configurations whose stability can be understood in terms of the conservation of a topological charge. In particular, we will explore two $1+1$ dimensional examples, the $\lambda\phi^4$ theory and the Gross-Neveu model at large N [32]. These offer a perfect opportunity to introduce all the necessary concepts to understand the key features of topological configurations, and the connection between the classical profiles and the quantum states to which they are connected in the corresponding quantum field theory.

Subsequently, we will discuss Q-balls [33], the prototypical example of non-topological solitons. Albeit similar to the previous examples for the role that classical nonlinearities play in ensuring their stability, Q-ball-like solutions are protected not thanks to topology but thanks to a Noether charge with which they are endowed. Their description will be important to offer an easier understanding of the example of a saturon which is the main focus of chapter 3.

1.1 The 1+1 dimensional kink

To introduce the concept of topological solitons, in this chapter, we will study at length a very specific 1+1 dimensional theory of a single scalar field ϕ. The Lagrangian reads:

$$\mathcal{L} = \frac{1}{2}\partial_\mu\phi\partial^\mu\phi - \frac{\lambda}{4}(\phi^2 - v^2)^2 \,. \tag{1.1}$$

Since the mass squared parameter $m^2 = \lambda v^2$ is negative, the theory admits two degenerate vacua, $\phi = \pm v$. The $\mathbb{Z}_2$ symmetry is then spontaneously broken. Perturbatively, the theory consists of fluctuations around one of the two vacua. However, the classical equations of motion admit static solutions $\phi_k(x)$ that asymptotically interpolate between different vacua, namely $\phi_k(\pm\infty) = \pm v$. These solutions represent stable, non-perturbative objects which strongly enrich the spectrum of the theory, both classically and, as we will see, quantum mechanically.

To find such solutions, one can consider the equations of motion:

$$\Box\phi - V'(\phi) = 0 \,, \tag{1.2}$$

and restrict oneself to the static configurations with $\dot{\phi} = 0$. The minimization of the action, for static configurations, reduces to the minimization of the static energy:

$$E = \int dx \left[\frac{1}{2}(\partial_x\phi)^2 + V(\phi)\right] \,, \tag{1.3}$$

which leads to the equation

$$\partial_x^2\phi - V'(\phi) = 0 \,. \tag{1.4}$$

An equation of this kind can be interpreted as a one-dimensional mechanical system, where the x coordinate plays the role of the "time". Then, the energy plays the role of an integral of motion, and the solution can be obtained explicitly. "Energy" conservation gives,

$$\phi'(x) = \sqrt{2V(x)} \,, \tag{1.5}$$

which leads to

$$x - x_0 = \int_{\phi(x_0)}^{\phi(x)} \frac{d\phi}{\sqrt{-2V(\phi)}} \,. \tag{1.6}$$

After integration, we obtain the so-called *kink* (or respectively *anti-kink*) solution:

$$\phi_k(x) = \pm v \tanh\left(\frac{m}{\sqrt{2}}(x - x_0)\right) . \tag{1.7}$$

Here, x_0 is an arbitrary parameter, which represents the position of the object. To obtain a finite energy state, we needed to impose the boundary conditions $\phi(\pm\infty) = \pm v$. The mass is readily obtained by integration:

$$M_k = \int dx\, (\partial_x\phi_k)^2 = \int dx\, 2V(\phi) = \frac{2\sqrt{2}}{3}\frac{m^3}{\lambda} \,, \tag{1.8}$$

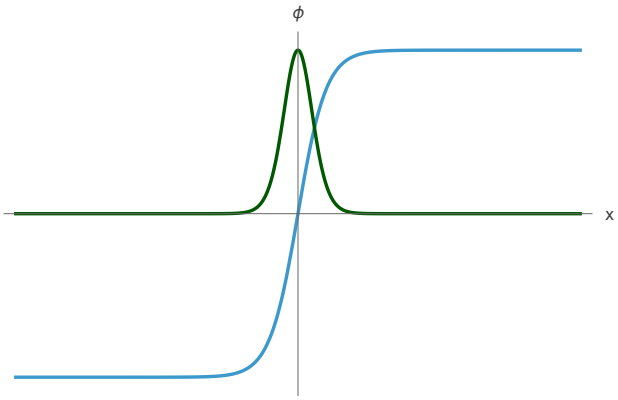

Figure 1.1: The classical kink (blue) and its energy density (green).

where we made use of the equations of motion.

The non-perturbative nature of the kink can be seen from the behaviour of its mass. Indeed, we can observe that its mass is inversely proportional to the dimensionless coupling of the theory, $M_k \sim m^2/\lambda$. This shall have an important meaning when we analyze the quantum theory. In particular, this means that if the theory is weakly coupled, the kink becomes a highly massive, rigid object, whose mass scale is much higher than the mass of the fundamental particle of the theory. On the other hand, the kink can become light if the theory approaches strong coupling. We will comment on this further in the next sections. To sum up, we found a fully non-perturbative static inhomogeneous field configuration. Now, we turn on investigating its properties, beginning with its stability properties.

1.1.1 Stability of the kink and topological charge

In this section, we prove the stability of the kink solution under perturbations, and we comment on the underlying fundamental reasons beyond it. First, let us observe that, in order to have finite energy, we needed our solution to go asymptotically to a point in the vacuum manifold $\mathbb{Z}_2$. Once this is established, let us consider its stability properties. In the specific case of a kink, we can prove its stability explicitly thanks to its saturation of the so-called Bogomolny bound on the energy [35]. Let us consider the energy of an arbitrary, static configuration:

$$E = \int dx \left[\frac{1}{2}(\phi')^2 + V(\phi)\right] . \tag{1.9}$$

By adding and subtracting $\phi'\sqrt{2V}$, we can rewrite the energy as a perfect square, plus a residual term:

$$E = \int dx \left\{\frac{1}{2}\left(\phi' - \sqrt{2V(\phi)}\right)^2 + \phi'\sqrt{2V(\phi)}\right\} \geq \left|\int dx\, \phi'\sqrt{2V(\phi)}\right| = \left|\int_{\phi(-\infty)}^{\phi(+\infty)} d\phi\, \sqrt{2V(\phi)}\right| . \tag{1.10}$$

This shows immediately that the energy is minimized, for the given boundary conditions, by solutions of the first-order equation:

$$\phi' \mp \sqrt{2V(\phi)} = 0\,, \tag{1.11}$$

namely, the kink itself. Of course, the bound then gets saturated by the kink mass. Solutions that saturate Bogomolny-type of bounds are called BPS solutions [35, 36], and play a special role in many theories, thanks to their inherent simplicity. Moreover, the deep property of them satisfying a first-order equation has deep connections to supersymmetry [37]. For the moment, however, we will not comment further in this direction.

Having proved the kink stability, let us now give a more powerful argument (see, for example, [38,39] for a review), which will also furnish us with a clear picture of the generic reason beyond this type of stable solutions. Let us consider the topological structure of the vacuum manifold. In particular, let us imagine a process where the kink were to decay in any finite energy state on top of one of the vacua of the theory. Since the asymptotic values of the field at infinity for the kink are not continuously connected to the ones of a symmetry-broken vacuum of the theory, such a process would require overcoming an infinitely high energy barrier. Indeed, the field would need to be outside of a vacuum for an infinitely large volume; this of course costs infinite energy and makes the process impossible, both classically and quantum mechanically. A solution that is stable thanks to the topological properties of the vacuum manifold of the theory is said to be a topological soliton.

We can make the stability evident by defining a *topological current*, and its associated *topological charge*. Let us consider the quantity

$$J_\mu = \epsilon_{\mu\nu}\partial^\nu\phi\,. \tag{1.12}$$

Such a current may, at first sight, appear trivial, since it is conserved without the field necessarily being on-shell:

$$\partial^\mu J_\mu = 0\,. \tag{1.13}$$

However, when considering the associated charge, we observe that it captures the nontrivial information about the asymptotic behaviour of the filled profiles:

$$Q = \int_{-\infty}^{\infty} dx J^0 = \int_{-\infty}^{\infty} dx \partial_x\phi = [\phi(\infty) - \phi(-\infty)]\,. \tag{1.14}$$

We see that the charge can take values in $\mathbb{Z}_2$. Its conservation shows that a kink acquires a conserved topological number, which supports its stability against decaying into the vacuum. In other words, fluctuations on top of a kink live in a different superselection sector with respect to vacuum fluctuations. It can be shown how, quantum mechanically, this type of topological stability can be rephrased in terms of an infinite occupation number of zero-momentum quanta [40].

We close this section with a discussion on how to generalize the concept of a topological charge to a generic theory in an arbitrary number $d = D+1$ of dimensions. Let us suppose

that a given theory of a field ϕ has a potential whose vacuum manifold is given by the manifold U. Normally, nontrivial vacuum manifolds appear thanks to symmetry breaking. Then, by symmetry, U will be a so-called symmetric space, namely, it can be written as a coset space $U = G/H$, where G is the symmetry group of the theory and H the unbroken subgroup. Finiteness of energy requires the field to approach the vacuum manifold asymptotically. In analogy to what has been discussed before, a configuration can be stable if it is impossible to continuously deform it into another one without remaining in the vacuum manifold. Thus, we can classify topological sectors by the group of continuous maps from the sphere at spatial infinity to the vacuum manifold, $\phi(x_\infty) : S^\infty \to U$, quotiented by continuous transformations. This is, by definition the D-th Homotopy group of the vacuum manifold U, usually denoted by $\pi_D(U)$. In the case of theories with gauge fields, similar considerations lead to an analogous classification for gauged topological defects like Nielsen-Olesen strings [41] or 't Hooft-Polyakov magnetic monopoles [42, 43].

1.1.2 Zero modes and Poincaré symmetry breaking

In this section, we analyze the properties of the kink solution with respect to Lorentz invariance. A kink, like all localized stable configurations, spontaneously breaks Poincaré invariance. In particular, it breaks both translations and boosts. At the classical level, indeed, the kink is parametrized by its center of mass, x_0, whose variation gives rise to a one-parameter family of distinct solutions, degenerate in energy. Moreover, by Lorentz invariance, we can boost the kink profile to obtain a kink moving at an arbitrary velocity v:

$$\phi_k^v(x) = \pm v \tanh\left(\frac{m}{\sqrt{2}}\gamma_v(x - vt - x_0)\right). \tag{1.15}$$

This boosted kink has the corresponding energy

$$E_k^v = \gamma_v M_k \,. \tag{1.16}$$

We already see from this analysis that we should be able to effectively describe the kink with an effective Lagrangian of a relativistic particle, as long as the interactions with other modes of the field can be neglected. We will show below that indeed this is the case.

Since there is a broken symmetry, we should identify the corresponding Goldstone mode. We can identify it by expanding around our "vacuum" kink solution, in the direction of the broken symmetry. Since we are breaking translational invariance, this amounts to an infinitesimal shift of the kink in the x direction. We are thus led to consider the following mode:

$$\phi_k(x + \eta(t)) = \phi_k(x) + \phi_k'(x)\eta(t) \,. \tag{1.17}$$

This shows that the Goldstone mode emerging from the broken translational invariance has a wavefunction proportional to the derivative of the kink solution. Its significance is clear: the Goldstone mode characterizes the motion in space of the kink itself. For this reason, we will refer to it, as customary, as the translational modulus, since it is the mode that parametrizes the position in space of an arbitrary moving kink state. Let us show

that its dynamics matches the physical picture. We can expand the original field-theoretic Lagrangian in the direction in field space corresponding to the translational modulus. Since the kink is a classical solution, its first-order variation vanishes. Expanding at quadratic order and integrating over the x coordinate, we obtain:

$$S = \int dxdt \left\{ -\left(\frac{1}{2}\phi_k'^2 + V\left(\phi_k\right)\right) + \frac{1}{2}\left(\phi_k'\right)^2 \dot{\eta}^2 \right\} = \int dt \left[M_k \left(-1 + \frac{1}{2}\dot{\eta}^2 \right) \right] . \tag{1.18}$$

This is the Lagrangian of a slowly moving, non-relativistic particle of the mass of the kink! It represents the low-energy effective Lagrangian of the zero-mode of broken translational invariance. In the next sections, we will discuss its cutoff in terms of the energy gap of the zero modes with respect to the other excited modes on top of the kink.

Let us make an important remark. Normally, in theories where the broken symmetry commutes with Lorentz invariance, the low-energy effective field theory lives on the same space where the original field theory lives. However, this changes for low-energy theories emerging from broken translational invariance. In full generality, let us imagine an arbitrary defect in a $D+1$-dimensional quantum field theory, which breaks p of the D translational directions. For example, we can think about a domain wall, or a string-theoretic D-brane. Then, the zero modes correspond to fluctuations of the object itself in the directions orthogonal to it. Namely, there are gapless fields living on the $D-p+1$ dimensional *world-volume* theory of the objects. In our examples, these would be transverse relativistic "sound waves" for the domain wall, or a subset of open string modes on the D-brane DBI theory. The usual shift-translational invariance, which translates into derivative interactions, reflects the fact that the position of the defect itself is arbitrary, and cannot influence the dynamics. For the kink, the only remaining unbroken direction is time translations. Therefore, the corresponding Goldstone mode lives on a $0+1$ dimensional, quantum mechanical theory. Finally, let us remark that the meaning of gaplessness needs to be interpreted appropriately in the light of the lower-dimensional theory: in the kink case, gaplessness means that the energy of a moving kink reduces to the "ground state" energy of the static kink continuously, in the zero momentum limit.

Let us now describe the symmetry-breaking process in quantum mechanical terms. Let us denote the quantum state corresponding to a localized kink by $|\phi_k\rangle$. Let us also consider the kink as a very heavy object, in such a way that a localized state in a region of order of its size L is a good approximate vacuum. As we will show later, this amounts to considering the kink in the weak coupling limit, where it is highly classical. Then, as customary, we define the order parameter for a broken symmetry as the variation $\delta\hat{O}$, of an operator $\hat{O}$, which has non-zero expectation value on the vacuum under consideration:

$$\langle\phi_k|\delta\hat{O}|\phi_k\rangle \neq 0\,. \tag{1.19}$$

The relevant operator is clearly the field itself $\hat{O} = \hat{\phi}$. Indeed, its variation $\partial_x\hat{\phi}$ satisfies

$$\langle\phi_k|\partial_x\hat{\phi}|\phi_k\rangle \neq 0\,. \tag{1.20}$$

Correspondingly, the integrated quantity

$$\mathcal{N}_\eta{}^2 = \int dx(\partial_x\phi_k)^2\,, \tag{1.21}$$

is exactly the norm (squared) of the associated zero mode, and together with the size of the object $L \sim 1/m$ it sets the scale f_P of the broken Poincaré symmetry: $f_P^2 = \mathcal{N}_\eta L$. This can be shown even more explicitly from the quantum field theoretic definition of Goldstone decay constant: given a broken symmetry with current J_μ and a Goldstone state with momentum p $|\pi(p)\rangle$, we define a generic decay constant f as:

$$\langle 0|J_\mu(0)\,|\pi(p)\rangle = \mathrm{i} f p_\mu\,. \tag{1.22}$$

For us, the current is the space-translation part of the energy momentum tensor: $T_{\mu 1}$. The (approximate) vacuum state is the localized kink solution, so we want to evaluate $T_{\mu 1}$ along the normalized zero mode direction, namely for $\phi(x) = \phi_k\left(x + \eta(t)/\sqrt{\phi'(x)}\right)$. Since our theory lives on the world-volume, the quantity to consider is the charge. We get at first order, for canonically normalized η:

$$T_{01} = (\partial_x \phi_k)\dot{\eta}\,. \tag{1.23}$$

Comparing with the usual expression for the decay constant for a Goldstone boson π, $J_\mu = f\partial_\mu \pi$, and taking into account that $\int(\phi')^2 = M_k = \mathcal{N}_\eta^2$, we obtain the formula above:

$$f_P^2 = \mathcal{N}_\eta L\,. \tag{1.24}$$

1.1.3 The quantum kink

In this section, we discuss the meaning of the kink solution within the quantized version of the theory. There are many ways to understand the role that kink states play in the quantum theory, all of which are different points of view that turn out to be equivalent to each other in the appropriate regime. First, we discuss the standard background field method, namely the quantization of the kink fluctuations on the top of the kink background [44]. We shall comment on its connection to the coherent state picture for multiparticle configurations. In the last part, we will discuss a semiclassical, WKB-like approach to obtain the quantum spectrum of a theory with classical bound states. Then, we will show how to apply it to non-perturbative solutions in a theory closely related to the $\lambda\phi^4$ theory, the so-called Sine-Gordon theory, where such methods can be fruitfully used to obtain its complete spectrum [45].

The first way to analyze the kink is through the quantization of its fluctuations. This amounts to expanding our original quantum field in a generic profile perturbing the kink classical background

$$\hat{\phi}(x) = \phi_k(x) + \delta\hat{\phi}(x)\,. \tag{1.25}$$

Before proceeding, let us remark that at weak coupling the kink is indeed a quasi-classical object. Indeed, an object can be expected to be classical if its Compton wavelength λ_c is much smaller than its actual size L. For the kink, the ratio between the two is controlled exactly by the coupling of the theory:

$$\frac{\lambda_c}{L} \sim \frac{m}{M_k} \sim \frac{\lambda}{m^2} \ll 1\,. \tag{1.26}$$

Correspondingly, the kink can be understood as a highly occupied "classical" state, kept together by collective interactions [13, 38, 40].

In the background field method, we want to quantize the operator $\delta\hat{\phi}$. Let us take a perturbative, weak-field approach. To this end, we expand the original Lagrangian for small $\delta\phi$ (we drop the hat from now on). Since we are expanding around a classical solution, there can be no linear tadpoles, and we obtain a quadratic theory for the fluctuation field:

$$\mathcal{L}_{\delta\phi} = \int d^2x \left[\frac{1}{2}\left(\partial_\mu \delta\phi\right)^2 - \frac{1}{2}V''\left(\phi_k\right)\delta\phi^2\right] + \mathcal{L}_{\text{int}}\,. \tag{1.27}$$

To quantize, we need to obtain the mode expansion that corresponds to harmonic oscillators. Therefore, we expand a generic profile as:

$$\delta\phi(x,t) = \sum_j c_j f_j(x) e^{-\mathrm{i}\omega_j t} + \text{h.c.}\,. \tag{1.28}$$

Note that since the kink is breaking translational invariance, the index j, is not labelled by momentum. It can, of course, have both a continuum and a discrete range. The mode wavefunctions f_j solve the static equation:

$$\left[-\frac{d^2}{dx^2} + V''\left(\phi_k\right)\right] f_j(x) = \omega_j^2 f_j(x)\,. \tag{1.29}$$

Then, one can promote the coefficients c_j's to ladder operators, which satisfy the canonical commutation relations, and the Hamiltonian assumes the canonical form

$$H = \sum_j \omega_j \left(\frac{1}{2} + c_j^\dagger c_j\right) + H_{\text{int}}\,. \tag{1.30}$$

Let us analyze the spectrum further. First, we know there cannot be any negative ω_j^2. Modes with imaginary frequencies would correspond to tachyons, and would signal an instability of the background. However, we proved above that the kink is stable; therefore, these types of modes are excluded. There has to be, however, a zero frequency mode: this is exactly the zero mode coming from the breaking of translational invariance discussed in the previous section. By taking the x derivative of the equations of motion for the kink

$$\phi_k'' + V'(\phi_k) = 0\,, \tag{1.31}$$

we see that the zero mode $f_0 = \eta = \phi'(x)$ is indeed a zero frequency solution:

$$\left(\frac{d^2}{dx^2} + V''(\phi_k)\right)\frac{d}{dx}\phi_k = 0\,. \tag{1.32}$$

We remark again that this mode does not correspond to an oscillator; instead, its Hamiltonian is that of a free particle on mass M_k

$$H_0 = \frac{1}{2}M_k\dot{\eta}^2\,. \tag{1.33}$$

The zero mode dynamics gives us a first confirmation of the classicality condition. The ground state of the center of mass coordinate of the kink η is, by translational invariance, completely delocalized for any finite mass of the kink. However, for very large values of the mass, the energy cost of localizing the wavepacket gets increasingly smaller, and a localized classical kink is a progressively better approximation of the associated quantum state.

As the next step, let us clarify what the physical meaning is beyond a decomposition of the form (1.25). Such a splitting of the quantum field into a classical solution and a fluctuation field can be seen as a canonical transformation:

$$\hat{\phi} = \phi_k + \delta\hat{\phi} \tag{1.34}$$

$$\delta\hat{\pi} = \hat{\pi}\,. \tag{1.35}$$

In particular, there exists a unitary operator that relates the fluctuation field $\delta\hat{\phi}$ to the original field $\hat{\phi}$. Under this transformation, the Hamiltonian transforms accordingly [46]:

$$H[\phi_k + \delta\hat{\phi}, \delta\hat{\pi}] = E_k + \frac{\delta H}{\delta\phi}(\phi_k, \pi_k)\delta\hat{\phi} + + \frac{\delta H}{\delta\pi}(\phi_k, \pi_k)\delta\hat{\pi} + \tilde{H}[\delta\hat{\phi}, \delta\hat{\pi}]\,, \tag{1.36}$$

where $\tilde{H}[\delta\hat{\phi}, \delta\hat{\pi}]$ is the Hamiltonian for the fluctuation fields. This corresponds to the Hamiltonian that one obtains by plugging the field transformation into the Lagrangian and dropping the total derivatives that appear using the equations of motion, and is the one governing the evolution for $\delta\hat{\phi}$ and the corresponding momentum. Thanks to the Hamilton equations and the staticity of the solution, the linear terms vanish, so we end up with:

$$H[\phi_k + \delta\hat{\phi}, \delta\hat{\pi}] = E_k + \tilde{H}[\delta\hat{\phi}, \delta\hat{\pi}]\,. \tag{1.37}$$

This allows us to define the kink state as the ground state of the operator $\tilde{H}$. Then, equation (1.37) tells us that the kink state as defined is indeed an eigenstate of the original Hamiltonian H, with classical energy E_k. Note that this refers to the true ground state of $\tilde{H}$, which, as commented, has the zero mode sitting in a momentum eigenstate. A localized kink should be thought of as a wave packet with a typical size of the order of the kink size. Note also the role of the stationarity of the kink solution: for a nontrivial, time-dependent, classical solution, the linear terms in (1.37) in general have a nontrivial effect. Moreover, for more generic profiles, $\tilde{H}$ is itself time-dependent, and as such, no clear definition of a ground state exists. This will become important in chapter 4, when discussing relativistic superfluids.

In a perturbative approach, we can approximate the vacuum of $\tilde{H}$ as the vacuum of the quadratic theory of the fluctuations. In this setting, we can explicitly understand the kink as a squeezed coherent state $|\phi_k\rangle$ on top of the fundamental vacuum [31]. Such a state satisfies $\langle\phi_k|\hat{\phi}|\phi_k\rangle = \phi_k$, and minimizes the energy of quadratic fluctuations.

It is instructive to use our previous discussion to show how one can calculate loop corrections to the kink mass [44]. We will follow the review of [39]. As expected, it will turn out that these are finite, once we add the counterterms used to regulate UV-divergences to the bare Lagrangian.

By looking at (1.30), the one-loop shift in the kink energy is naively divergent, and given by:

$$\delta E_k = \frac{1}{2}\sum_j \omega_j \,. \tag{1.38}$$

However, we need to remember that the vacuum of the theory has itself a divergent vacuum energy. Hence, the quantity of interest is:

$$\delta E_k = \frac{1}{2}\left(\sum_j \omega_j - \sum_k \omega_k^{(v)}\right) , \tag{1.39}$$

where $\omega_k^{(v)} = \sqrt{2m^2 + k^2}$ are the frequencies given by the dispersion relations for the modes in the vacuum. To proceed further, we need more details on the spectrum of fluctuations around the kink, these can be found, for example, in [39]. Here, we just state the results. Besides the zero mode, there's a single bound state with frequency $\omega_1^2 = 3m^2/2$, and then a continuum of modes with frequencies $\omega_k = \sqrt{2m^2 + k^2}$ labelled by the asymptotic momentum k. The details of the continuum modes are unimportant; the only property that is relevant for our purposes is that, compared with free plane waves, they undergo a phase shift at infinity given by

$$\delta(k) = -2\arctan\left(\frac{3\sqrt{2}}{2}\frac{mk}{m^2 - k^2}\right) . \tag{1.40}$$

Let us now regulate the space with an IR cutoff L. Then, the momenta of the continuum modes for the kink excitations and for the vacuum get discretized as:

$$k_n L - \delta(k_n) = \pi n \tag{1.41}$$

$$k_n^{(v)} L = \pi n \,. \tag{1.42}$$

We see that the difference of the two respective momenta labeled by the same n is infinitesimally small for large L: $\Delta k_n = k_n - k_n^{(v)} = \delta(k_n)/L$. We can now calculate (1.39):

$$\delta E_k = \sum_n \left(\sqrt{2m^2 + k_n^2} - \sqrt{2m^2 + k_n^{(v)2}}\right) . \tag{1.43}$$

Expanding in series for small $\delta(k_n)/L$ and converting the sum back to an integral in the $L \to \infty$ limit, we obtain:

$$-\frac{1}{2\pi}\int_0^\infty dk\, \frac{k\delta(k)}{\sqrt{k^2 + 2m^2}} \,. \tag{1.44}$$

This integral can be evaluated. Taking into account also the contribution of the bound state, it can be shown that one obtains:

$$\delta E_k = \left(\frac{\sqrt{6}}{12} - \frac{3\sqrt{2}}{2\pi}\right) m - \frac{3\sqrt{2}m}{2\pi}\int_0^\infty \frac{dk}{\sqrt{k^2 + 2m^2}} \,. \tag{1.45}$$

Observe that, in addition to a finite term, a divergent contribution is still present. Nicely enough, this perfectly cancels with the divergent contribution coming from the counterterms. Indeed, the counterterm Lagrangian is

$$\mathcal{L}_{ct} = \int d^2x \, \frac{1}{2}\delta m^2 \phi^2 \,, \tag{1.46}$$

which leads to an energy contribution of the form:

$$\delta E_{ct} = -\frac{1}{2}\delta m^2 \int dx \, \phi_k(x)^2 \,. \tag{1.47}$$

The counterterm δm^2 can be obtained by the one-loop correction to the propagator, and it reads:

$$\delta m^2 = \frac{3\lambda}{2\pi}\int_0^\infty \frac{dk}{\sqrt{k^2+2m^2}} \,. \tag{1.48}$$

We observe that δE_{ct} conspires to exactly cancel the divergence in the one-loop kink energy (1.45). We can state the final, finite correction to the energy in the dimensionless coupling λ/m^2

$$E_k = \frac{2\sqrt{2}}{3}\frac{m^3}{\lambda} + \left(\frac{\sqrt{6}}{12} - \frac{3\sqrt{2}}{2\pi}\right) m \,. \tag{1.49}$$

This notable result shows, among other things, how a consistent definition of a non-trivial quantum state results in finite-energy properties even when taking into account loop corrections. We will see how something similar happens for a time-dependent non-trivial U(1) superfluid state in chapter 4.

1.1.4 Quantum kinks: the WKB approximation

In this section, we discuss an alternative way to connect a class of classical solutions to corresponding quantum bound states in the corresponding quantum field theory. The approach, due to Dashen Hasslacher and Neveu (DHN) [44,45,47,48], consists of developing an extension of the WKB approximation to a quantum field theoretic setting. This allows us to connect periodic, "bounded" solutions in the field space to actual bound states in the theory. As it is common for semiclassical approximations, in general, it is expected to be more precise the larger the classical action of the solution under consideration is in units of $\hbar$. Nevertheless, in some situations it can even lead to exact results.

In this section, we will introduce the method in the context of the 1+1 dimensional Sine-Gordon theory, a close relative of the $\lambda\phi^4$ theory discussed above. Compared to the latter, the Sine-Gordon theory has a richer nontrivial spectrum, where WKB methods can be exemplified with more clarity. The Sine-Gordon Lagrangian is that of a bosonic field, endowed with a periodic potential:

$$\mathcal{L} = \frac{1}{2}\partial_\mu\phi\partial\phi^\mu - \frac{m^4}{\lambda}\left(\cos\left(\frac{\sqrt{\lambda}}{m}\phi\right) - 1\right) \,. \tag{1.50}$$

It is immediately clear that the vacuum manifold of this theory is $\mathbb{Z}$; correspondingly, topologically nontrivial configurations that interpolate between different vacua carry a $\mathbb{Z}$-valued topological charge. It can be shown by trivial integration, that the Sine-Gordon equivalent of the kink solution in $\lambda\phi^4$ is given by:

$$\phi(x) = \frac{2v}{\pi} \tan^{-1}\left[e^{m(x-x_0)}\right] . \tag{1.51}$$

However, Sine-Gordon admits more nontrivial nonperturbative solutions. In particular, by considering a kink anti-kink superposition, one can obtain a family of classical profiles that represent classical bound states of a kink and an anti-kink: the so-called breather solutions. They are parametrized by a continuous parameter s, and they read:

$$\phi_s(x,t) = \frac{2v}{\pi} \tan^{-1}\left\{\frac{1}{s}\sin\left(\frac{mst}{\sqrt{1+s^2}}\right)\left[\cosh\left(\frac{mx}{\sqrt{1+s^2}}\right)\right]^{-1}\right\} . \tag{1.52}$$

These solutions carry no topological charge, and correspondingly they need to have a nontrivial time dependence in order to be non-dispersive. However, their time evolution is purely periodic with period $T = 2\pi\sqrt{1+s^2}/ms$, i.e., they track closed orbits in the field space. Their mass is

$$M_s = \frac{M_k}{\sqrt{1+s^2}} . \tag{1.53}$$

Intuitively, one would expect that, once we move to the quantum theory, this continuous family of closed orbits would translate into a discrete set of bound states. We now introduce the WKB formalism needed to show it. In the following, we will mainly follow the original papers and [39].

First, let us understand intuitively how a semiclassical quantization procedure works. Let us consider a one-dimensional quantum mechanical system, whose classical counterpart admits periodic solutions of energy E and period $T(E)$. Let us denote the action of these solutions as $S(E)$. Semiclassically, such a family of orbits will generate a discrete set of bound states satisfying the condition:

$$\int_T p(q)dq = 2\pi n , \tag{1.54}$$

where the integration is taken on one period of oscillation. Note, that the above condition can be rewritten in terms of the action. From

$$\int_T pdq = \int_T p\dot{q}dt = \int_T (H+\mathcal{L})\,dt = ET(E) + S(E) = 2\pi n . \tag{1.55}$$

Now, we immediately see how the WKB condition can be extended to field theory. For a family of periodic solutions of energy E, period $T(E)$ and action $S(E)$, we need to impose:

$$\int_T dxdt\,(\mathcal{H}+\mathcal{L}) = ET(E) + S(E) = 2\pi n . \tag{1.56}$$

Let us apply this condition to the breather. The on-shell action reads:

$$S(T) = \frac{32\pi m^2}{\lambda}\left\{\cos^{-1}\left(\frac{2\pi}{mT}\right) - \left[\left(\frac{mT}{2\pi}\right)^2 - 1\right]^{-1}\right\}. \tag{1.57}$$

The quantization condition (1.56) gives us the following spectrum for the breathers:

$$M_n = \frac{16m^3}{\lambda}\sin\left(\frac{n\lambda}{16m^2}\right). \tag{1.58}$$

Before proceeding with a more formal argument for (1.56), we can ask ourselves as a trivial check if we can reproduce the continuum of states corresponding to the kink itself moving with velocity v using the approach above. Indeed, such a treatment is possible. To this end, let us for a moment compactify the space in a torus or radius L. Then, we expect the momenta to become discrete. Indeed, let us consider a kink in motion. This will be a periodic solution, with energy $E = M_k\gamma_v$ and period $T = L/v$. Then, a straightforward application of (1.56), gives us the quantization condition for momenta:

$$E_n = \sqrt{M_k^2 + p_n^2}, \quad p_n = \frac{2\pi n}{L}. \tag{1.59}$$

Now, we can turn on proving (1.56) more rigorously. The idea of DHN in [47], was to consider the trace of the resolvent operator:

$$G(E) = \mathrm{Tr}\,\frac{1}{H-E} = \sum_n \frac{1}{E-E_n} = \mathrm{i}\,\mathrm{Tr}\int_0^\infty dT e^{\mathrm{i}(E-H)T} \tag{1.60}$$

The quantity $\mathrm{Tr}\,e^{-iHT}$ can itself be represented through a path integral with periodic boundary conditions of period T. This allows us to write the resolvent as:

$$G(E) = \int_0^\infty dT \int_T \mathcal{D}[\phi] e^{\mathrm{i}(S[\phi]+ET)}. \tag{1.61}$$

Bound state energies correspond to poles of the resolvent. To obtain them, we can proceed semiclassically, evaluating the integral above in a saddle point approximation. The full proper WKB requires expanding the action at quadratic order around all classical solutions ϕ_{cl} which have periodicity T, or an integer divisor of T, and performing the Gaussian integral. This has to be performed case by case, and gives one-loop corrections to (1.56). Here, we perform a cruder approximation. We can estimate the dominant contribution to both integrals as the value of the integrand at the saddle. Then, we estimate the path integral as $\int \mathcal{D}[\phi]e^{\mathrm{i}S} \sim e^{\mathrm{i}S[\phi_{cl}]}$. The second integral gives us a condition that connects the energy with the classical action: $dS_{cl}(T)/dT = -E_{cl}$. This forces the period T to be the one corresponding to the solution ϕ_{cl}. Finally, we need to take into account that each classical solution of period T, also contributes to all the path-integrals with periodic boundary conditions equal to nT, for an arbitrary integer n. Consequently, we can express $G(E)$, modulo a dimensionful scale, as:

$$G(E) \approx \sum_{n=1}^{\infty} e^{\mathrm{i}n[S_{cl}(E)-ET(E)]} := \sum_{n=1}^{\infty} e^{\mathrm{i}nW(E)} = \frac{e^{\mathrm{i}W(E)}}{1+e^{\mathrm{i}W(E)}} \,. \tag{1.62}$$

We can now identify the poles of $G(E)$: they appear exactly when:

$$S_{cl}(E) - ET(E) = 2\pi n \,. \tag{1.63}$$

This proves (1.56). Of course, the full WKB treatment would require the evaluation of the Gaussian integral. That would amount to correcting the tree-level classical energy with the one-loop contribution given by the sum of the zero point energies $\omega_i/2$ for the sum of all the i-th modes on top of the classical background, and treating the UV-divergences with the counterterm Lagrangian, similar to what we did for the static kink profile in the previous section, but taking into accunt the periodicity in time of the solution [49]:

$$S(\phi_{cl}) + S_{ct}(\phi_{cl}) + T\left(E(\phi_{cl}) + E_{ct}(\phi_{cl}) + \frac{1}{2}\sum_i \omega_i\right) = 2\pi n \,, \tag{1.64}$$

where we included in E_{ct} also the counterterm that renormalizes the zero point energy. In the case of the Sine-Gordon model, DHN [45] were able to show that this amounts only to a redefinition of the coupling constant in (1.58):

$$\frac{\lambda}{m^2} \to \frac{\lambda}{m^2}\left(1 - \frac{\lambda}{8\pi m^2}\right)^{-1} \,. \tag{1.65}$$

In the next chapter, we will report how the same method has been used by the same authors in another interesting 1+1-dimensional model, the so-called Gross-Neveu model at large N, to obtain the exact spectrum of bound states. This will be relevant for chapter 2, when we will discuss the phenomenon of saturation and give some examples of saturated states.

1.2 The 1+1-dimensional Gross-Neveu model

In this section, we briefly discuss the basic properties of another non-trivial 1+1-dimensional model, the Gross-Neveu model [32]. The reasons for dedicating some time to it are numerous. First, it will endow us, in chapter 2, with a prominent example of a theory exhibiting the phenomenon of saturation in a controlled setting. Second, it allows us to briefly discuss the power of large-N physics. Large-N theories, as we will see, will play an important role in both chapter 2 and chapter 3. Finally, it is a beautiful example of an integrable theory, where the methods exposed in the previous subsection had a great impact in understanding its properties [48]. The Gross-Neveu model is defined by the following Lagrangian of a set of N fermionic Dirac fields ψ^i in the fundamental representation of a global $SU(N)$ group.

$$\mathcal{L} = \mathrm{i}\bar{\psi}_i \partial\!\!\!/ \psi^i + \frac{g^2}{2}\left(\bar{\psi}_i \psi^i\right)^2 \,. \tag{1.66}$$

It becomes of particular interest in the limit where the number of flavours N goes to infinity. Indeed, the so-called large-N limit makes the theory simpler. To understand the essence of this phenomenon, we first need to clarify how the $N \to \infty$ limit is taken. Indeed, a perturbative analysis immediately shows that perturbative unitarity would be lost if N were taken to infinity at fixed coupling g^2. This follows from the structure of the loop expansion: adding additional loops leads to additional factors of N from the traces over the flavour space. Clearly, this implies that the series explodes, and the loop expansion breaks down immediately. To define a sensible limit, we are thus led to the renowned 't Hooft limit [50], where we take simultaneously:

$$N \to \infty, \quad g^2 \to 0, \quad g^2 N := \lambda \text{ finite}. \tag{1.67}$$

The quantity λ is called the 't Hooft coupling, and controls the now convergent (actually, asymptotic) loop expansion in the large-N limit. Let us now clarify the significance of such a limit and why it is so convenient. This can be shown in a simple form in the path integral approach. Let us consider, for example, the partition function:

$$Z = \int \mathcal{D}[\psi] e^{\frac{\mathrm{i}}{\hbar} S[\psi]} . \tag{1.68}$$

We can perform a rescaling of the fields, to bring the quantum coupling outside of the action. From now on, we omit the flavour index i. If we consider $\psi' = g\psi$, the action takes the form

$$S = \frac{1}{g^2} \int d^2x \left[\mathrm{i}\bar{\psi}' \partial\!\!\!/ \psi' + \frac{1}{2} \left(\bar{\psi}' \psi' \right)^2 \right] = \frac{N}{\lambda} \int d^2x \left[\mathrm{i}\bar{\psi}' \partial\!\!\!/ \psi' + \frac{1}{2} \left(\bar{\psi}' \psi' \right)^2 \right] . \tag{1.69}$$

This implies that, in the limit of $N \to \infty$ at fixed λ, we are actually making the theory semiclassical! The path integral will be strongly dominated by saddle points, and higher-order quantum corrections will be suppressed by powers of $1/N$. In the next chapter 2, we will briefly see how a similar approach allows us to gain great control also in a QCD setting, in the limit with a large number of colors.

Here, we can use the power of large-N to show that the Gross-Neveu model exhibits the important phenomenon of *dimensional transmutation*. At the same time, we will show that the fermion bilinear condenses in the vacuum, and that correspondingly the fermions acquire a mass. To this end, it is useful to introduce an auxiliary field σ, performing a so-called Hubbard Stratonovic transformation [51]. We rewrite the Lagrangian as:

$$\mathcal{L} = \mathrm{i}\bar{\psi}_i \partial\!\!\!/ \psi^i + \sigma \bar{\psi}_i \psi^i - \frac{N}{2\lambda} \sigma^2 . \tag{1.70}$$

The field σ is non-dynamical, and integration over $\mathcal{D}[\sigma]$ gives the constraint: $\sigma = \bar{\psi}_i \psi^i$ and restores the original Gross-Neveu Lagrangian. The advantage of such a formulation is that the Lagrangian is now quadratic in the fermionic fields. We can use this property to argue that σ, or equivalently the fermionic bilinear $\bar{\psi}_i \psi^i$, develops a vacuum expectation value. At the same time, we will see that the effective potential tells us how to renormalize the

coupling, making the theory asymptotically free. Let us calculate the effective potential for σ. Assuming a constant field configuration $\sigma = \text{const}$ and integrating over the quadratic Lagrangian for the fermionic fields, we obtain:

$$\int \mathcal{D}[\sigma]\mathcal{D}[\bar{\psi},\psi]\exp\left[\mathrm{i}S\right] = \int \mathcal{D}[\sigma]\exp\left[-\mathrm{i}\int \frac{N}{2\lambda}\sigma^2\right]\int \mathcal{D}[\bar{\psi},\psi]\exp\left[\mathrm{i}\int \bar{\psi}\left(\mathrm{i}\partial\!\!\!/ + \sigma\right)\psi\right] \quad (1.71)$$

$$= \int \mathcal{D}[\sigma]\exp\left[-\mathrm{i}\int \frac{N}{2\lambda}\sigma^2 + \mathrm{Tr}\ln\left(\mathrm{i}\partial\!\!\!/ + \sigma\right)\right]. \quad (1.72)$$

Taking the fermionic trace gives us the effective potential:

$$V(\sigma) = \frac{N}{2\lambda}\sigma^2 - N\int \frac{d^2p}{(2\pi)^2}\ln\left(\frac{p^2+\sigma^2}{p^2}\right). \quad (1.73)$$

Notice that the potential is controlled by an N prefactor. This shows that a saddle point around the minimum of such a potential has fluctuations suppressed by $1/N$, which vanish in the large-N limit. Thus, the minimization of the effective potential gives the exact result for $N \to \infty$. It remains to renormalize V. The integral (1.73) is logarithmically divergent as

$$(\sigma^2/4\pi)\left[1 + \ln(\Lambda^2/\sigma^2)\right], \quad (1.74)$$

in terms of a UV cutoff Λ. It can be made convergent by defining the renormalized 't Hooft coupling at scale μ:

$$\frac{1}{\lambda(\mu)} = \frac{1}{\lambda} + \frac{1}{2\pi}\log\left(\frac{\mu^2}{\Lambda^2}\right). \quad (1.75)$$

Then, the effective potential takes the finite form:

$$V = N\left[\frac{\sigma^2}{2\lambda(\mu)} + \frac{1}{4\pi}\sigma^2\left(\log\left(\frac{\sigma^2}{\mu^2}\right) - 1\right)\right]. \quad (1.76)$$

This tells us two things. First, it exhibits the phenomenon of dimensional transmutation very transparently. By minimizing (1.76), we see that σ develops a vacuum expectation value at a scale exponentially smaller than the cutoff:

$$\sigma_0 = \mu e^{-\pi/\lambda(\mu)}. \quad (1.77)$$

By imposing that the scale σ_0 is physical, and hence a RG-invariant quantity, we traded a dimensionless coupling with a dimensionful scale. This allows us to rewrite the effective potential in terms of the physical scale:

$$V(\sigma) = \frac{N\sigma^2}{4\pi}\left(\ln\frac{\sigma^2}{\sigma_0^2} - 1\right). \quad (1.78)$$

Note that the v.e.v of σ also gives a mass to the fermionic fields.

Moreover, the invariance of σ_0 under changes of μ defines the beta function:

$$\beta(\lambda) = \frac{d}{d\ln\mu}\lambda(\mu) = -\frac{\lambda^2(\mu)}{\pi}\,. \tag{1.79}$$

Since β is negative, the coupling constant decreases with energy. The Gross-Neveu model is thus asymptotically free, and a well-defined theory at all energies.

One can do more: Dashen Hasslacher and Neveu were able to find explicit space-dependent solutions for profiles of the σ field, coupled to the fermions [48]. This allowed them to apply the WKB method discussed in the previous section to obtain the semiclassical bound-state spectrum of the theory. In large-N, the semiclassical spectrum is expected to become exact. We do not report here the derivation since it is extremely technical; however, we report the results. It turns out that the model exhibits an N-controlled tower of bound states, labelled by $n = 1, ...N$, with masses

$$M_n = \sigma_0 \frac{2N}{\pi} \sin\left(\frac{n}{N}\frac{\pi}{2}\right)\,. \tag{1.80}$$

Of course, the mass of the fundamental fermion, $m_f = \sigma_0$, is recovered for $n = 1$. These bound states are degenerate, with high degeneracy. Their entropy is:

$$e^{S_n} = \frac{2N!}{n!(2N-n)!}\,. \tag{1.81}$$

This fact, as we will see in the next chapter, was crucial for Dvali and Sakhelashvili to connect the top bound state to the phenomenon of saturation [19].

1.3 Non-topological solitons: Q-balls

In this section, we discuss the basics of another type of non-perturbative configurations, so-called Q-balls, that appear in field theory. Their characteristics carry many similarities with the type of solutions that are the main focus of chapter 3, and as such are a good setting to demonstrate some of their properties. Q-balls are stable solutions of interacting quantum field theories, which, unlike the topological solitons discussed above, are protected by a Noether charge. They were first introduced by Lee and Wick, and others [33, 52]. In this section, we mainly follow the discussion of Coleman in [34], and the very nice review of Lee and Pang [53]. The prototypical example of a theory admitting Q-balls is one of a complex scalar ϕ, admitting a $U(1)$ symmetry. For the moment, let us leave the potential $U(|\phi|)$ fairly generic. The Lagrangian is:

$$\mathcal{L} = \partial_\mu\phi^\dagger\partial^\mu\phi - U(|\phi|)\,. \tag{1.82}$$

Let us also set ourselves in $d = 3+1$. We look for charged solutions of the form:

$$\phi(x) = e^{\mathrm{i}\omega t}\varphi(r)\,, \tag{1.83}$$

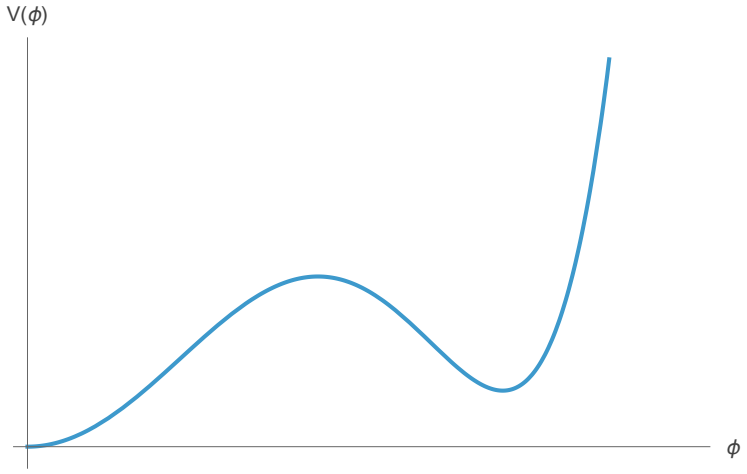

Figure 1.2: A typical potential that admits Q-ball solutions

where ω is a frequency of oscillation, which for the moment we leave unspecified, and we assume spherical symmetry. Intuitively, such solutions can be imagined as a multiparticle state with a high number of charged particles, held together by collective self-interactions. In particular, for any configuration one can use the $U(1)$ charge to count the particle number:

$$N = Q = \mathrm{i} \int d^3x \left(\phi^\dagger \dot{\phi} - \dot{\phi}^\dagger \phi \right) . \tag{1.84}$$

For a Q-ball-like profile, the expression above specifies to

$$Q = \omega \int d^3x \varphi^2(r) . \tag{1.85}$$

To understand the appearance of Q-ball profiles with finite size, let us plug the ansatz (1.83) in the original Lagrangian to obtain an effective Lagrangian for φ. The effect of the phase rotation is to generate an effective potential $\mathcal{V}$, by the addition of an extra term of the form ωQ, which resembles a grand-canonical potential:

$$\mathcal{L}_{\text{eff}} = \partial_\mu \varphi^\dagger \partial^\mu \varphi - U(\varphi) + \omega^2 \varphi^2 := \partial_\mu \varphi^\dagger \partial^\mu \varphi - \mathcal{V}(\varphi) . \tag{1.86}$$

We can readily obtain the equations of motion in spherical coordinates. They read:

$$\frac{\partial^2}{\partial r^2}\varphi + \frac{2}{r}\frac{\partial}{\partial r}\varphi - U'(\varphi) + \omega^2 \varphi = 0 . \tag{1.87}$$

The existence of a Q-ball solution is reduced to a one-dimensional mechanical problem of a particle moving in the inverted potential $-U + \varphi^2\omega^2/2$ with respect to the "time" r. The first derivative term can be understood as a "time" dependent friction contribution. For a generic potential, the existence of a Q-ball amounts to the existence of a solution to eq (1.87) which starts at a certain value of the field φ^* at $r = 0$, and reaches $\varphi = 0$ at infinite "time" $r = \infty$ with zero velocity. For this to happen, we need some conditions

on the potential U and on ω. To have any hope, we would like the shape of the potential to look similar to Fig. 1.2, namely to have a metastable minimum at a given $|\phi| \neq 0$. To this end, we require the coefficient of the quadratic term, let us call it m^2, to be positive and to dominate over ω, $m > \omega$. This is of course not sufficient, since we also want the new minimum to be metastable and not absolutely stable. If we denote by φ_0 the new minimum, the latter condition amounts to requiring

$$\omega^2 > 2U(\varphi_0)/\varphi_0^2 := \omega_0 \,. \tag{1.88}$$

Under these conditions, the existence of a solution with the properties described above can be seen from Coleman's undershoot/overshoot argument [34]. If we imagine releasing a ball at a given starting point φ^* in our auxiliary one-dimensional system, the ball will start rolling down the potential hill, and then climb up again. Clearly, releasing it where $\mathcal{V} < 0$ doesn't allow it to climb back up all the way to $\mathcal{V} = 0$ at infinity. On the other hand, if we start sufficiently close to the high maximum of the inverted potential (corresponding to the metastable minimum discussed above), the energy loss induced by friction becomes negligible, and the ball can roll with sufficient energy to reach $r = 0$ with nonzero speed, thereby overshooting. By continuity, there has to exist a value φ^* such that the field rolls exactly to 0 at $r = \infty$. This value is the v.e.v. of the Q-ball, and the corresponding solution is the radial profile of the Q-ball solution.

It is instructive to understand what happens to the profile of the Q-ball while we vary ω. In particular, let us try to push ω towards its minimum value $U(\varphi_0)/\varphi_0^2$. Then, the two maxima of the inverted potential become degenerate. In this limit, to avoid undershooting the field needs to stay for a long "time" very close to its maximum value. The Q-ball radius correspondingly becomes infinite, as does the charge $Q \sim L\varphi^{*2}\omega$.

Lastly, one can address the question of stability. The proof of absolute stability has been given in Coleman in the large Q limit [34]. Kusenko analyzed the thick-wall, large ω case [54]. Here, we shortly argue for the stability with respect to its disassembly into $N = Q$ fundamental quanta of mass m. Let us work in the large Q limit. By what we said above, this is also a large size limit, where the size R is much larger than the thickness. Then, we can imagine that up to surface terms, the energy for the bubble is of order

$$E \sim \frac{1}{2}\varphi^{*2}R^3\omega^2 + U(\varphi^*)R^3 \,. \tag{1.89}$$

The radius R, or equivalently the volume V, can be obtained by minimizing E for a given $Q \sim \varphi^{*2}R^3\omega$. This leads to the volume $V \sim Q/\sqrt{2\varphi^{*2}U(\varphi^*)}$, and energy:

$$E = Q\frac{\sqrt{2U(\varphi^*)}}{\varphi^*} \,. \tag{1.90}$$

Also, for large Q we can assume thin-wall bubbles satisfying $\varphi^* \simeq \varphi_0$. Then, we can calculate the energy-to-charge ratio:

$$\frac{E}{Q} = \frac{\sqrt{2U(\varphi^*)}}{\varphi^*} \leq m \,, \tag{1.91}$$

by the condition $\omega \leq m$. This shows us that for the bubble it is inconvenient to disassemble into its constituent quanta. We conclude by noting that, even if Q-balls are stable, they can be made to evaporate if coupled to other fields that offer an appropriate decay channel. This was studied in particular by Cohen, Coleman, Georgi and Manohar for the case of a massless fermionic field [55]. There, they coupled the Q-ball field ϕ to a Weyl spinor ψ by:

$$\mathcal{L}_\psi = \mathrm{i}\psi^\dagger \sigma^\mu \partial_\mu \psi - \mathrm{i}g\phi\psi^\dagger \sigma_2 \psi^* + h.c.\,. \tag{1.92}$$

In the thin-wall limit and at weak coupling, they obtain that the Q-balls evaporate, with a decay rate proportional to their area, and with a depletion rate per unit area of [55]:

$$\frac{dN}{dtdA} = 3\pi \frac{g\phi_0}{\omega_0} \frac{\omega_0^3}{192\pi^2}\,. \tag{1.93}$$

In chapter 3, we will discuss a similar scenario, of the evaporation of a 1+1-dimensional bubble in a theory endowed with a large-N symmetry, and we will connect it to the phenomenon of saturation.

Chapter 2

The phenomenon of saturation

In this chapter, we introduce the phenomenon of saturation. First introduced by Dvali in [16–18], saturated states, so-called saturons, are in essence quantum field theoretic states which possess the maximal possible entropy allowed by unitarity. These states, of which black holes are one but far from the only example, arise in several quantum field theories as self-sustained multi-particle configurations when a relevant collective coupling becomes of order one. Such states, albeit being in a deeply classical region of the Hilbert space, nevertheless exhibit paramount quantum aspects which are lost in the classical limit. In particular, they are characterized by a huge, maximal, microstate entropy. Their fully quantum field theoretic characterization is thus essential for an adequate description of their dynamics and of the phenomena for which they are responsible.

In the first section, we start with an introduction to the semiclassical theory of black holes. Then, we discuss the quantum N-portrait description of black holes [13], and we show how it can be seen as an invitation to the phenomenon of saturation.

In the second section, we give a general overview of the phenomenon of saturation, and we describe its implications for generic quantum field theoretic systems. Then, in the following sections we discuss specific examples from various physically relevant theories, at the same time introducing the necessary background for a self-contained discussion of the example at hand.

2.1 Black holes

Black holes are one of the most fascinating objects predicted by general relativity. Already at the classical level, they are home of great interest for many both theoretical as well as phenomenological reasons. However, their role becomes even more prominent once we regard general relativity as a quantum, effective theory of gravity. In a quantum setting, as we shall see, black holes are not only objects of interest, but they become an inescapable ingredient for the consistency of the theory itself. In the following, we shall denote by G the Newton's constant, and by $M_{\rm pl} = \sqrt{\hbar/G}$ the Planck mass (with the associated Planck length $L_{\rm pl} = 1/M_{\rm pl}$).

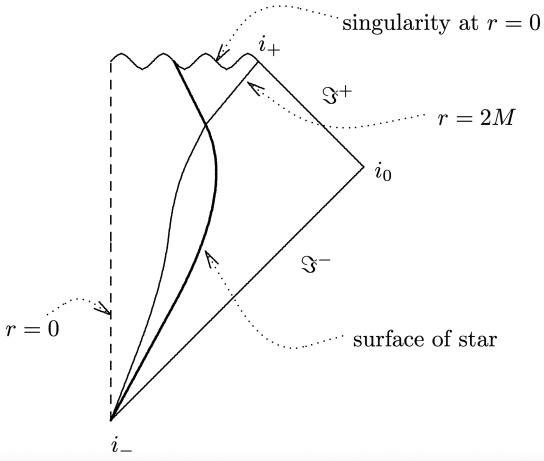

Figure 2.1: The Penrose diagram of a black hole. Picture taken from [1]

2.1.1 Classical black holes

Before adventuring in the quantum realm, let us start by reviewing the fundamental properties of classical and semi-classical black holes. The starting point of a classical black hole is the Schwarzschild solution, which describes a chargeless and spinless static black hole:

$$ds^2 = -\left(1 - \frac{2GM}{r}\right) dt^2 + \left(1 - \frac{2GM}{r}\right)^{-1} dr^2 + r^2 d\Omega^2 \,. \tag{2.1}$$

As it is well known, a Schwarzschild black hole has a horizon at radius $R \sim GM$, and a physical curvature singularity at $r = 0$. Let us remark that, at the horizon, the metric can be made arbitrarily weakly curved by increasing the black hole mass. Classically, everything that is beyond the horizon is doomed to fall into the singularity, and cannot reach future infinity, as shown, for example, by the Penrose diagram description of a black hole in Fig. 2.1. In terms of the asymptotic coordinates of an observer at infinity, we can understand the Horizon as the region of spacetime where the weak-field approximation of general relativity around the Minkowski vacuum breaks down. To explain this, let us consider the Einstein Hilbert action $S = M_{\rm pl}^2 \int \sqrt{-g} R$ expanded around the Minkowski metric $\eta_{\mu\nu}$ in the canonically normalized graviton field $g_{\mu\nu} = \eta_{\mu\nu} + h_{\mu\nu}/M_{\rm pl}$. Schematically, the action has the form

$$S = S_{\rm free} + \sum_n \frac{\partial^2}{M_{\rm pl}^2} \frac{h^n}{M_{\rm pl}^{(n-2)}} \,. \tag{2.2}$$

The horizon develops exactly when the dimensionless h is of order 1, or equivalently when the canonically normalized graviton is of the order of the Planck mass, $h \sim M_{\rm pl}$. This is precisely the regime where the linearized approximation breaks down, and classical nonlinearities become all equally important. Note that, even if they are all non-negligible, they are still subdominant with respect to the kinetic term, thereby safely in the weak coupling regime.

In a theory where, besides pure gravity, we allow gauge fields with associated gauge charges, black holes can carry fingerprints of such charges Q, consistently with the fact that their conservation is expressed in the form of a flux at infinity by Gauss's law. If, moreover, we take into account the angular momentum charge $J = aM$, associated to the asymptotic Poincaré symmetry of asymptotically flat spacetimes, we arrive at the most general black hole solution, described by the Kerr-Newman metric [56] :

$$\begin{aligned} ds^2 = &-\frac{\Delta - a^2 \sin^2\theta}{\Sigma}\, dt^2 - \frac{2a \sin^2\theta\,(r^2 + a^2 - \Delta)}{\Sigma}\, dt\, d\phi \\ &+ \frac{\left[(r^2+a^2)^2 - a^2 \Delta \sin^2\theta\right]}{\Sigma} \sin^2\theta\, d\phi^2 + \frac{\Sigma}{\Delta}\, dr^2 + \Sigma\, d\theta^2 \\ \Delta = r^2 - 2Mr + a^2 + Q^2, &\qquad \Sigma = r^2 + a^2 \cos^2\theta\,. \end{aligned} \tag{2.3}$$

Despite its complication, such a solution is an essentially unique description of black holes. In particular, Birkhoff's theorem proves that every spherically symmetric solution to the vacuum Einstein's equations reduces to the Schwarzschild metric, or its charged extension, the Reissner-Nordstrom metric. Moreover, every axially symmetric stationary vacuum solution belongs to the Kerr-Newman class of metrics. Of course, realistic black holes, when they form, are neither stationary nor spherically symmetric. However, their nontrivial dynamics, described for example by quasi-normal mode physics, quickly settles at equilibrium into one of the cases above. Let us remark on the importance of such results, which are commonly known as classical no-hair theorems: irrespectively of the details that lead to back hole formation, or of the matter content that actually creates the black hole itself, once a classical black hole is formed, it is essentially characterized only by its mass, its gauge charges and its angular momentum.

Another fundamental result of the theory of classical black holes is the Penrose singularity theorem: essentially, Penrose proved that black hole will be created under a very general set of assumptions, making them an unavoidable prediction of general relativity. Intuitively, we can say that we expect to form a black hole every time a certain mass M is localized in a region of physical size R smaller than its own Schwarzchild radius: $R < GM$.

In the seventies, it was observed that classical black holes follow laws that resembled closely the laws of thermodynamics. In particular, the first law states that every infinitesimal change of the mass M, charge Q or angular momentum J of a black hole are related to each other by the so-called Smarr law [57]:

$$dM = TdS + \Omega dJ + \Phi dQ\,, \tag{2.4}$$

where $T = M_{\rm pl}^2/M$ is an energy scale soon to be identified with the Hawking temperature, $S = A/4L_{\rm pl}^2$ is the black hole area in Planck length units, Ω is a quantity connected to the angular velocity at the horizon and Φ the electric potential. Note that, even if we wrote the law in a form ready for its quantum mechanical interpretation, at the classical level the proportionality constants of the various quantities are not fixed.

Even more important is the second law of black holes' dynamics, rigorously proven by Hawking [8]: under appropriate conditions, the area of a black hole can never decrease in

time:

$$\frac{dA}{dt} \geq 0\,. \tag{2.5}$$

Classically, we see that a black hole looks like a featureless object that swallows information and never releases it. However, once we turn on quantum mechanics the whole story changes.

2.1.2 Semiclassical black holes

Once we turn on quantum mechanics, black hole physics becomes extremely richer. Before briefly describing the main points of semiclassical black hole physics, and before detailing the quantum description given by the N-portrait, let us briefly comment on the utmost importance of black holes in quantum gravity. At the heart of the role that black holes play in gravity is the combination of the uncertainty principle and the universal properties that govern black hole formation.

In classical physics, there is no intrinsic price to probe shorter and shorter length scales: one can always, for example, engineer a classical wave with arbitrarily high frequency, but arbitrarily low energy, by reducing its amplitude appropriately. This is not the case in quantum physics: the Heisenberg uncertainty principle, in a relativistic setting, tells us that in order to probe a lengthscale L there is a minimum energy price to pay $E \sim 1/L$. Now, let gravity enter the game. First, let us recall that gravity is by definition universal, so it couples democratically to all forms of energy. Let us imagine that we try to probe a smaller and smaller length scale in a quantum theory of gravity. To this end, we need to localize a certain energy $E \sim 1/L$ in a size L. Without gravity, there would be no obstruction to such a procedure. However, we now encounter an inescapable limit: we will reach the point when the size L becomes smaller than the Schwarzschild radius of the associated energy $E \sim 1/L$:

$$L \sim 1/E \sim GE\,. \tag{2.6}$$

At this point, we have no hope to proceed further: we have just created a black hole, and every increase of energy will only result in a bigger and bigger black hole, thereby shielding us even more from the short distances that we were trying to probe. Black holes gave us an intrinsic bound on the shortest scales that we can probe, the celebrated Planck length $L_{\rm pl}$. What quantum mechanics and general relativity together are telling us is that the high-energy region of quantum gravitational physics is inevitably dominated by black hole physics.

Moreover, since the more we push into the UV, the larger the black hole, we naturally come to the conclusion that a complete theory of quantum gravity needs to be a theory formulated in terms of states at spacetime infinity, namely an S-matrix theory [58]. The other side of the coin of the fact that black holes forbid probing distances smaller than the Planck length, is that black holes also furnish a maximal value for the mass of every elementary particle. Indeed, consider an elementary particle of mass m. There is a quantum length-scale associated with it, its Compton length $\lambda_c \sim 1/m$. On the other hand, it is

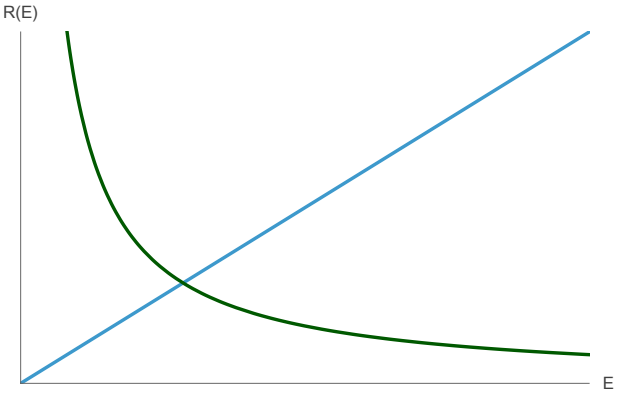

Figure 2.2: A plot of the Compton wavelength (in dark green) and of the gravitational radius (in blue) of an object as a function of its mass E. They intersect at the Planck mass $M_{\rm pl}$.

also endowed with a gravitational radius, $R_g \sim Gm$. For proper elementary particles, the gravitational radius is smaller than the Compton wavelength, so the particle never probes strong field gravity by itself. However, if the mass of the particle were trans-Planckian, then the Compton wavelength would become smaller than the gravitational radius: the particle has become a black hole. Therefore, black holes also tell us that there is a maximal mass, $M_{\rm pl}$, for elementary species. Above it, the spectrum has to be controlled by black holes.

Now that we have clarified the fundamental importance of black holes in quantum gravity, let us discuss their properties. From the so-called laws of black holes thermodynamics, people were speculating that black holes could be endowed with a real entropy, proportional to the area, and with a corresponding temperature. However, the nature and the validity of these proposals were not fully clear. The situation changed with the seminal work of Hawking [12] in 1975: By a semiclassical computation, Hawking showed that semiclassically, black holes radiate with a thermal spectrum and a quantum mechanical temperature:

$$T = \frac{1}{8\pi GM}\,. \tag{2.7}$$

This, in turn, put on firmer ground the hypothesis made by Bekenstein a few years earlier [11], that a quantum black hole has an entropy proportional to the area:

$$S = \frac{A}{4L_{\rm pl}^2}\,. \tag{2.8}$$

To obtain this result, Hawking considered a quantum field in the fixed background of a classical black hole. A black hole is not a static solution: there is no globally defined timelike Killing vector field, since at the horizon the vector ∂_t that generates translations with respect to asymptotic time switches sign and becomes spacelike. Correspondingly, the effective quantum theory in the background of the black hole sees a time-dependent Hamiltonian, which in turn leads to particle creation. Hawking showed that in the asymptotic future, the spectrum of created particles is universal and independent of the details of the

black hole formation; it corresponds to a thermal spectrum where (for bosonic particles) the number of particles n_E at energy E is:

$$n_E = \frac{1}{e^{E/T} - 1}\,. \tag{2.9}$$

Here we do not report the derivation, which can be found in many books, for example, see [1]. We want to stress, however, the precise limit taken by Hawking in his calculation [13, 59]. In order to be allowed to keep the black hole background fixed, one needs to decouple quantum gravitational effects. The only way to do so is by sending the Planck mass to infinity, while at the same time we send the black hole mass to infinity, keeping the radius finite. The double scaling limit is then:

$$M \to \infty, \quad M_{\rm pl} \to 0, \quad R = \frac{M}{M_{\rm pl}^2} \ \text{ finite.} \tag{2.10}$$

In this limit, the black hole becomes an infinite reservoir, that can radiate eternally thanks to its infinite mass. Of course, in a fully quantum theory, the Planck mass is finite, and black holes radiate, losing their mass in the process. It is of the utmost importance to keep in mind the assumptions beyond Hawking computation, in order not to extrapolate its results beyond their regime of validity.

Let us now comment on the black hole entropy. Surprisingly enough, in stark contrast to the classical picture, we discovered that quantum black holes carry a huge entropy, $S \sim AM_{\rm pl}^2$. This entropy is an intrinsic quantum feature, as it is clear from the appearance of the Planck mass in its definition. Moreover, the entropy follows an area law. Even though its existence is already apparent from semiclassical physics, its nature is fully quantum, and it requires every quantum description of a black hole to come up with the proper microstate degeneracy to account for such behaviour.

Starting from black hole physics, Bekenstein imagined a scenario where an object of size R energy E and entropy $S_{\rm obj}$ is thrown into a black hole [60]. Imposing the validity of the generalized second law,

$$\Delta S_{\rm gen} = \Delta S_{\rm bh} + \Delta S_{\rm obj} \ \geq 0\,, \tag{2.11}$$

he obtained a bound for the maximum entropy content of a field-theoretic localized object. The bound reads:

$$S \leq 2\pi ER\,. \tag{2.12}$$

In the next section, this bound will be explained in terms of a more fundamental bound emerging from untarity. Finally, let us note that in the classical limit, the value of the black hole entropy doesn't go to zero as one could naively expect; instead, it explodes to infinity. One could wonder how one can reconcile an infinite entropy with the featureless classical black holes constrained by the no-hair theorems. The only way out is that these modes decouple in the classical limit, thereby freezing their dynamics and becoming impossible to excite. In section 2.2, we will interpret the black hole entropy in light of the

general phenomenon of saturation. There, on one hand we will be able to understand the appearance of the area law in terms of the fundamental concept of unitarity of quantum field theories, and on the other hand we will show how black holes are not the only objects that follow such a law.

2.1.3 Black hole evaporation and information retrieval

The existence of a Hawking temperature implies that black holes evaporate. If one were to trust the (semi)-classical description of a black hole, as a state without any hairs, he would immediately be led to an apparent paradox. Indeed, the naive treatment of black hole evaporation describes the decay process through a self-similar effective equation, where the mass of the black hole is the unique parameter. One uses the Stefan-Boltzmann law to relate the variation of the mass to the total radiated power $P \sim T^4$, to obtain

$$\frac{dM}{dt} \sim \frac{1}{M^2}\,. \tag{2.13}$$

This equation predicts the evaporation of a black hole in a finite time

$$t \sim MS\,. \tag{2.14}$$

On the other hand, it looks like the black hole had no way to radiate the information associated to the initial conditions that led to its formation, since the radiation is assumed to be thermal. This discrepancy constitutes the so-called information paradox. However, let us point out that such reasoning is misleading. First, the no-hair theorem holds for classical black holes, which, as such, do not evaporate. On the contrary, the area law formula tells us that quantum black holes are highly entropic states. Therefore, this fact alone should make us think that their quantum dynamics, even when remaining within the gravitational EFT at sub-Planckian scales, should be much richer than a self-similar "semiclassical" evaporation [59]. In particular, scrambling and inner entanglement are expected to play an important role [61–63]. Indeed, as we shall argue below, a self-similar evolution is actually incompatible with the evaporation rate (2.13) itself on general grounds [59]. Therefore, the assumption of self-similar evaporation up to the Planckian regime is completely unjustified. In the next section and in Chapter 4, we will discuss how the quantum dynamics of a semiclassical state can deviate significantly from its own classical counterpart, in a manner that cannot be captured just by semiclassical quantities. Indeed, for large times, all correlation functions become important, and a semiclassical description in terms of a few parameters such as the mass becomes inadequate [23, 64].

The other side of the same coin is that the exact thermality of the black hole spectrum is obtained in the very specific limit of (2.10). However, this is a limit where there is no backreaction, and the black hole does not evaporate. The question then becomes, how large the corrections to thermality in the finite mass case are? We can estimate them by checking the rate of departure from thermality in the semiclassical evaporation law [59]:

$$\frac{\dot{T}}{T^2} \sim T^2 \sim \frac{1}{S}\,. \tag{2.15}$$

Such corrections, integrated over the long lifetime (2.14), cumulate to deviations of order one. Therefore, the rate (2.13) itself gives us information about the structure of the necessary corrections. In particular, it forbids self-similarity, since quantum corrections of order $1/S$ cannot be captured classically. Let us also note that exponentially small corrections of the form e^{-S} are incompatible with the weak coupling regime of the gravitational EFT, where the thermalization rate is related to weakly coupled rescattering processes [59] (see also [65] for a string-theoretic argoument).

In accordance with what was discussed above, in 1993, Page showed that, generically, one can expect information to start to come out at most at the so-called Page's time, which corresponds to the black hole half-life [66]:

$$t_p \sim RS\,. \tag{2.16}$$

Beyond this timescale, semiclassical evolution cannot be trusted, and we need a fully quantum description.

All the generic features discussed above find a concrete realization in the fully quantum description of black holes given by the so-called quantum N-portrait [13, 63, 67]. In the next section, we introduce the N-portrait, and outline its main characteristics.

2.1.4 The quantum N-portrait

The quantum N-portrait is a microscopical quantum description of a black hole, proposed by Dvali and Gomez in [13]. Here, we discuss the basic features following the original papers [13–15], and explain the implications for the semiclassical puzzles that were hinted at in the section above.

The starting point of the N-portrait is Einsteinian gravity as an effective field theory (EFT). Let us observe that large black holes, at least at the scale of the horizon, are fully in a weakly curved regime of gravity. This implies that the dimensionless quantum coupling that controls the gravitational interactions,

$$\alpha_{gr} \sim \frac{p^2}{M_{\rm pl}^2}\,, \tag{2.17}$$

is much smaller than one. Therefore, we are fully within the EFT regime of validity (with one small caveat for the modes responsible for the entropy, which we will discuss later). As a consequence, irrespective of the UV-completion of gravity, we should be able to describe a black hole within the degrees of freedom of the EFT itself. Since the black hole solution is a quantum state which, to a good approximation, is well-approximated at least for the early stages by the classical Schwarzschild metric, its quantum mechanical counterpart should be a multi-graviton state that in expectation value reproduces the classical metric. Obviously, in case the black hole is formed in a theory where there are also non-gravitational species, there can be subleading contributions encoding the matter constituents that created the black hole itself. Therefore, the N-portrait describes the black hole as a multiparticle state

with a large but finite occupation number of gravitons N, with typical energy set by the inverse size of the black hole,

$$E \sim \frac{1}{R}. \tag{2.18}$$

It turns out, that these gravitons form a loose bound state held together by collective interaction exactly at the moment of black hole creation. Therefore, a black hole can be seen as a condensate at the critical point of a quantum phase transition. This property allows us to describe all relevant properties in terms of the fundamental quantity N, the occupation number of gravitons. The criticality properties that emerge are exactly the ones needed to understand many black holes mysteries.

Let us now substantiate the claims above. If we consider gravitons of energy $E \sim 1/R$ for a macroscopic radius $R \gg L_{\rm pl}$, their individual pairwise interactions are extremely small. Indeed, the gravitational coupling at the relevant scale is $\alpha_{gr} \sim (L_{\rm pl}/R)^2 \ll 1$. However, we know that classical nonlinearities can still be very important also at weak coupling. At the quantum level, they emerge as collective effects from many graviton states. In these settings, we can describe interactions through a mean-field like approach, where every particle feels the collective potential generated by all the other particles. This is similar to what happens in the Hartree approximation for many-body multiparticle systems.

For a moment, let us consider a generic set of N particles of energy $E \sim 1/R$, whose interactions are controlled by a weak coupling α. These particles can form a bound state if the individual kinetic energies are balanced by the collective binding energy $E_p = \alpha N/R$ generated by the system. This leads to the condition:

$$\frac{1}{R} - \frac{\alpha N}{R} = 0\,, \tag{2.19}$$

or

$$\alpha N = 1\,. \tag{2.20}$$

Note that the bound state condition (2.20) is not specific to gravitational systems, and describes generically the condition to obtain multiparticle bound states at weak coupling. This same condition will appear again in the next section. Thanks to the weak coupling condition, we can also estimate the total energy of the bound state to be of the same order as the sum of the kinetic energies of the constituent quanta:

$$E_{\rm tot} \sim \frac{N}{R} \sim \frac{1}{\alpha R}\,. \tag{2.21}$$

Let us now focus on the gravitational case. Since gravity is coupled to the energy momentum tension, its quantum coupling is momentum dependent as discussed above. Therefore, equation (2.20) can be solved for an arbitrary radius R. This allows us to fix all the relevant quantities in terms of the parameter N:

$$E_{\rm tot} \sim M_{\rm pl}\sqrt{N}, \quad R \sim \sqrt{N}/M_{\rm pl} \sim M/M_{\rm pl}^2\,. \tag{2.22}$$

In particular, we see that the bound state condition is satisfied exactly whenever the size of the bound state coincides with the gravitational radius associated to the total energy! Therefore, we can identify the creation of a loose bound state with the process of black hole creation.

This matches exactly with a back-of-the-envelope estimation for the number of gravitons associated with a classical metric profile that matches the one of a black hole. Let us consider the classical gravitational field generated by a static source of energy $E_{\rm tot}$ and size R. It generates a gravitational potential $\phi_g(r) \sim GM/r$. By Fourier analysis, such a potential gets its dominant contribution to the energy of the system from gravitons of wavelength $\lambda \sim R$. Since the total energy is $E_{\rm tot} \sim N/R$, their number is:

$$N \sim M^2/M_{\rm pl}^2\,. \tag{2.23}$$

Again, we see that we recover eq (2.22) exactly when the size matches the gravitational radius $R \sim R_g \sim M/M_{\rm pl}^2$. Finally, we can ask what happens if one tries to add more energy to the black hole. The semiclassical intuition tells us that it should result in a black hole of a larger size. At the quantum level, this is encoded in the concept of maximal packing. Indeed, the uncertainty principle tells us that the minimal energy price to pay for localizing a quantum in a given size R is $E \sim 1/R$. Therefore, the minimal energy to localize N quanta in such a size is $E_{\rm tot} \sim N/R$. As a consequence, gravitons in a black hole are maximally packed, $N \sim MR$. This implies that every increase in the graviton number has to be accompanied by an increase in the black hole size. Finally, let us point out what the classical limit is for a black hole state in the N-portrait. It corresponds to the $N \to \infty$ limit, while keeping the radius fixed:

$$N \to \infty, \quad L_{\rm pl} \to 0, \quad R = \sqrt{N} L_{\rm pl} \ \text{ finite.} \tag{2.24}$$

Note that in this limit the entropy $S \sim N$ diverges as expected.

Now that we have established the foundations of the N-portrait, let us dive deeper into its consequences. As we discussed above, the black hole is understood as a bound state at the critical point of a phase transition. It is the property of criticality that allows us to explain the appearance of a huge number of almost gapless modes, responsible for the huge entropy.

To elucidate this aspect, we will discuss the role of criticality in a toy model of interacting bosons, introduced in [14], and then expanded in subsequent works [63, 68–70]. In the next section, we follow the original treatment. The type of phase transition that we are concerned with is a transition at a given particle number between a homogeneous state and a localized configuration. For example, in [71,72], the authors studied the vacuum structure of an attractive system of bosons on a circle. There, they showed that for a critical value of the parameters, one can develop a quantum phase transition: the ground state moves from a uniform phase to a nonuniform phase where translations are spontaneously broken, in the form af a so-called bright soliton. At the point of the phase transition, the Bogoliubov modes of the uniform phase collapse and become gapless up to $1/N$ corrections: this leads to a highly degenerate state where, thanks to criticality, it becomes extremely cheap to

excite the condensate. To illustrate, we briefly illustrate a variation of said model [14]. Let us consider the following Lagrangian of a complex scalar field in a box of size R:

$$H = L_0 \int d^3x \psi(x)^\dagger \nabla^2 \psi(x) - g \int d^3x \psi(x)^\dagger \psi(x) \psi(x)^\dagger \psi(x) \,. \tag{2.25}$$

Here, L_0 is a parameter of dimension length, and g is the (dimensionful) coupling constant. In terms of ladder operators, the Hamiltonian reads:

$$H = \sum_k k^2 a_k^\dagger a_k - \frac{1}{4}\alpha \sum_{k,p,k'} a_{k+p}^\dagger a_{k'-p}^\dagger a_k a_{k'} \,, \tag{2.26}$$

with $\alpha = 4gR^2/VL_0$. Let us study the system at a finite occupation number N. In the homogeneous phase, the ground state is a Bose-Einstein condensate of zero-momentum particles. Therefore, we can apply the Bogoliubov approximation for a_0; $a_0 = a_0^\dagger \sim \sqrt{N}$. The quadratic Hamiltonian that follows represents the excitations on top of the condensate:

$$H = \sum_{k\neq 0} \left(k^2 + \alpha N/2\right) a_k^\dagger a_k - \frac{1}{4}\alpha N \sum_{k\neq 0} \left(a_k^\dagger a_{-k}^\dagger + a_k a_{-k}\right) \,. \tag{2.27}$$

Its form is however not diagonal. Its diagonalization through a Bogoliubov transformation $a_k = u_k b_k + v_k^* b_k^\dagger$ identifies the Bogoliubov modes. In [14], it is shown that they satisfy the dispersion relation:

$$H = \sum_k \epsilon(k) b_k^\dagger b_k \tag{2.28}$$

$$\epsilon(k) = \sqrt{k^2\left(k^2 - \alpha N\right)} \,. \tag{2.29}$$

From here, we can identify the critical point at $\alpha N = 1$. Here, the first Bogoliubov mode becomes gapless and turns tachyonic for larger values of α. Correspondingly, the system undergoes a phase transition. The black hole is expected to lie exactly at a quantum critical point of this sort. The gaplessness up to $1/N$ of the first R^2 modes gives an explanation for the huge entropy: if we imagine mildly populating these modes, the combinatorics gives $S \sim N$. Note that the number of gapless modes becomes infinite in the $N \to \infty$ limit. However, at the same time, they decouple since their coupling goes as $1/N$. In subsequent works [70, 73, 74], it was clarified that the equivalent of these Bogoliubov modes for black holes are higher angular momentum modes of the black hole of Planckian energies. These modes, that in the vacuum would be extremely heavy to excite, become almost gapless in the black hole background thanks to the phenomenon of assisted gaplessness [25].

Finally, let us explain how the N-portrait addresses Hawking radiation. Recall that the black hole should be considered as a multigraviton state with N constituents of momentum $1/R$. Such constituents can rescatter among themselves, and the rescattering permits them to leave the condenstate. Each single rescattering event is strongly suppressed by the quantum coupling $\alpha^2 \sim 1/N^2$. However, at the same time, there is an enhancement due to the high multiplicity or particles involved. The total scattering rate reads:

$$\Gamma_{\rm tot} \sim N^2 \alpha^2 E \sim N^2 \frac{1}{N^2}\frac{1}{R} \sim \frac{1}{R} \,. \tag{2.30}$$

Therefore, the condensate depletes with a spectrum peaked at momentum $1/R$, with rate $1/R$. If we want to produce gravitons with a higher momentum, we would need to consider $N \to 2$ processes to accommodate for the kinematics; these processes are known to be exponentially suppressed as e^{-N}. This gives the illusion of a thermal Boltzmann-like tail. Finally, note that since gravity couples democratically to all species, analogue processes exist that can mediate the emission of quanta of every species of the theory within the allowed kinematic regime. Finally, note that the rate remains finite in the semiclassical limit $N \to \infty$. To sum up, the process of quantum depletion reproduces all aspects of the Hawking evaporation.

However, the N-portrait can do more. If we remain in the fully quantum regime at finite N, we can estimate corrections to the leading emission rate. They come from rescattering processes that involve a graviton with another constituent whose multiplicity is not enhanced by a factor of N [15]. This identifies the leading corrections as $1/N$ corrections, in accordance with the general arguments given in the previous section. Such corrections allow us to retrieve information, albeit in a macroscopically long time. The timescale of retrieval,

$$t_{\text{ret}} \sim R/N \sim RS\,, \tag{2.31}$$

is exactly the one predicted by Page (2.35).

This concludes our description of the N-portrait. In the next section, we will discuss of the above features of black hole physics can be understood in terms of the more general phenomenon of saturation.

2.2 Saturation in QFT

In the previous section, we discussed the main features of semiclassical and quantum black holes. In particular, we showed how a huge entropy emerged for a black hole, which has the form of an area law. Moreover, we discussed how in a quantum model of a black hole, the N-portrait, such entropy can be understood as emerging from the existence of a huge number of gapless modes up to $1/S$, supported on the black hole. All of this brought us a long way; however, there are still some questions that one could imagine asking. Some may seem unique from the context of black hole physics: is there any particular role that this huge entropy plays? Is there any reason at all for which it should scale as the area of the black hole in Planck units? Another set of questions, which, as we will see, are deeply connected to the first set, regards the extent of the generality of these peculiar properties of black holes. In particular, we could wonder if there are any other states, in other quantum field theoretic non-gravitational theories, that can exhibit a behaviour analogous to the one of black holes. If this were the case, then it may be possible to connect the surprising area law entropy to some deeper and more general principle.

These questions have indeed been recently discussed by Gia Dvali and collaborators [16–18]. Answering these questions resulted in the understanding of the area law as emerging from a more fundamental bound. Such a bound is valid for any quantum field theoretical object localised in a size R, and it bounds the maximal microstate entropy of said object

in terms of the relevant, dimensionless quantum coupling α of the theory:

$$S \leq \frac{1}{\alpha}\,. \tag{2.32}$$

It turns out that, whenever this absolute bound is saturated, the maximal entropy also assumes the form af an area law, expressed in units of the Goldstone decay constant of the Poincaré symmetry broken by the localisation of the object, f_P:

$$S \leq A f_P^{d-2}\,. \tag{2.33}$$

This bound is also equivalent to the Bekenstein bound (2.12). However, it turns out that the above bounds are more fundamental. There are cases where the Bekenstein bound is less stringent than the coupling and area law bound. In these cases, the theory is still inconsistent because of violations of unitarity [17]. The set of objects that saturate these bounds have been called saturons. They appear in many different non-gravitational theories [16, 18–21, 75]. In section 2.3 and in the next Chapter 3, we will discuss some examples.

The reformulation of the area law entropy bound in terms of the quantum coupling, besides its intrinsic interest, gives it a deeper meaning. As we will show, saturated objects emerge when the theory under consideration is at the boundary of perturbative unitarity. This bound can therefore be understood as emerging from the most fundamental principle of unitarity. The surprises do not stop here. One can check that, whenever a saturon exists in a given theory, it exhibits properties that are completely analogous to the ones of black holes. In particular, at the classical level such states are stable, and the maximal amount of information encoded in the modes responsible for the huge entropy becomes infinite, but its retrieval at the same time is impossible. Quantum mechanically, such states radiated with a rate completely analogous to the Hawking rate

$$\Gamma \sim \frac{1}{R}\,. \tag{2.34}$$

The information content, in full analogy with black holes, is shielded in the semiclassical limit, and quantum mechanically can be retrieved thanks to $1/S$ corrections only after a timescale that matches Page's time:

$$t_{\text{ret}} \sim SR\,. \tag{2.35}$$

One can therefore say that black holes can be interpreted as one instance of a more general universality class of objects, saturons.

The value of this point of view feeds back in both directions between quantum field theory and black holes physics. On the one hand, the phenomenon of saturation, inspired by black holes, allows us to single out new exciting phenomena. On the other hand, the study of saturons in easier, more controlled settings than quantum gravity, combined with the input given by the universality properties of saturation, can function as a powerful tool to understand new aspects of black hole physics. One instance of this is the so-called

memory burden effect [25, 26], which is associated with the later stage of the evaporation process of a saturon. It was shown how a saturon, after Page's time, dramatically changes its behaviour under evaporation. In particular, it turns out that the huge information load stored in the entropy modes resists the decay of the saturon. This results in a complete departure from the semiclassical evolution, and a system can effectively be stabilized or slow down its evaporation rate significantly. Let us remark that such a process is due to the quantum backreaction of the almost gapless modes, of pure quantum origin, on the saturon itself. As such, this type of effect requires the knowledge of the full quantum dynamics, and it is impossible to capture in a semiclassical description where the saturated state, in all its complexity, is approximated by a semiclassical profile, say the one-point function of a field operator. This type of phenomena therefore offer an opportunity to make predictions about the later stages of black hole life, which is of clear interest both theoretically and phenomenologically [27, 76–81]. Finally, the study of saturation has led to the realization of the importance of understanding the full quantum dynamics beyond many strong-field classical phenomena. This corpuscular picture has led to important results, for example in the context of the quantum exclusion of de-Sitter states [22, 23, 75], and has been extended to many non-gravitational systems [16–21, 28, 29, 31, 82–84]. In recent years, many instances of saturons have been found in different, non-gravitational theories, supporting the picture of black holes as part of a broader universality class of states [16, 19–21].

In the next section, we explain how the bounds (2.32) and (2.33) emerge in a generic quantum field theoretic setting from the requirement of unitarity.

2.2.1 Entropy bounds and unitarity

Let us now discuss how we can obtain the bound (2.32). We will mainly follow the treatment given in [17]. To understand the connection between highly entropic objects and unitarity bounds, let us focus on a general quantum field theoretic example. We consider, without loss of generality, a scalar field with attractive interactions, controlled by a quantum coupling α. We shall focus on multi-particle states of such a theory, with a large occupation number n. Moreover, we shall endow the field with some highly degenerate quantum numbers, in quantity N. For example, we could think about a scalar field in the fundamental representation of a large flavour group $SU(N)$, with quartic self-interactions. Furthermore, let us consider n quanta of the given field. Let us define both the 't Hooft coupling $\lambda_t := N\alpha$, which controls the loop expansion of the theory, and the collective coupling $\lambda_c := n\alpha$, which controls the strength of the collective interaction of the n quanta.

There are two key observations that we shall make. The first one is that there's a price to pay to create a bound state of n fundamental quanta at a given size R, held together by collective interaction, while remaining at weak coupling. In particular, for the quanta to generate collective effects strong enough to hold themselves together, their number needs to satisfy the self-sustainability condition

$$n\alpha = 1\,. \tag{2.36}$$

We can understand such a condition by imagining a mean field approximation, valid for a

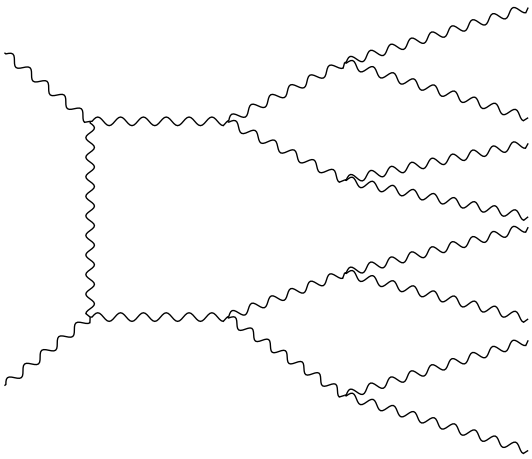

Figure 2.3: A $2 \to n$ scattering process at tree level.

large number of constituents $n \gg 1$. In this framework, a bound state originates when the kinetic energy $E \sim 1/R$ of a single quantum balances the collective potential $V \sim \alpha n/R$, leading to the condition (2.36). Note that this is exactly the condition imposed in the N-portrait at the threshold for black hole formation. Let us observe that a similar relation is also satisfied by solitons and other "non-perturbative" configurations at weak coupling.

The second observation is that, once a bound state is formed, it will participate as a, possibly approximate, asymptotic state in the S matrix of the theory. Therefore, we shall ask ourselves what the probability is of creating such an object in a scattering process. For simplicity, we will consider a 2-particle scattering. At first sight, it looks like a $2 \to n$ process needed to create a bound state of this kind gives a completely negligible contribution. Indeed, one can generically prove that a $2 \to n$ process is inevitably suppressed at large n by the non-perturbative factor [85–89]:

$$\sigma_{2\to n} \sim e^{-n} \,. \tag{2.37}$$

Let us prove the bound above. Perturbatively, a process like the one above requires a number of vertices of at least order n. Therefore, it may seem that the amplitude explodes due to the multiplicity of the Feynman diagrams:

$$\sigma_{2\to n} \sim \alpha^n n! \,. \tag{2.38}$$

However, we shall recall that the perturbative series is asymptotic Therefore, its regime of validity is limited to the point where successive contributions start diverging. Moreover, the series better approximates its real, nonperturbative value when it is summed up to the point of optimal truncation. Such a point can be estimated by imposing the stationarity of (2.38) with respect to n. This happens when:

$$\alpha n = 1 \,. \tag{2.39}$$

Consequently, for a $2 \to n$ process at the limit of perturbative unitarity, the amplitude is exactly controlled by the point of maximal truncation. By evaluating (2.38), and using the Stirling approximation, one recovers (2.37). Notice that this is an upper bound; the nonperturbative value could receive further suppressions.

Given all of the above, the natural question to ask is whether there is any way in which such a ridiculously small probability can be enhanced to the point where such a bound state can be produced with an order one probability. We shall show that this happens exactly when the 't Hooft coupling of the theory is of order one. The corresponding bound state is the saturon. The enhancement comes through the means of a large entropy. Indeed, even if each single instance of the saturon is highly suppressed, the total production rate needs to weigh in the enhancement coming from the different configurations of the same saturon, namely, its microstate entropy S.

Let us now estimate such an entropy. In the setting discussed above, the saturon is a bound state of n constituents, each of which can come in N different, degenerate flavours. For example, let us consider for definiteness a classical profile $\phi^i_{cl}(x)$ representing the bound state, where i is some internal index. One can imagine it as a coherent state[1] with constituents of typical momentum $k \sim 1/R$, of the form:

$$\exp\left[\int dk \sqrt{2E_k}\phi^i_{cl}(k) a^{i\dagger}_k\right]|0\rangle = \exp\left[\int dk \sqrt{n^i_k} a^{i\dagger}_k\right]|0\rangle\,. \tag{2.40}$$

Therefore, our bound state will live in the large fully symmetric representation of n tensor products of the internal symmetry group. In large N, the degeneracy of states $n_{\rm st}$ is

$$n_{\rm st} \simeq \binom{n+N}{N}\,. \tag{2.41}$$

By using the self-sustainability condition (2.36), one can write the entropy in terms of the 't Hooft coupling:

$$S = \ln\left(n_{\rm st}\right) \simeq \frac{1}{\alpha}\ln\left((1+\lambda_t)\left(1+\frac{1}{\lambda_t}\right)^{\lambda_t}\right)\,. \tag{2.42}$$

We observe that, when

$$\lambda_t \sim \alpha N \sim 1, \tag{2.43}$$

the entropy reaches the value $S \sim 1/\alpha$. Therefore, the probability of producing a saturon in a scattering process becomes of order 1:

$$\sigma_{2\to n} \sim e^{-1/\alpha} e^{1/\alpha} \sim 1\,. \tag{2.44}$$

If the entropy were to increase any further, unitarity would be violated nonperturbatively. Notice that a resummation of perturbative diagrams cannot cure this violation, since the

[1] As we will discuss in Chapter 4, strictly speaking, such a state would require appropriate dressing. We shall not enter here in these subtleties.

latter arises from a fully nonperturbative production probability. We can then state the absolute bound on microstate entropy for a localized object:

$$S \leq \frac{1}{\alpha}\,. \tag{2.45}$$

This is saturated when both the 't Hooft coupling and the collective coupling of the state are of order 1, $N \sim n \sim 1/\alpha$.

At the same time, we can show that the entropy takes the form of an area law, in units of the decay constant of the broken Poincaré symmetry f_P. Indeed, any object that is localized in space breaks translational invariance with a strength

$$f_P = \frac{1}{R\sqrt{\alpha}} = \frac{\sqrt{N}}{R}\,. \tag{2.46}$$

It is immediately clear that at saturation, we obtain

$$S \leq R^2 f_P^2\,. \tag{2.47}$$

The connection with the inverse coupling bound is explained by the fact that the decay constant enters into the definition of the quantum coupling of the modes that break Poincaré symmetry spontaneously. The dimensionless coupling for such a mode is momentum dependent as p^2/f_P^2, with a momentum $p \sim 1/R$ of the order of the inverse size of the saturon. Therefore, the relevant quantum coupling for such a mode scales as an area, from which the bound follows. Notice that in the saturation limit the same decay constant controls also the coupling α_G of the entropy modes, which in our example emerge as Goldstone excitations of the global symmetry $SU(N)$, through the scale of the breaking of the internal symmetry $f_G = f_P$.

Next, we can remark on the role of black holes in this picture. Black holes are the prototypical example of a saturon. By the discussion in section 2.1.4, they saturate both the coupling bound (2.32) and the area law. In particular, notice that since at the horizon black holes break Poincaré symmetry at the Planck scale, $\langle h_{\mu\nu}\rangle \sim M_{pl}$, the area law is in complete accordance with the general form (2.33). Moving to their connection to unitarity, normally one assumes that, for every trans-Planckian scattering process in a quantum gravitational theory, the dominant channel is black hole production. This follows directly from the generic principle that every process in which a given energy is localized in a size smaller than the corresponding Schwarzschild radius produces a black hole, as discussed in the previous section. Nevertheless, from a microscopic point of view, the actual realization of such a process may seem mysterious. For example, one could wonder how it is possible that a two-graviton scattering, albeit sufficiently energetic, could produce a huge, classical object like a macroscopic black hole. This discussion clarifies how this can happen: the $2 \to N$ graviton process needed to create a black hole is enhanced thanks to the entropy of the black hole. This is further supported by explicit calculations both in the effective field theory and string theory [90]. This clarifies the paramount role of the black hole entropy

in appropriately enhancing the production process in order to overcome the exponentially suppressed probability: the circle closes.

Finally, we point out that black holes play a peculiar role in gravity, compared to other theories that admit saturons. In particular, let us consider the self-sustainability condition (2.36). In a renormalizable theory, the coupling runs only logarithmically. Therefore, equation (2.36), together with the condition (2.43) on the 't Hooft coupling, determines the momentum scale at which unitarity is saturated, and consequently the size and energy of the saturon. In particular, in these cases, saturons appear only at a very specific kinematic window. It can be shown that, correspondingly, the saturation of scattering amplitudes through saturon production happens only as a narrow resonance of width α.

For gravity, this is fundamentally different. Here, the quantum coupling is itself momentum dependent. Thus, we can obtain saturated states for an arbitrary size. In other words, gravity admits a (quasi)-continuum spectrum of saturons. This remarkable property is essential to clarify the role that black holes play in unitarizing the high-energy behaviour of quantum gravity. In gravity, high-energy, trans-Planckian physics is shielded by black hole creation [10, 91, 92]. Namely, the theory protects itself from violating unitarity in the deep UV by trading high energy quanta for high multiplicity, low energy classical states, in the form of larger and larger black holes. In other words, scattering trans-Planckian gravitons (or any other particle) can only produce a larger and larger, more classical black hole. Since the latter are controlled by IR physics, they are under full control and preserve unitarity. This shows how black holes make the UV-IR correspondence possible, and in doing so unitarize the theory. Theories of this kind are named classicalizing theories, after [10].

2.2.2 Evaporation and information retrieval

We have seen that generic saturons have information properties in all aspects similar to those of black holes. Now, we discuss how they behave with respect to the possible retrieval of this information. The upshot is that even in this aspect, their behavior is analogous to black holes. Let us begin with the analogue of the semiclassical Hawking limit. In our setting, this corresponds to sending:

$$\alpha \to 0, \;\; N \to \infty, \;\; \lambda_t = 1 \text{ finite}. \tag{2.48}$$

In this limit, the entropy of a saturon becomes infinite. At the same time, the quantum coupling α_G that controls the interaction of the memory modes responsible for the entropy vanishes, $\alpha_G \sim 1/(f_G R)^2 \to 0$. Therefore, the information patterns become unreadable for a classical observer. Notice that the theory remains interacting, since the collective coupling remains nonzero in this limit. However, all the interactions become insensitive to all the modes whose excitation levels do not scale appropriately with N. In this limit, if an appropriate channel allows it, the saturon can decay. Its decay rate is completely analogous to that of a black hole:

$$\Gamma \sim \frac{1}{R}\,. \tag{2.49}$$

The reason for this behaviour also strictly follows the analogue discussion made for the N-portrait in 2.1.4. Namely, the evaporation is the result of a rescattering of constituents of momentum $1/R$ at weak coupling α, enhanced by the multiplicity N^2 of pairs of the saturon. Therefore, $\Gamma \sim \alpha^2 N^2/R \sim 1/R$.

In order to efficiently retrieve the information content of the saturon, we need to relax the semiclassical limit and keep both N and α finite. The information can thus be retrieved through $1/N \sim 1/S$ corrections to the leading order process in N. The information retrieval time matches the Page's time for black holes:

$$t_{\text{ret}} \sim RS\,. \tag{2.50}$$

Notice that the same $1/\alpha$ correction that leads to a finite timescale for the extraction of information can be interpreted in terms of the quantum coupling of the memory modes responsible for the saturon entropy.

With this, the discussion on the general properties of saturated systems is complete. As we have shown, it turns out that saturons exhibit properties completely analogous to those of black holes. This shed new light both on black hole physics and on the phenomenon of saturation itself. In the next section, we proceed by briefly summarizing two examples of saturons in large-N, renormalizable theories. Then, in the next Chapter 3, we will focus on a third $1+1$ dimensional example in great detail, to demonstrate explicitly how such properties arise in a concrete example.

2.3 Two examples of a saturon in large-N theories

Up to now, we have only discussed saturated states in general terms. In this section, we will give two concrete examples in calculable theories. For both, the power of large-N physics is instrumental in creating the necessary conditions for a saturon to emerge.

2.3.1 Saturons in Gross-Neveu

As a first example, let us report here about the findings of [19]. In 2021, Dvali and Sakhelashvili observed that a saturon can be found even in an integrable theory, namely the Gross-Neveu model at large N. We have already presented the basics of the model in section 1.2. Here, we just follow the original work and we detail the saturon characteristics. Let us recall that in the Gross-Neveu model there is a tower of bound states (1.80) labelled by an integer $n = 1...N$. Moreover, their multiplicity is given by (1.81). It turns out that the maximally entropic bound state is the one lying in the top multiplet, with $n = N$. Its entropy scales as

$$S \sim 2N\,, \tag{2.51}$$

up to logarithmic factors. It can be shown that, while the mass of such a bound state scales with the fermion mass as Nm_f in large-N, its size remains N-independent and is set by the fermion mass.

$$R \sim 1/m_f\,. \tag{2.52}$$

Now, recall that the 't Hooft coupling is $\lambda = \alpha N$. Moreover, the phenomenon of dimensional transmutation tells us that it becomes of order one at the scale of the fermion mass, which is exactly the scale associated with the localization of the bound state under consideration. This is the defining relation for the entropy of a saturon: since at the relevant scale 't Hooft coupling is of order one, the bound state saturates the coupling bound (2.32). At the same time, the entropy follows an area law. To clarify it, observe that the scale of Poincaré symmetry breaking in d dimensions is

$$f_P \sim N/R^{(d-2)} \,. \tag{2.53}$$

Therefore, in $1+1$ dimensions, the area law has to be interpreted as a factor of order one, multiplying the inverse coupling N. This shows that, as expected, the area law bound (2.33) is also matched. Furthermore, Dvali and Sakhelashvili showed that the decay, in the large N, semiclassical limit, happens with a $1/R$ when allowed. To this end, they coupled the fermionic field of Gross-Neveu to an external adjoint "pion" field π_{ij} with the interaction

$$\frac{m_f}{f_\pi}\pi_{ij}\bar{\psi}_i\gamma_5\psi_j \,. \tag{2.54}$$

Taking into account that unitarity bounds the "pion" decay constant $f_\pi \sim \sqrt{N}$, they estimate the rescattering rate of two of the saturon constituents into a "pion" to obtain:

$$\Gamma \sim \frac{m_f}{f_\pi^2} g^4 N^3 \sim 1/R \,. \tag{2.55}$$

Corrections in the form of $1/N$ effects allows us to retrieve information at the timescale (2.35). This concludes the analysis, and shows that the Gross-Neveu model at large-N contains an instance of a saturon.

2.3.2 Baryons in large-N QCD

The second example we want to discuss is the one of baryons in large-N QCD. We shall show how, in a specific limit connected to the saturation of unitarity, baryons are perfect examples of saturons.

QCD in large-N has been famously introduced by 't Hooft [50,93], who first considered the number of colours $N_c := N$ as an ideal expansion parameter for non-abelian gauge theories. We shall see that, in order to build a connection with saturation, we will later need to consider the Veneziano limit [94], where the number of flavours N_f is also large $N_f \sim N_c \sim N$. The advantage of the large-N limit is similar in spirit to the one that we explained for the Gross-Neveu model in 1.2. One trades a large number of degrees of freedom for a theory that becomes "semiclassical" in spirit. Here, we do not give a full treatment of QCD at large N, since it would be beyond the scope of the current thesis. However, we feel it may be interesting to briefly state its basic properties, before focusing on the Baryon spectrum.

As 't Hooft showed in his seminar paper [50], the perturbative expansion in large-N is organized in the form of a topological expansion. The theory is dominated by planar diagrams, while diagrams of more complicated topologies get additional suppression of $1/N$ in powers of the genus of the Riemann surface where they lie.

This very characteristic property allows for the extraction of a great deal of information on the theory [50, 95, 96]. In particular, it turns out that

- In the $N \to \infty$ limit, the theory is a free theory of mesons and glueballs.
- The particles are infinite in number.
- At finite but large N the heavy glueballs have decay rates suppressed by $1/N$, and interactions suppressed by $1/N^2$. Mesons have decay rates suppressed by $1/\sqrt{N}$, and interactions suppressed by $1/N$.
- Chiral symmetry is spontaneously broken. The pion decay constant f_π scales with N (in units of Λ_{QCD}) as $\sqrt{N}$ [95, 97].

Large-N QCD admits also baryonic states, whose nature we will discuss now. It turns out that, in the Veneziano limit, baryons in large N are perfect examples of saturons [16,17]. Compared to their $N = 3$ relatives, baryons in large-N share many similarities, but also notable differences. In particular, in large-N baryons are semiclassical, multiparticle states. This can be understood from the fact that color confinement implies that baryons need to be completely antisymmetric in color. Therefore, they need to be built by N quarks. Moreover, since they are fully antisymmetrized in the color indices, their spatial wavefunctions are symmetric. Their multiparticle nature makes them perfect candidates for an analysis based on a mean-field approach. Indeed, Witten showed [95] that they can be understood in a Hartree approximation, where each constituent interacts with the collective potential of all the others. This has several immediate consequences:

- As expected from the analysis above, their mass scales as N in units of Λ_{QCD}.
- Their size, however, remains constant in N and set by $R_b \sim \Lambda_{QCD}^{-1}$.
- The baryon baryon scattering rate scales as N thanks to the multiplicity of the baryon constituents. Taking into account that the mass also scales as N, this results in a finite scattering rate.
- The baryon anti-baryon production rate from meson meson scattering is exponentially suppressed non-perturbatively as e^{-N}. This follows generally from the multiparticle nature of baryons, analogously to what has been discussed in section 2.2.1.

Moreover, it is interesting to note that baryons in large-N have a representation in the chiral effective theory as topological solitons, the so-called Skyrmions [95, 98, 99].

To connect baryons to saturation, we need to endow them with the necessary entropy. Therefore, we shall consider the limit of a large number of flavours $N_f \gg 1$. This greatly

enhances the baryonic degeneracy n_{states}, since baryons transform as a symmetric tensor of rank N_f [16, 17]:

$$n_{\text{states}} \sim \binom{N_c + N_f - 1}{N_f}. \tag{2.56}$$

If we introduce the 't Hooft couplings for both flavours and colour numbers $\lambda_f \sim g^2 N_f$ and $\lambda_c \sim g^2 N_c$, the entropy goes as [17]:

$$S \simeq \frac{1}{g^2} \ln \left[\left(1 + \frac{\lambda_c}{\lambda_F}\right)^{\lambda_F} \left(1 + \frac{\lambda_F}{\lambda_c}\right)^{\lambda_c} \right] . \tag{2.57}$$

Such an entropy saturates the coupling bound (2.32) exactly when the number of flavours matches the number of colours $N_f \sim N_c \sim N$. This is precisely the unitarity limit for the theory, since for $N_c \lesssim N_f$ the beta function changes sign, and the theory loses asymptotic freedom. Therefore, baryons at the unitarity limit are saturons. Notice that the entropy is such that it balances the exponential suppression for meson-meson scattering into baryon/anti-baryon. Thus, in the same limit, one can expect a saturation of the meson cross-section at the scale $R_b \sim \Lambda_{QCD}^{-1}$ by baryon pairs. At the same time, the baryons satisfy the area law form of the bound (2.33). Taking into account the baryon size and the scaling of the pion decay constant, we get

$$S = (R_b f_\pi)^2 , \tag{2.58}$$

which is precisely the area of the baryon in units of the appropriate decay constant. To conclude, we have shown that large-N QCD offers us another textbook example of saturated states. In the next Chapter, we will study in great detail another fully controllable saturon in a $1+1$ dimensional theory, with particular emphasis on its evaporation properties.

Chapter 3

A model of a saturated soliton and its evaporation

In this chapter, following [2], we discuss in great detail a specific example of a saturon in a renormalizable $1+1$ dimensional theory. This theory, first studied in its $3+1$ dimensional version in [20], allows us, thanks to its simplicity, to demonstrate all the properties discussed in the previous chapter in a fully controlled manner. In particular, after having proven that the theory under consideration actually contains a saturon in the form of a thick-wall bubble, and having exhibited all its characteristic features, we will focus on retrieving the Hawking-like evaporation rate (2.34). Thanks to the simplified setting, we shall be able to calculate the evaporation rate for a generic bubble both semiclassically, in an analogue of the Hawking computation, as well as in a fully quantum mechanical approach. Namely, in the first approach, we consider the saturon as a fixed background sourcing particles, in a zero backreaction limit. In the latter, we resolve the saturon as a fully quantum multiparticle state, and we obtain its evaporation rate from the quantum decay process of its constituent quanta. In both cases, we shall obtain analytical results, that match in the appropriate limit. This constitutes a strong support both for the general phenomenon of saturation, and for the corpuscular picture of a black hole given by the N-portrait. Finally, thanks to the quantum picture, we shall discuss corrections to the semiclassical behaviour.

3.1 A model of a saturon

3.1.1 The classical soliton

The model under consideration is the one of a vacuum bubble originally introduced in [17], and then studied in depth in its stabilized version in [20].

The theory is defined by the following Lagrangian:

$$\mathcal{L} = \frac{1}{2}\,\mathrm{tr}\left[(\partial_\mu \Phi)\,(\partial^\mu \Phi)\right] - V[\Phi] \tag{3.1}$$

$$V[\Phi] = \frac{\alpha}{2}\,\mathrm{tr}\left[\left(f\Phi - \Phi^2 + \frac{I}{N}\,\mathrm{tr}\left[\Phi^2\right]\right)^2\right], \tag{3.2}$$

where Φ is a scalar field in the adjoint representation of the $SU(N)$-group. Since we are in $1+1$ space-time dimensions, Φ and f are dimensionless, while the parameter α has dimensionality of $[\mathrm{mass}]^2$. We shall denote the dimensionless coupling as $\tilde{\alpha}$:

$$\tilde{\alpha} \equiv \frac{\alpha}{m^2} = \frac{1}{f^2}\,. \tag{3.3}$$

We shall work in the limit of large N and large f. This is a weak quantum coupling regime. At large N we also define the collective ('t Hooft) coupling as $\lambda := N/f^2$. The coupling is bounded by unitarity as

$$N/f^2 \lesssim 1\,. \tag{3.4}$$

To obtain saturated states, we shall consider the theory close to the unitarity bound for the collective 't Hooft coupling.

The potential (3.2) admits the $SU(N)$-invariant vacuum, together with a family of degenerate vacua where the $SU(N)$ symmetry undergoes spontaneous symmetry breaking to maximal subgroups of the form $SU(N-K)\times SU(K)\times U(1)$, with $0<K<N$. Here, we will examine two nearby cases: the symmetric $SU(N)$ vacuum and the vacuum in which the symmetry is broken to $SU(N-1)\times U(1)$. While in the former the field v.e.v is obviously zero, in the latter the field gets a v.e.v. given by

$$\Phi^\beta_\alpha = \frac{f}{\sqrt{N(N-1)}}\,\mathrm{diag}((N-1),-1,\ldots,-1)\,. \tag{3.5}$$

Notice that in the $SU(N)$-symmetric vacuum, all excitations are massive, with a mass $m\sim\sqrt{\alpha}f$. In contrast, the $SU(N-1)\times U(1)$ vacuum hosts $2N$ gapless Goldstone degrees of freedom.

The theory supports vacuum bubble solutions connecting the two vacua, separated by a wall of thickness of order m^{-1}.

In $1+1$ dimensions, a bubble corresponds to a kink and an antikink positioned a distance $2L$ apart. In the limit of infinite separation, a kink (or antikink) centered at $x=0$ has the form

$$\phi(x) = \frac{f}{2}\left(1 \pm \tanh\left(\frac{mx}{2}\right)\right), \tag{3.6}$$

while its energy is

$$E_k = \frac{1}{6}\frac{m^3}{\alpha} = \frac{1}{6}\frac{m}{\tilde{\alpha}}\,. \tag{3.7}$$

We consider bubbles where the interior is in the broken-symmetry vacuum while the exterior remains in the symmetric one. For $L \gg m^{-1}$, the field profile approaches $\phi(x) \simeq f$ inside ($|x| < L$) and $\phi(x) = 0$ outside ($|x| > L$). The bubble core thus contains the $2N$ massless Goldstone excitation species mentioned above. If none of these modes are present, a bubble of finite size is unstable: the kink and antikink attract and eventually annihilate. On the other hand, if the Goldstone species are populated the bubble can be stabilized, as shown in [20]. Stable bubbles are given by the following profiles:

$$\Phi_\alpha^\beta = \left(U^\dagger V U\right)_\alpha^\beta \tag{3.8}$$

$$U(t) = \exp\left[-\mathrm{i}\theta^a(t)T^a\right] \tag{3.9}$$

$$V_\alpha^\beta(x) = \frac{\phi(x)}{\sqrt{N(N-1)}}\,\mathrm{diag}((N-1), -1, \ldots, -1)\,, \tag{3.10}$$

where T^a are the $SU(N)$ generators, and both the time-independent profile $\phi(x)$ and the time-dependent Goldstone field $\theta(t)$ satisfy appropriate equations. In particular, $\phi(x)$ is a profile interpolating between different vacua inside and outside of the bubble, while $\theta(t)$ represents a rotation in the internal flavour space of the bubble, which makes the solution charged under $SU(N)$.

If we specialize, without loss of generality, the ansatz (3.8) to a single-flavour uniform rotation, $\theta^a = \delta_1^a \omega t$, and we insert into the Lagrangian, the bubble profile ϕ solves the effective equation

$$\partial_x^2\phi + \mathcal{V}'(\phi) = 0\,, \tag{3.11}$$

where

$$\mathcal{V}(\phi) = \frac{1}{2}\phi^2\left(\omega^2 - \alpha(\phi - f)^2\right)\,. \tag{3.12}$$

Stationarity is specified by $\phi(0) = \phi_0 \neq 0$, with $\phi'(0) = 0$, and the asymptotic condition $\phi(x) \to 0$ as $|x| \to \infty$.

To prove that such a solution exists, in the $3+1$ dimensional model, Dvali, Valbuena and Kaikov [20] proceeded along the lines of the undershoot-overshoot argument given by Coleman for the Q-ball case, which we discussed in section 1.3 of chapter 1. Here, we adapt such an argument to the $1+1$ dimensional problem. Thanks to the lower dimensionality, it is possible to obtain analytical profiles for the bubble solutions, similarly to the two-dimensional Q-balls discussed in [53].

Interpreting x as a fake "time" maps the problem to a particle with coordinate ϕ moving in the potential (3.12). For $\omega^2/\alpha f^2 < 1$ (or, equivalently, for $\omega^2 < m^2$), the above potential has two maxima, $\phi = 0$ and $\phi_{\max} = \frac{f}{4}(3 + \sqrt{1 + \frac{8\omega^2}{\alpha f^2}})$, separated by a minimum at $\phi_{\min} = \frac{f}{4}(3 - \sqrt{1 + \frac{8\omega^2}{\alpha f^2}})$. In addition to $\phi = 0$, the potential also becomes zero at the points $\phi_0 = f \pm \frac{\omega}{\sqrt{\alpha}}$.

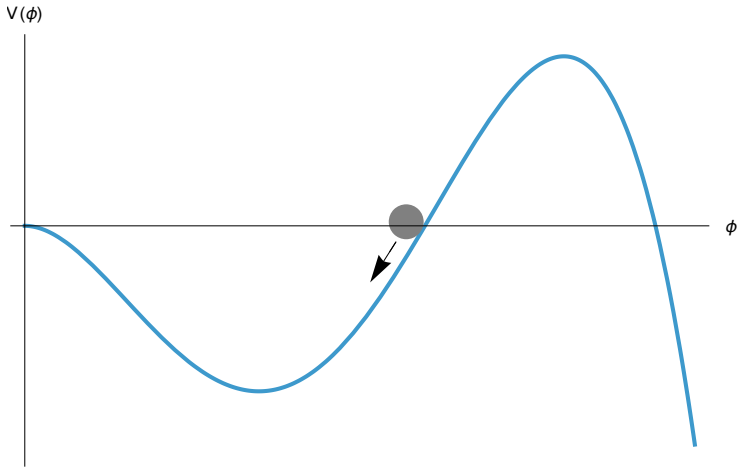

Figure 3.1: The effective potential for the ϕ field. The bubble solution corresponds to the field rolling down from the zero value at "time" $r = \infty$ to the finite value ϕ_0 at "time" $r = 0$, and back to $\phi = 0$.

Within this parameter range the motion is that of a bounce: from rest at $\phi = 0$ at $x = -\infty$, the trajectory rolls down, climbs to $\phi_0 = f - \frac{\omega}{\sqrt{\alpha}}$, stops, and goes back to $\phi = 0$ as $x \to +\infty$. The turning point

$$\phi_0 = f\left(1 - \frac{\omega}{f\sqrt{\alpha}}\right) \tag{3.13}$$

fixes the v.e.v. of the field at the center of the bubble, therefore, its height. Also, the bubble size R is the effective "time" of the complete trip, which in turn is set by ω.

In the limit $\omega \to 0$, the bounce point becomes the maximum, $\phi_0 = \phi_{\max} = f$, and the particle remains there for an infinite duration before returning. Consequently, the kink and anti-kink are at infinite distance, and the bubble becomes a superposition of a kink and anti-kink with an infinite size $R \to \infty$.

To sum up, choosing a certain frequency ω for the Goldstones in the bubble interior uniquely fixes the size R and the height ϕ_0 of the bubble profile as in (3.13). Also, the $SU(N)$-charge of the bubble is given by

$$Q = \int dx(\phi_b(x))^2\,\omega\,. \tag{3.14}$$

In the $1+1$ dimensional case, for $\omega \to 0$ the size of the stationary bubble R increases only logarithmically. Namely, in the thin-wall approximation $m \gg \omega$, we have

$$R \sim \frac{1}{m}\ln\left(\frac{m}{\omega}\right)\,. \tag{3.15}$$

We can understand this behaviour since, in the thin-wall approximation, the bubble size (3.15) can be found by extremizing the R-dependent potential energy

$$V(R) = \frac{1}{2}Rf^2\omega^2 - 2E_k e^{-mR}, \tag{3.16}$$

subject to the fixed charge constraint, which in the thin-wall regime implies $f^2 R\omega \simeq Q$. The second term in the potential comes from the attractive force between a kink and an anti-kink, which in $1+1$ dimensions is suppressed exponentially. This is in contrast with the $3+1$ dimensional bubble studied in [20], where the size goes quadratically with the inverse frequency.

Thus, in the thin-wall limit, $\phi_0 \simeq f$. Moreover, we have

$$R\omega \sim \frac{\omega}{m} \ln\left(\frac{m}{\omega}\right) \ll 1 \tag{3.17}$$

and

$$\frac{\omega}{\phi_0} \ll \sqrt{\alpha}\,. \tag{3.18}$$

For thick-wall bubbles, on the other hand, all the scales in the game become comparable. Such bubbles are characterized by $\omega \sim m$, $R\omega \sim 1$ and $\phi_0 < f$.

Thanks to the low dimensionality, we can do more: the bubble profile $\phi_b(x)$ can be obtained analytically. This follows from the existence of an integral of motion similar to the one coming from the Bogomolny bound in the case of the kink, discussed in section 1.1.1. Indeed, the bubble profile satisfies the first-order equation:

$$d_x\phi_b = \sqrt{-2\mathcal{V}(\phi_b)}\,. \tag{3.19}$$

which can be integrated explicitly to obtain [1]:

$$\phi_b(r) = \frac{m-\omega}{\sqrt{\alpha}} \left(\frac{m+\omega}{m+\omega\cosh\left(\sqrt{m^2-\omega^2}r\right)} \right)\,. \tag{3.20}$$

Correspondingly, the energy of the bubble is

$$E_b = \int_{-\infty}^{\infty} (d_x\phi_b)^2\,, \tag{3.21}$$

which, after integration, leads to

$$E_b = -\frac{2}{3}mf^2\left(1-\frac{\omega^2}{m^2}\right)^{3/2} + mf^2\sqrt{1-\frac{\omega^2}{m^2}} + \\ + \frac{\omega^2 f^2}{m}\ln\left(\frac{m}{\omega} - \frac{m}{\omega}\sqrt{1-\frac{\omega^2}{m^2}}\right)\,. \tag{3.22}$$

In the thin-wall limit ($\omega/m \to 0$) this energy is equal to twice the energy of a static kink (3.7),

$$E_b \simeq 2E_k \simeq \frac{1}{3}\sqrt{\alpha}f^3 = \frac{1}{3}\frac{m}{\tilde{\alpha}}\,, \tag{3.23}$$

as expected from the previous discussion. However, the order of magnitude of the energy also stays the same in the thick-wall limit $\omega \sim m$.

[1] In a different context, this solution was previously obtained by Juan Sebastián Valbuena Bermúdez. We thank him for sharing it.

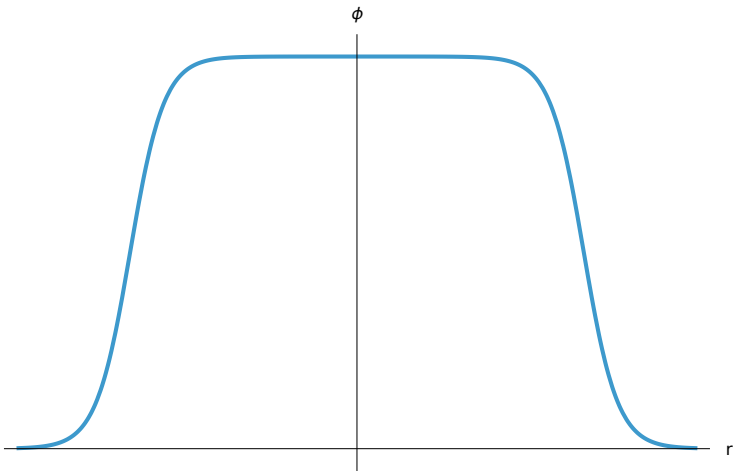

Figure 3.2: The bubble profile for the ϕ field.

3.1.2 The Goldstone modes

It is of great importance for connecting the bubble to the phenomenon of saturation, to analyze its gapless excitations. They originate from the symmetries broken by the bubble itself, namely, Poincaré symmetry and the internal $SU(N)$ symmetry. We shall discuss both of them.

Breaking of Poincaré symmetry

The breaking of translational invariance is described by a translation modulus $\eta(t)$, which corresponds to an infinitesimal translation of the bubble without a change in its shape. This is completely analogous to the case of the kink discussed in section 1.1.2. Its profile follows from differentiating the background:

$$\phi_b(x+\eta(t)) = \phi_b(x) + (\partial_x \phi_b(x))\,\eta(t) \quad + \ldots . \tag{3.24}$$

The mode's norm is

$$\mathcal{N}_\eta = \int_{-\infty}^{\infty} (\partial_x \phi_b)^2 \,, \tag{3.25}$$

and, combined with the size R, sets the Poincaré-breaking scale as in 1.1.2:

$$f_P^2 = \mathcal{N}_\eta R \sim \frac{(mR)}{\tilde{\alpha}} = (mR)\, f^2 \,. \tag{3.26}$$

Breaking of the internal symmetries

Now, we focus on the $SU(N)$ Goldstone modes. To this end, without loss of generality, we parametrize a rotation along one of the broken generators with $\theta(x_\mu)$. The resulting mode has the effective action:

$$S_\theta = \int d^2x \phi_b^2(x)(\partial_\mu \theta)^2 \,. \tag{3.27}$$

To analyze the modes, we decompose the field using separation of variables:

$$\theta(x,t) = \sum_k \Theta_k(x)\zeta_k(t)\,, \tag{3.28}$$

where the time amplitudes satisfy $\ddot{\zeta} = -k^2\zeta$. The spatial modes therefore obey the equation:

$$\Theta_k'' + 2\frac{\phi_b'}{\phi_b}\Theta_k' + k^2\Theta_k = 0\,, \tag{3.29}$$

with prime denoting ∂_x.

We can observe that a normalized zero mode exists at $k = 0$:

$$\Theta_0 = \left(\int dx \phi_b^2(x)\right)^{-\frac{1}{2}} \equiv \frac{1}{\sqrt{\mathcal{N}_\theta}}\,. \tag{3.30}$$

Its norm links to the bubble charge as $\mathcal{N}_\theta = Q/\omega$. Its meaning is clear: together with analogous modes for the remaining broken generators, it accounts for the $SU(N)$ flavor degeneracy, obtained by uniformly rotating the bubble in flavour space.

Notice that there is also a non-normalizable $k = 0$ solution [100]:

$$\tilde{\Theta}(x) = \int_0^x \frac{dy}{\phi_b^2(y)}\,, \tag{3.31}$$

for which $\int_0^{+\infty} dx \phi_b^2 \tilde{\Theta}_0^2 = \infty$. Obviously, such a mode is nonphysical.

Let us remark that in the thick-wall regime, $(mR) \sim 1$, the scales of Poincaré and $SU(N)$ breaking match. This is a crucial fact to explain the bubble's entropy saturation and its connection with the black-hole entropy.

3.1.3 An interesting non-zero mode

Among the non-zero excitations, we can identify a breathing mode, with a gap set by ω. We shall show its existence in the thin-wall limit. In this regime, the bubble is approximated by a kink and an anti-kink at a distance R. As discussed in the section above, the configuration is stabilized by a repulsive $SU(N)$ charge countering the exponentially weak attraction. Linearizing small displacements around the equilibrium point gives

$$E = 2E_k\frac{\dot{\delta}(t)^2}{2} + \frac{1}{2}\frac{\partial^2 V}{\partial L^2}\bigg|_{L=R}\delta(t)^2\,, \tag{3.32}$$

where the potential comes from the quadratic expansion of equation (3.16),

$$V(L) = \frac{1}{2}Lf^2\omega^2 - 2E_k e^{-Lm}, \tag{3.33}$$

about the minimum defined by $\partial V/\partial L = 0$, $L = R$ at fixed Q .

This expression can be understood as emerging for small velocities from its relativistic generalization

$$L_{\rm rel} = 2E_k\sqrt{1-(\dot{R})^2} - V(R)\,, \tag{3.34}$$

after an expansion for $R(t) = L + \delta(t)$.

Therefore, we have that

$$2V''(R) = -m^2E_ke^{-Rm} = -mQ^2/f^2R^2 = -mf^2\omega^2\,, \tag{3.35}$$

and the oscillations in size around the bubble minimum are controlled by: $V''(R)/E_k \sim \omega^2$. Consequently, the canonically normalized fluctuation then obeys the harmonic equation

$$\ddot{\delta}(t) + \omega_\delta^2\delta(t) = 0\,, \tag{3.36}$$

with $\omega_\delta \sim \omega$.

3.1.4 The quantum picture

Up to now, we have discussed the classical properties of the bubble. However, as argued at length in the previous chapters, any classical configuration should be interpreted as a proper quantum state in the QFT. This shall also be central in chapter 4. In particular, as discussed in section 2.2, in order to capture the phenomena relevant for saturation one is especially interested in the quantum resolution of a saturon candidate, since many of the peculiar properties are apparent only beyond the classical limit. Therefore, we dedicate this paragraph to describing the quantum resolution of the bubbles under consideration.

Quantum mechanically, as argued in 2.2, the bubble is a coherent bound state sustained by collective interactions [17,20]. In the non-stationary realization of [17], Goldstone modes remain unexcited and the state is composed chiefly of quanta of the radial degree of freedom $\phi(x)$. For the stationary configuration of [20], the case relevant here, Nambu–Goldstone modes constitute a relevant part of the state, since they play a crucial stabilizing role.

We shall consider the two constituents separately. First, we consider the radial field. Its main contribution to the total energy comes from the energy of the wall, which scales as $E_\phi \sim \int |\boldsymbol{\nabla}\phi|^2 \sim m\phi_0^2$. Each of the quanta has energy of order m, while the size of the wall sets their wavelength as m^{-1}. Therefore, their occupation number is

$$N_\phi \sim \frac{E_\phi}{m} \sim \phi_0^2\,. \tag{3.37}$$

On the other hand, the Goldstone charge is encoded in the interior Goldstone quanta, oscillating with frequency ω. The associated energy is $E_G \sim \int \dot{\phi}^2 \sim \phi_0^2\omega^2 R$. This gives an occupation number

$$N_G \sim \frac{E_G}{\omega} \sim \omega R\phi_0^2\,. \tag{3.38}$$

Using (3.14) one recovers the identity

$$N_G = Q\,, \tag{3.39}$$

as expected since the charge resides in Goldstone excitations.

For a generic bubble, we observe that

$$\frac{N_G}{N_\phi} \sim \omega R\,. \tag{3.40}$$

Consequently, in the thin-wall regime $R\omega \ll 1$, radial quanta dominate. In the thick-wall case, instead, $N_G \sim N_\phi$, implying an approximately even redistribution between radial and Goldstone constituents.

The microstate entropy of the bubble

Similarly to the case of the black hole and the other examples of saturons discussed in sections 2.1 and 2.3, a fundamental difference between the classical and quantum picture emerges in the entropy of the state. Indeed, also in our scenario, the quantum bubbles are endowed with a large, but finite entropy. As we shall shortly see, the modes responsible for this huge degeneracy have small gaps suppressed by the number of constituents, which also control the strength of their coupling. In the classical limit, at the same time, the entropy becomes infinite, and the gap vanishes, decoupling the modes.

To analyze the entropy of the bubbles, we follow the counting given in [17, 20] for the $3+1$ dimensional case, since the same logic applies essentially unchanged to bubbles in $1+1$ dimensions. This shall allow us to identify thick-wall bubbles as saturons.

The microstate degeneracy can be obtained in two equivalent ways. One is the interior viewpoint, where we understand the bubble degeneracy in terms of possible configurations of the Goldstone particles. The other is the exterior viewpoint, which observes the bubble residing in the symmetric vacuum. There, the bubble appears as a multiparticle state transforming in a large tensorial representation of $SU(N)$, so the entropy is governed by the representation's dimension. As discussed in [20], for our scenario the representation is the totally symmetric irreducible representation included in the tensor product of adjoint representations, in number equal to the total occupation number. This directly mimics, for example, the degeneracy counting of baryons in the Veneziano limit of section 2.3.2.

From the interior viewpoint, the vacuum is a Goldstone vacuum with $N_{sp} \simeq 2N$ gapless species. The fixed total occupation numberN_G can be distributed among these modes without altering the macroscopic bubble, so the states are labeled by patterns $|n_1, \ldots, n_{N_{sp}}\rangle$ summing to N_G, and the entropy becomes a combinatorial count.

Both approaches lead to the entropy [17, 20]:

$$S \sim 2N \ln \left[\left(1 + \frac{2N}{N_G}\right)^{\frac{N_G}{2N}} \left(1 + \frac{N_G}{2N}\right) \right]\,. \tag{3.41}$$

To obtain a saturated state, we shall consider the entropy above at the unitarity limit $f^2 = N$, and look for the saturation of the bounds (2.32) and (2.33). Notice that in the same limit also the occupation number of Goldstones becomes of order $N_G \sim N$. The counting of equation (3.41) shows that, at the critical 't Hooft coupling, the bound is saturated by thick-wall bubbles:

$$S \sim 2N \sim f^2 \,. \tag{3.42}$$

Thus, thick-wall bubbles at the unitarity limit are saturons.

Since saturated bubbles are thick-wall, this will be our primary regime of interest. The thin-wall case will also be analyzed, since its tractability allows precise results that we then extrapolate to the thick-wall limit.

Approximate gaplessness

We close the section on the quantum description of the bubbles with a remark on the gaplessness of the modes discussed in section 3.1.2. It is important to note that the exact gaplessness for both the translational and the "rotational" zero modes holds only in the classical limit or at infinite N. Quantum mechanically, which in our setting is equivalent to finite N and finite occupation numbers, all these modes are lifted by a tiny gap of order

$$\Delta\omega_0 \sim \frac{1}{NR} \,. \tag{3.43}$$

Such a lift is of fundamental importance and reflects the consequence of the breaking of translational invariance by the localized bubble configuration. As discussed also in section 1.1.2, such a breaking can only be exact in the classical limit. Therefore, for a localized configuration, this necessarily leads to a non-zero gap in the quantum theory.

Let us now explain how this gap can be understood for both sets of modes. For the translational mode, the solution wavepacket localized in a radius R will necessarily spread in a superposition of solitons at different locations, with a characteristic time of

$$\Delta t = \frac{1}{\Delta\omega_0} \sim NR \,. \tag{3.44}$$

This spreading lifts the gaplessness of the translation mode by (3.43). At the same time, this spread affects the spatial profiles of all other localized modes, lifting every would-be zero mode to the minimal gap set by (3.43).

In particular, the modes of broken $SU(N)$ symmetry also get lifted, since they are themselves localized on the bubble. We can understand such a lift as a spreading in the $SU(N)$ space: at finite N, since we are in a localized region set by R, the would-be degenerate "vacua" obtained by rotating the bubble are not exactly orthogonal. Consequently, their Goldstones also exhibit gaps of order (3.43). Notice that the $1/N$ gaplessness is strikingly similar to the entropy modes of black holes [15, 68], and has the same physical origin.

In thick-wall saturated bubbles, the two gaps track each other because N controls both the internal $SU(N)$ and the Poincaré sectors. On the other hand, in under-saturated cases the corresponding gaps need not to coincide: they scale with the relevant occupation numbers and localization radii. Finally, let us stress that the smallness of the gap leaves the saturation of (2.32) and (2.33) unaffected, since the entire microstate manifold lies within the energy window $\sim 1/R$.

3.1.5 Coupling to fermions

The bubble solutions that we discussed up to now are stable, both classically and quantum mechanically. Their stability is due to charge conservation, similar to the Q-ball stability discussed in section 1.3 [33, 52, 53, 55]. The decay requires exporting that charge to the exterior. However, since the exterior is the $SU(N)$-invariant vacuum, all charge carriers have a mass gap set by the mass of the fundamental particle m. Therefore, there is an unavoidable energy price to pay, which ensures stability. At the same time, the stability can be understood as an instance of the so-called memory burden effect [25, 27], as shown in [19, 20, 27]. Indeed, the charge content of the bubble is encoded in the Goldstones configurations, which, as discussed above, contain a large amount of information encoded in their almost-gapless modes. Therefore, we can understand the stability in terms of information: the bubble represents a system with a high capacity of information storage. Such information requires the existence of the bubble in order to be stored cheaply: outside of the bubble there are no gapless modes. Therefore, an eventual decay of the bubble would enforce different microstates to unload their information content in different asymptotic states. However, this creates a huge energy barrier, thereby ensuring the stability of the bubble.

In order to enable the decay of the bubble, we shall couple it to a field that can extract the Goldstone charge from the bubble interior without paying the high energy price. To this end, we couple the adjoint field ϕ to a massless fermionic field in the fundamental representation of $SU(N)$, ψ_α, via the following terms in the original Lagrangian:

$$\mathcal{L} = \mathcal{L}_\Phi + \mathrm{i}\bar{\psi}^\alpha \partial\!\!\!/ \psi_\alpha - g\bar{\psi}^\alpha \Phi^\beta_\alpha \psi_\beta \,. \tag{3.45}$$

This offers an efficient decay channel for the bubble, and, as we shall see, it leads to the bubble evaporation. The dynamics of the particle-creation process is in some aspects similar to the decay of a non-topological soliton with $U(1)$-charge discussed in [55, 101]. The goal in the present case is the understanding of the universal features of the process in the regime of saturation which, in particular, allows establishing a clear parallel with the decay of a black hole.

3.1.6 The large-N limit

In this paragraph, we want to specify the equivalent of the semiclassical limit for the bubble, and the conditions that the model should satisfy in order to preserve unitarity. We have

already discussed how the 't Hooft coupling shall remain smaller than one: $\lambda := N/f^2 \leq 1$. The introduction of fermionic fields defines an additional interaction between the fermions, mediated by the Φ field. By analyzing the $2 \to 2$ tree-level scattering among the fermionic particles, we note that it is controlled by the dimensionless coupling constant $g^2/\alpha f^2$. The corresponding 't Hooft coupling is defined and constrained as $\beta := g^2 N/\alpha f^2 \lesssim 1$.

We are now in the position to discuss the semiclassical limit. This is the $N \to \infty$ limit analogous to the one discussed in the case of baryons in large-N QCD and in Gross-Neveu in sections 2.3.2 and 2.3.1 respectively. Therefore, the double scaling limit is:

$$f^2 \sim N \to \infty \quad \frac{\alpha}{m^2} \sim \frac{g^2}{m^2} \sim \frac{1}{N} \to 0 \tag{3.46}$$

$$m^2 \sim \alpha N \; = \; \text{finite}\,. \tag{3.47}$$

In particular, this implies that the quantity $g\phi_0$, which effectively controls the strength of the interaction between the bubble and the fermionic field, remains finite, as it should. In this limit, the interactions of the theory are fully controlled by the 't Hooft couplings λ and β. Unitarity is saturated when $\lambda \sim \beta \sim 1$. This is the limit where, as shown in section 3.1.4, a thick-wall bubble becomes a saturon. Notice, that at the unitarity bound the limit $N \to \infty$ and the requirement that we keep the bubble radius R (and hence m) finite, completely determines the behaviour of the system

$$f^2 \sim N, \quad \alpha \sim \frac{m^2}{N}, \quad g^2 \sim \frac{m^2}{N}\,. \tag{3.48}$$

Notice that in full analogy to the general discussion of section 2.2, in this semiclassical limit the entropy modes decouple, and the bubble becomes an infinite reservoir of inaccessible information.

3.1.7 Analysis of the fermions-bubble system

After establishing how the theory's parameters relate in the large-N limit, we classify the interaction regimes between the bubble and the fermions. The scales that remain finite as $N \to \infty$ are the bubble size R, the frequency ω, and the effective fermion mass inside the bubble $m_\psi \sim g\phi_0$. At the unitarity bound, this mass behaves as

$$m_\psi \sim g\phi_0 \sim m\left(1 - \frac{\omega}{m}\right) = m - \omega\,. \tag{3.49}$$

For any value of the coupling, the inequality $m_\psi \leq m$ holds, and the equality is reached in the thin-wall limit stated above.

Let us first discuss thin-wall bubbles, $R\omega \sim 1$, for the various allowed values of the fermion coupling g. We have the following regimes:

- For the fermion coupling at the unitarity limit, the fermion mass inside the bubble is both larger than the Goldstone frequency: $m_\psi \sim g\phi_0 \sim m \gg \omega$, and than the inverse

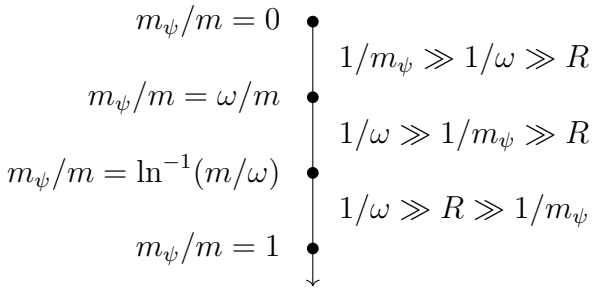

Figure 3.3: Possible regimes for a thin-wall bubble.

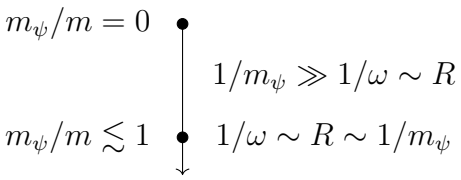

Figure 3.4: Possible regimes for a thick-wall bubble.

length $Rm_\psi \gg 1$. The latter condition follows from $Rm_\psi \sim (m_\psi/m)\ln(m/\omega) \sim \ln(m/\omega)$. This in turn implies that, for a fermion of energy of order ω, the penetration length inside the bubble, $\lambda_\psi \sim 1/m_\psi$, is also much smaller than the bubble size. In section 3.3, we shall see how this implies that the fermion production can only happen close to the boundary of the bubble.

- To proceed, we can modify the effective fermionic mass by lowering the coupling below the unitarity bound. As m_ψ decreases, when $m_\psi/m \sim \ln^{-1}(m/\omega)$, the fermion penetration length becomes larger than the bubble size: $Rm_\psi \sim 1$.
- Next, if we further decrease m_ψ, the mass becomes also smaller than the Goldstone frequency ω.

The situation is different for thick-wall bubbles, where $R\omega \sim 1$.

- Let us first consider thick-wall bubbles with the fermionic coupling at the unitarity bound. Here the effective mass is smaller, albeit of the same order, than the energy of the Goldstones: $m_\psi \sim g\phi_0 \sim m - \omega \lesssim \omega$. Therefore, fermions are almost allowed to be on shell also in the bubble core.
- By further lowering g, we enter a regime where $m_\psi \ll 1/R \sim \omega$, while R and ω of course remain of the same order.

The list above encompasses all the regimes of mutual interaction among the bubbles and the fermions. When investigating the bubble evaporation in the following section, we shall take into account the various hierarchies of scales that can appear.

3.2 The semiclassical evaporation rate

In this section, we discuss the bubble's evaporation rate, as obtained with semiclassical methods. This means that we shall consider the bubble as a fixed, rigid, background which sources fermions. This approximation becomes exact in the large-N limit (3.46), since for a bubble with an infinite number of constituents, any backreaction to an emission at a finite rate is negligible. Therefore, the bubble becomes an eternal, time-dependent background that is an infinite reservoir for fermion production. This means that for $N \to \infty$ we can consider the bubble as a good vacuum for the fermions, and quantize the fermionic fields on top of it. The time-dependent vacuum will induce an effective time dependence in the Hamiltonian for the fermions, thereby leading to particle creation.

This limit can be investigated both for thin-wall and thick-wall bubbles. Of course, the most relevant case for saturation is the one of thick-wall bubbles. However, their exact profile does not permit an analytic solution for fermionic modes. Therefore, we shall first focus on thin-wall bubbles, where the modes can be obtained analytically in the approximation of an infinitely steep wall. Afterwards, we shall extrapolate the analytic form of the spectrum to the thick-wall bubble. Obviously, by approximating a bubble with a double Heaviside Theta function-like profile, we are committing to an approximation where the validity of the calculation is restricted to the modes with a momentum $k < m$ smaller than the wall-thickness. However, the result still gives the correct parametric behaviour as a function of the relevant parameters of the theory. We will investigate the radiation of a thin-wall bubble both in the regime $g\phi_0 \ll \omega$ or in the opposite one, $g\phi_0 \gg \omega$, by an appropriate expansion in the relevant small quantity.

Now, we shall proceed to the derivation of the spectrum. Without loss of generality, we shall consider a bubble with a macroscopically occupied Goldstone mode: $\theta^a = \delta^a_1 \omega t$. In the $N \to \infty$ limit relevant for our calculation, the v.e.v of the field inside the bubble simplifies, taking the following form:

$$V^{(N\to\infty)}{}_\alpha{}^\beta(x) = \phi_b(x)\,\mathrm{diag}(1,0,\ldots,0)\,. \tag{3.50}$$

Notice that the quantity $g\phi_0$, which controls the interaction between the bubble and the fermions, remains finite in this limit. Therefore, all the quantities remain regular as well.

The origin of particle creation can be understood as the consequence of the time-dependent Hamiltonian for the fermionic fields induced by the oscillating bubble background. As it is customary, a time-dependent Hamiltonian induces a nontrivial mixing in the ladder operators, associated to the time dependence of the vacuum state in the non-trivial background. The ladder operators at early and late times are connected by a Bogoliubov transformation, whose coefficients encode the radiation rate of the bubble itself. In what follows, we shall denote the two-momentum components by $k_0 = \epsilon$ and $k_1 = k$. Also, by flavour symmetry, the particle production will be non-trivial in the two flavors that non trivially rotate under the chosen flavour T_1, to which we shall restrict our attention. Moreover, unless stated otherwise, for convenience we shall use a unique index i which runs over the tensor product of the spinor and the flavor spaces since our calculation

will mix the two types of indices. Conventionally, we label with $i = 1, 3$ the two spinor components of the first flavor and with $i = 2, 4$ the two spinor components of the second flavor.

Finally, there is a time-dependent symmetry of the fermionic system in the background of the bubble, generated by a simultaneous time-translation and an $SU(2)$-rotation in the flavor space, $Q = \partial_t - \omega T_1$. This allows us to label the modes according to the associated charge, which can be interpreted as the energy ϵ of the modes after a time-dependent fermion redefinition $\psi' = U\psi$, with $U(t)$ given by equation (3.8). Since on the other hand translational invariance is broken by the bubble itself, we shall express the asymptotic and internal momentum k of the modes as a function of ϵ, and not vice-versa, as it is customary. This will make the matching of the mode behaviour between the different regions more transparent.

Let us now consider the fermionic modes. We can generically expand the fermionic field as:

$$\psi = \sum_n c_n \mathbf{f}^n(x,t)\,, \tag{3.51}$$

where n is an index that runs over the eigenvectors of the quadratic operator describing the equation of motion of the fermion in the bubble background and $\mathbf{f}^n$ are the corresponding eigenmodes. We left the expansion generic, since as discussed above both space and time-translations are broken by the bubble. On the other hand, at spatial asymptotic infinity the fermions do not feel the presence of the bubble. Therefore, their mode expansion is the one of a free theory. Then, we can expand in plane waves as:

$$\begin{aligned}\psi = &\int_0^\infty d\epsilon \sum_i \frac{1}{\sqrt{2\omega_k}} c^i_{L/R} \mathbf{u}^\epsilon_i e^{\mathrm{i}(k^i(\epsilon)x - \epsilon t)} + \\ &+ \int_{-\infty}^0 d\epsilon \sum_i \frac{1}{\sqrt{2\omega_k}} c^{\dagger i}_{L/R} \mathbf{u}^\epsilon_i e^{\mathrm{i}(k^i(\epsilon)x - \epsilon t)}\,,\end{aligned} \tag{3.52}$$

where $\mathbf{u}_i$ are the polarization spinors, which take into account also the choice of direction in flavour space.

To define the in- and out-vacua appropriately, we shall consider the asymptotic behavior of the mode functions. Indeed, even if the background makes the Hamiltonian time dependent and changes the instantaneous ground state, far from the bubble the field approaches stationary regions, which select preferred ground states at infinite time $t \to \pm\infty$. This is because in the infinite past or future all the scattering states have dispersed to infinity. Therefore, they do not feel the presence of the bubble anymore, and they behave as free wave-packets governed by the free Hamiltonian outside of the bubble.

Hence, we decompose each mode into incoming and outgoing components according to their momentum. On the left of the bubble, incoming waves with positive frequency carry positive momentum, while incoming waves with negative frequency carry negative momentum. On the right, the assignments switch.

This decomposition matches the evolution of normalizable wavepackets. Incoming modes create or annihilate a packet at $t = -\infty$ and are responsible for its propagation to-

wards the bubble at early times, and outgoing modes determine the content at $t = +\infty$ and control the late time evolution. Therefore, we define the asymptotic vacuum at $t = \pm\infty$ as the state annihilated by all the ladder operators with positive momentum from $x \to -\infty$ and with negative momentum from $x \to +\infty$. This corresponds to the physical fact that no incoming particles appear from either side. Similarly, we define the late-time vacuum as the state without any outgoing particles from either side. Let us remark that if there were no bubble, these two vacua would be equivalent to each other and to the usual Fock vacuum.

Now, let us discuss the role of the bubble. Due to its presence, the fermionic modes mix in time. A purely incoming mode at $t = -\infty$ evolves into a superposition of incoming and outgoing modes by $t = +\infty$. This by itself wouldn't be sufficient to have particle creation. However, the $SU(2)$ rotation generated by the bubble evolution:

$$U(t) = e^{\mathrm{i}\omega t T_1} = W \begin{pmatrix} e^{\mathrm{i}\frac{\omega}{2}t} & 0 \\ 0 & e^{-\mathrm{i}\frac{\omega}{2}t} \end{pmatrix} W^\dagger \,, \tag{3.53}$$

with W a matrix diagonalizing U, mixes a mode of frequency ϵ to another with frequency $\epsilon - \frac{\omega}{2}$. For $|\epsilon| < \frac{\omega}{2}$, this leads to a nontrivial Bogoliubov relation between in- and out-operators of the form:

$$c_i{}^{\mathrm{out}} = \sum_j \alpha_{ij} c_j{}^{\mathrm{in}} + \beta_{ij} c_j^{\dagger \mathrm{in}} \,, \tag{3.54}$$

which signals particle production. To obtain the rate, we shall compute the precise coefficients of (3.54).

The mode analysis simplifies after a change of variables that eliminates the explicit time dependence. As suggested by the symmetry of the system discussed above, we perform the fermionic redefinition $\psi' = U\psi$. With this choice, the original equation of motion

$$\mathrm{i}\partial\!\!\!/\psi + gU^\dagger V(x) U\psi = 0 \,, \tag{3.55}$$

became the time-independent equation

$$-\gamma_0 \omega T^1 \psi + \mathrm{i}\partial\!\!\!/\psi + gV(x)\psi = 0 \,. \tag{3.56}$$

A closed analytic solution does not exist for arbitrary $V(x)$. On the other hand, as anticipated, the thin-wall limit, in which the bubble is modeled by a double Heaviside Theta profile, allows for an analytic treatment. This is because, in that limit, the continuity of the mode profile at the interface at the boundary of the bubble fixes the fermionic modes completely. Therefore, from now on we shall focus on this regime.

Here we can write the modes of Eq (3.56) as:

$$\psi_\epsilon(x,t) = \begin{cases} \sum_j \tilde{c}^j \tilde{\mathbf{u}}_j^\epsilon e^{\mathrm{i}\left(\tilde{k}_j(\epsilon)x - \epsilon t\right)} & |x| < R \\ \sum_j c^j_{L/R} \mathbf{u}_j^\epsilon e^{\mathrm{i}(k_j(\epsilon)x - \epsilon t)} & |x| > R \,. \end{cases} \tag{3.57}$$

We denote quantities related to the solution inside the bubble with a tilde, and we sum over both spin and flavor indices.

In the two regions far from the bubble, the dispersion relation is the one of a two-flavor massless fermion, with a flavour-dependent frequency shift produced by the fermionic rotation:

$$k_{1/2}(\epsilon) = \pm\epsilon \pm \frac{\omega}{2}\,. \tag{3.58}$$

Within the bubble, both fermions develop an effective mass $m_\psi \sim g\phi_0$ and couple to the excited Goldstones, which yields a more complicated flavor-dependent dispersion relation:

$$k_{1/2}^2 = \epsilon^2 - \left(\frac{m_\psi}{2}\right)^2 + \left(\frac{\omega}{2}\right)^2 \pm \frac{1}{2}\sqrt{4\omega^2\epsilon^2 + m_\psi^4 - \omega^2 m_\psi^2}\,. \tag{3.59}$$

Notice that the polarization vectors are also modified accordingly inside the bubble. We observe that, for a range of frequencies, the corresponding momenta can turn imaginary in the bubble core, indicating that on-shell propagation is kinematically forbidden inside the bubble. This is because the energy falls below the effective mass. Even so, these modes, which are analogous to tunneling modes between the two asymptotic regions in quantum mechanics, are of course perfectly legitimate.

This decomposition has been written in terms of the frequency ϵ, which is a conserved quantity. The frequencies ϵ can be both positive and negative. The coefficients c^i have to be interpreted either as creation or annihilation operators, depending on their frequencies. This is crucial for understanding how particle creation from the vacuum can occur, since particle creation can occur only when the Eq (3.54) mixes modes with positive and negative frequencies. If we undo our time-dependent fermionic field redefinition, it is clear from the equation (3.58) that this happens for $\epsilon \leq \frac{\omega}{2}$. Indeed, given that ϵ is conserved, the only mixing that can take place is among the modes that in the time-dependent basis have frequencies ϵ' and $\epsilon' - \frac{\omega}{2}$. Consequently, positive and negative frequencies overlap only in the range discussed above. Outside of this range, particle creation from the vacuum is excluded in the semiclassical limit. However, we still have a non-trivial scattering against the bubble.

By imposing the necessary continuity conditions, we can obtain c_L^i as a function of c_R^i

$$c_\epsilon^{L\,i} = S_\epsilon{}^i{}_j c_\epsilon^{R\,j}\,. \tag{3.60}$$

Such a matrix contains all the necessary ingredients for extracting the coefficients of the Bogoliubov transformation (3.54). The complete expression for S_{ij} is quite lengthy and was obtained analytically with the help of Mathematica; we do not report it here. Instead, we consider its asymptotic series in two regimes, expressed either for $g\phi_0 \ll \omega$ or for $g\phi_0 \gg \omega$. For illustrative purposes, we write explicitly the Bogoliubov coefficients for one of the outgoing ladder operators in the small $g\phi_0/\omega$ regime:

$$
\begin{aligned}
c^{L\dagger}_{1,\text{out }\epsilon} = c^{L\dagger}_{2,\text{in }\epsilon}&\left(\frac{\mathrm{i}g\phi_0\sin(R(2\epsilon-\omega))}{2\epsilon-\omega}\right) + c^{R}_{3,\text{in }\epsilon}\left(\frac{\mathrm{i}g\phi_0\sin(2R\epsilon)}{2\epsilon}\right)\\
&+ c^{R\dagger}_{1,\text{in }\epsilon}\left(-\frac{2\mathrm{i}\epsilon^2(g\phi_0)^2e^{-\mathrm{i}R\omega}\sin(4R\epsilon)}{(\omega^2-4\epsilon^2)^2} + \frac{8\mathrm{i}\epsilon^3(g\phi_0)^2\sin(R\omega)}{\omega(\omega^2-4\epsilon^2)^2}\right.\\
&\quad - \frac{\omega\epsilon(g\phi_0)^2e^{-\mathrm{i}R\omega}\cos(4R\epsilon)}{(\omega^2-4\epsilon^2)^2} + \frac{\omega\epsilon(g\phi_0)^2(\cos(R\omega)-3\mathrm{i}\sin(R\omega))}{(\omega^2-4\epsilon^2)^2}\\
&\quad \left. + \frac{\omega^2(g\phi_0)^2\sin(4R\epsilon)(\sin(R\omega)+i\cos(R\omega))}{2(\omega^2-4\epsilon^2)^2} - \frac{\omega^3(g\phi_0)^2e^{-\mathrm{i}R\omega}\sin^2(2R\epsilon)}{2\epsilon(\omega^2-4\epsilon^2)^2}\right)\\
&+ c^{L}_{4,\text{in }\epsilon}\left(\frac{2\epsilon^2(g\phi_0)^2(\sin(R\omega)+\mathrm{i}\cos(R\omega))\sin(R(4\epsilon-\omega))}{(\omega^2-4\epsilon^2)^2} - \frac{8\mathrm{i}R\epsilon^3(g\phi_0)^2}{(\omega^2-4\epsilon^2)^2}\right.\\
&\quad + \frac{\omega\epsilon(g\phi_0)^2e^{-2\mathrm{i}R\omega}\left(e^{4\mathrm{i}R\epsilon}-e^{2\mathrm{i}R\omega}\right)}{(\omega^2-4\epsilon^2)^2} - \frac{2\mathrm{i}R\omega\epsilon^4(g\phi_0)^2}{(\omega^2-4\epsilon^2)^2}\\
&\quad + \frac{\omega^2(g\phi_0)^2e^{-2\mathrm{i}R(\omega+2\epsilon)}\left(2e^{2\mathrm{i}R\omega}-3e^{2\mathrm{i}R(\omega+2\epsilon)}+e^{8\mathrm{i}R\epsilon}\right)}{4(\omega^2-4\epsilon^2)^2}\\
&\quad + \frac{3\mathrm{i}R\omega^2\epsilon^3(g\phi_0)^2}{(\omega^2-4\epsilon^2)^2} + \frac{\mathrm{i}R\omega^3\epsilon^2(g\phi_0)^2}{2(\omega^2-4\epsilon^2)^2}\\
&\quad \left. + \frac{\omega^4(g\phi_0)^2(1-e^{-4\mathrm{i}R\epsilon})}{16(\omega^2-4\epsilon^2)^2} - \frac{\mathrm{i}R\omega^4\epsilon(g\phi_0)^2}{4(\omega^2-4\epsilon^2)^2} + 1\right)\,.
\end{aligned}
\tag{3.61}
$$

The spectrum of evaporation follows directly from the Bogoliubov coefficients. Let us discuss it in both regimes $g\phi_0 \ll \omega$ and $g\phi_0 \gg \omega$. Since, as discussed in section 3.1, the regime relevant for saturation is $g\phi_0 \lesssim \omega$, let us begin with this region of parameters. Recall that even if we considered the evaporation process for a thin-wall bubble, the spectrum can be extrapolated to a thick-wall, saturated bubble in its parametric scaling.

In this regime, the density of created particles per frequency per unit volume at the leading order in a series expansion in the small parameter $g\phi_0/\omega$ is given by:

$$
\rho_\epsilon = \frac{g^2\phi_0^2\sin^2(2R\epsilon)}{4\epsilon^2}\,,
\tag{3.62}
$$

for $|\epsilon| < \frac{\omega}{2}$.

Moreover, it turns out that, as it should, the radiation conserves the $SU(N)$ flavor and is democratic in particles and antiparticles. The fact that the first-order expression does not contain ω explicitly is an "accident" of the first-order truncation, and explicit ω dependence reappears in higher orders.

The total particle density can be obtained by integration over the frequencies in the

allowed range:

$$\begin{aligned}\Gamma &= \int_0^{\frac{\omega}{2}} \mathrm{d}\epsilon\ \rho_\epsilon \\ &= \frac{g^2\phi_0^2\left(2R\omega\,\mathrm{SinIntegral}(2R\omega)+\cos(2R\omega)-1\right)}{4\omega}\,.\end{aligned} \tag{3.63}$$

From the rate above, we can finally obtain the evaporation rate for a saturated bubble, in which $R\omega \sim 1$. It reads:

$$\Gamma \sim \frac{g^2\phi_0^2}{4\omega} \sim \frac{1}{R}\,. \tag{3.64}$$

As expected from the universality properties of saturons, the particle emission rate is given by the inverse size of the bubble. Also, the typical energy of the radiation is $E \sim 1/R$. These features, surprisingly similar to the Hawking rate for black holes, and in agreement with the results obtained in [19, 20] for the decay of different models of saturons in the language of QFT S-matrix scattering amplitudes, strongly support the connection between black holes and generic saturons. The next section shall be devoted to reproducing in this model the same result in a fully quantum language.

In the complementary regime relevant for a thin-wall bubble at unitarity, the spectrum admits an expansion in the small parameter $\omega/g\phi_0$. Using the same semiclassical method introduced earlier, the decay rate takes the form

$$\Gamma = \omega \tanh^2\left(Rg\phi_0\right). \tag{3.65}$$

This result matches with the decay rate of the thin-wall bubble at weak coupling, equation (3.63), namely $\Gamma \sim g^2\phi_0^2R^2\omega$, within the window $\omega \lesssim g\phi_0 \lesssim 1/R$. The agreement indicates a smooth crossover between the two parameter regimes.

The same expression, even if strictly speaking is valid for $g\phi_0 > \omega$, also supports an extrapolation toward a thick-wall saturated bubble. The extrapolation proceeds by tuning $g\phi_0 \sim 1/R$ and $\omega \sim 1/R$ at the same time. In this limit, equation (3.65) reproduces the expected saturon evaporation rate (3.64) up to factors of order unity.

The overall picture that emerges describes the decay across all the regimes and links them to each other consistently. In the next section, we shall reproduce these phenomena in a quantum picture of the bubble, and show that the semiclassical features are correctly captured in the appropriate limit.

3.3 The quantum description of evaporation

In this section, we consider the bubble as a quantum coherent state, and we derive its evaporation from the quantum rescattering of its constituents. This is similar in spirit to the approach taken in the N-portrait [13], and in other works on other saturons [19, 20], as discussed in section 2.2. We shall demonstrate, that the quantum analysis correctly reproduces the semiclassical results. Obviously, the quantum picture is nevertheless more

fundamental, and allows us to estimate the necessary corrections to the semiclassical limit, in the form of $1/N$ corrections. The latter is recovered in the large-N limit (3.46) as discussed in the previous section.

In the quantum picture, the dominant process is a decay of a Goldstone particle of frequency ω into a fermion-antifermion pair.

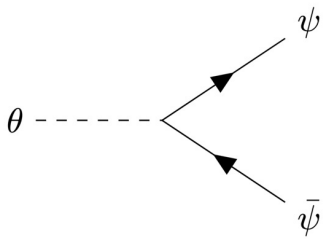

Figure 3.5: The dominant channel that leads to the bubble evaporation.

In an ordinary Goldstone vacuum, an on-shell massless Goldstone boson does not decay. The situation changes for a Goldstone mode confined to the bubble. As we will show below, this happens because the bubble spontaneously breaks spatial translations. Therefore, the localized Goldstone obeys a dispersion relation that is different from that of a massless particle in a Poincaré-invariant vacuum. Since the vacuum with a spontaneously broken $SU(N)$ exists only inside the bubble, for an observer at infinity, a Goldstone mode of frequency ω localized on the bubble appears as an internal excited level of the massive bubble. Such an excitation can relax by decaying into a pair of free fermions, and no kinematical obstruction arises thanks to the broken Poincaré invariance.

We can now estimate the quantum decay rate. First, let us consider the one-Goldstone process. Later, we shall take into account the enhancement factor coming from the multiplicity of Goldstone constituents.

For a single particle of frequency ω, the decay rate in terms of the dimensionless quantum coupling g/ω is:

$$\Gamma \sim \frac{g^2}{\omega}\,. \tag{3.66}$$

Notice that the above rate omits the effect caused by the localized spatial overlap of the Goldstone and fermionic modes. Within the bubble, where the Goldstones are living, the fermions get an effective mass $m_\psi \sim g\phi_0$, which, for a low-energy mode, restricts the penetration length of its wavefunction to a size of order $1/m_\psi$. Consequently, an efficient decay of a bubble Goldstone into fermions occurs only in a region of thickness of order the penetration length, near the bubble boundary. This gives rise to a suppression factor coming from the wavefunction overlap, which depends on which of the regimes discussed in section 3.1.7 we are considering.

Let us discuss such factors generically, by estimating the decay rate of a Goldstone particle θ of energy ω into a pair of asymptotic fermions of energy ω_1 and ω_2 and corresponding momenta $|p_1| = \omega_1$ and $|p_2| = \omega_2$.

The total decay rate at tree level is:

$$\Gamma = \frac{1}{T}\int \frac{dp_1}{2\omega_1}\frac{dp_2}{2\omega_2}\frac{|\langle\theta|g\int d^2x\theta\bar{\psi}\psi|\bar{\psi}\psi\rangle|^2}{\langle\theta|\theta\rangle}\,. \tag{3.67}$$

We shall denote by θ_ω the mode function that corresponds to a Goldstone particle with frequency ω, and by ψ_i the mode associated with an asymptotic fermion of energy ω_i. Now, we discuss the normalization of such modes. Since the Goldstone field is localized within the bubble size R, the modes of the Goldstone particles which live on the bubble are normalized by a factor $1/\sqrt{\omega R}$. On the other hand, the fermionic field in the background of the bubble is expanded in a continuum of modes, since the fermion is massive inside the bubble but massless outside. Therefore, they follow the usual continuum normalization, $<\psi_i|\psi_i>=(2\pi)\omega_i\delta(0)=(2\pi)\omega_i V$, where V denotes the spatial volume and $\frac{1}{V}\sim dp$.

Next, we discuss the spatial profiles of the modes. As already stated above, the Goldstones live on the bubble. The fermionic modes, however, can have different behaviours. Outside of the bubble, they always oscillate freely. Inside, there are two different regimes. For energies smaller than the fermionic mass, the modes will be exponentially decaying inside with the penetration length $l_p\sim 1/m_\psi$. This is because, inside the bubble the modes behave approximately like $\psi_i(x)\sim\exp\left(\mathrm{i}x\sqrt{\omega^2-m_\psi^2}\right)$. On the other hand, if the energy ω is larger than the fermionic mass induced by the bubble, the fermion also propagates on shell within the bubble, carrying an effective momentum of order $k\sim\sqrt{\omega^2-m_\psi^2}$.

We now have all the ingredients to estimate the decay rate. Summing over polarizations, we obtain:

$$\Gamma\sim g^2\frac{1}{R\omega}\int\frac{dp}{\omega_1}\frac{dq}{\omega_2}\left|\int dx\,\theta^*_\omega\bar{\psi}_1\psi_2\right|^2\omega_1\omega_2\,\delta(\omega-\sum_i\omega_i)\,. \tag{3.68}$$

To obtain the wavefunction overlap, let us distinguish between the various scenarios.

First, we look at the thin-wall limit, $R\omega\ll 1$. Here, close to the unitarity bound for fermions, $m_\psi\gg\omega$, the integral is approximately independent of the value of the asymptotic momenta and equal to

$$\left|\int dx\,\theta^*_\omega\bar{\psi}_1\psi_2\right|^2\sim\left|\int_0^R dx\,e^{i\omega x}e^{-2m_\psi x}\right|^2 \tag{3.69}$$

$$\sim\begin{cases}\frac{1}{m_\psi^2} & m_\psi\gg 1/R\\ R^2 & m_\psi\ll 1/R\,.\end{cases} \tag{3.70}$$

The ω_i-dependence of the wavefunction-overlap factor can be recovered from ω/m_ψ corrections, which are contributing to the phase space integral. However, energy conservation keeps them suppressed compared to the leading-order contribution. When $\omega\geq m_\psi$, the fermions can be produced on-shell. Such a regime is relevant both for thin-wall and thick-wall bubbles, and leads to a similar overlap factor as

$$\left|\int dx\,\theta^*_\omega\bar{\psi}_1\psi_2\right|^2\sim\begin{cases}R^2 & \omega\ll 1/R\\ \frac{1}{\omega^2}\sim R^2 & \omega\sim 1/R\,.\end{cases} \tag{3.71}$$

Therefore, after estimating the phase space integral, we finally obtain the parametric scaling for the decay rate of a single Goldstone:

$$\Gamma \sim \begin{cases} \frac{g^2}{\omega}\frac{1}{m_\psi^2}\frac{\omega}{R} & m_\psi \gg 1/R \\ \frac{g^2}{\omega}(\omega R) & m_\psi \ll 1/R\,. \end{cases} \tag{3.72}$$

This rate is enhanced by the Goldstone occupation number $N_G \sim \phi_0^2 R\omega$. Correspondingly, the total decay rate is given by:

$$\Gamma_g^{\rm tot} \sim \Gamma N_G \sim \Gamma(\omega R)\phi_0^2\,. \tag{3.73}$$

We are now ready to obtain the full rate, and compare with the semiclassical results. In the regime where $g\phi_0 \gg \omega$, relevant for thin-wall bubbles when the fermionic coupling is close to its unitarity bound, the penetration length is much smaller than $1/\omega$ as well as the size of the bubble R. Therefore, the small overlap induces a suppression of the order $(\omega/R)(m_\psi)^{-2}$, leading to the total rate:

$$\Gamma \sim \frac{g^2\phi_0^2}{\omega}\frac{\omega^2}{m_\psi^2} \sim \frac{g^2\phi_0^2\omega}{m_\psi^2} \sim \omega\,. \tag{3.74}$$

This fully matches the corresponding semiclassical one (3.65), once we take into account that for thin-wall bubbles at the unitarity bound $g\phi_0 \sim m \gg 1/R$ holds.

Now, we consider thin-wall at weak coupling, where $g\phi_0 \ll \omega$. Here, as shown above the fermionic penetration length is of the same order or larger than the size of the bubble, $g\phi_0 \ll 1/R$. Therefore, the dominant suppression comes from the localization of the Goldstone mode within the size R, which leads to a rate suppressed by a factor of order $R\omega$:

$$\Gamma \sim \frac{(g\phi_0)^2}{\omega}(R\omega)^2 \sim \omega(Rm_\psi)^2\,. \tag{3.75}$$

Again, the decay rate matches with the one obtained by the semiclassical computation in (3.63). Such a rate can be extrapolated to saturated thick-wall bubbles with $R\omega \sim 1$ to obtain:

$$\Gamma \sim \frac{g^2\phi_0^2}{\omega} \sim \omega \sim \frac{1}{R}\,, \tag{3.76}$$

that reproduces the generic decay rate of saturated states.

3.3.1 An analytic regime for the de-excitation of the bubble Goldstones

After the generic analysis of the quantum decay rate, we shall focus in this section on a specific regime, where we can give a clear analytic treatment of the decay process. We will consider the deep thin-wall regime, when the bubble walls are far apart and ω is smaller

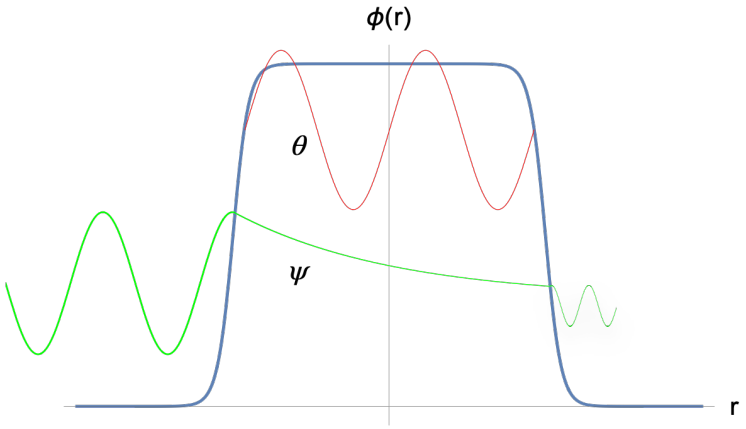

Figure 3.6: A graphical representation of the fermionic and Goldstone modes in the background of the bubble.

than all the other scales in the game, so that the system can be considered static for an exponentially long time:

$$1/\omega \gg R,\ \omega \ll m_\psi\,. \tag{3.77}$$

In this regime, the relevant Goldstone and fermion modes are the ones with frequencies $\omega_k \leq \omega$.

Generically, the spectrum of arbitrary modes is obtained by analyzing the linearized theory around the background. A generic configuration is expanded in a tower of states characterized by the frequencies ω_k:

$$\theta(x,t) = \sum_k \Theta_k(x)\zeta_k(t) = \sum_k \Theta_k(x)\, e^{\mathrm{i}\omega_k t}\frac{\hat{a}_k}{\sqrt{\omega_k}} + h.c., \tag{3.78}$$

$$\psi(x,t) = \frac{1}{\sqrt{L}}\sum_{k,\pm}\Omega_{k\pm}(x)\,\hat{b}_{k\pm}e^{\mathrm{i}\omega_k t}\mathbf{u}_\pm + h.c.\,. \tag{3.79}$$

We are denoting as $\Theta_k(x), \Omega_{k\pm}(x)$ the mode functions for the Goldstone and the fermion field respectively, as $\mathbf{u}_\pm$ the fermion polarization spinors in the dimensionless normalization, and as $\hat{a}_k, \hat{b}_{k\pm}$ the corresponding ladder operators. Also, for clarity, we are using a normalization for the modes within a box of finite size L, which later must be taken to infinity.

If we focus on the low energy modes in the regime (3.77), we can obtain the profiles of the relevant wavefunctions analytically. Let us first consider fermionic modes, with frequencies $\omega_k \leq \omega$. Under our assumptions, we can approximate their profiles by the profiles of their $\omega_k = 0$ counterparts. In particular, in the $\omega \to 0$ limit, the polarization spinors $\mathbf{u}_\pm$ correspond to $\pm\mathrm{i}$ eigenvalues of γ_x, and the mode functions $\Omega_\pm(x)$ are eigenfunctions of γ_x, $\gamma_x\psi = \pm\mathrm{i}\psi$:

$$\Omega_\pm(x) = \Omega_\pm(\mp\infty)\exp\left(\mp g\int_{\mp\infty}^{x}\phi_b(y)dy\right)\,, \tag{3.80}$$

where $\phi_b(x)$ is the bubble wall profile (3.20).

Similarly, the mode for the Goldstone of frequency ω can also be approximated as the associated zero mode, weighted by the bubble profile. As we discussed in section 3.1.2, the Goldstone mode with $\omega_k = 0$ is normalized as $\Theta_0(x) = 1/\sqrt{\mathcal{N}_\theta}$, according to equation (3.30).

Their overlap in the interaction Lagrangian follows directly (we drop the label ω because of the weak ω-sensitivity):

$$\int dx\, g\, \phi_b(x)\, \Omega_\pm^2(x) \;=\; \int dx \frac{1}{2} d_x(\Omega_\pm(x)^2) \tag{3.81}$$

$$=\; \Omega_\pm(\pm\infty)^2 - \Omega_\pm(\mp\infty)^2\,, \tag{3.82}$$

and it is of order one for $1/m_\psi \ll R$, and of order $m_\psi R$ for $1/m_\psi \geq R$.

The knowledge of the modes' profiles allows us to obtain the effective Hamiltonian describing their interaction, and consequently, the transition rate of the bubble.

Let us denote by $\hat{b}_{1,2}$ the ladder operators of the fermions of frequencies ω_1 and ω_2 into which the excited Goldstones decay. Similarly, we denote by $\hat{a}_\omega$ the ladder operator referring to the Goldstone modes of the bubble with frequency ω, which are the excited modes constituting the bubble. For both of them, as we already said, due to the condition (3.77), the profiles closely match the ones of the respective zero modes.

Also, let us remark that the kinetic term for the Goldstone mode is normalized canonically as:

$$H \supset \int dx\, \phi_b^2 \Theta_0^2(x) \dot{\zeta}^2(t) = \omega \hat{a}_\omega^\dagger \hat{a}_\omega\,. \tag{3.83}$$

The interaction term in the Hamiltonian is (we omit the spinorial structure for simplicity):

$$\int dx\, g\phi_b \theta \bar{\psi}\psi = \int dx\, g\phi_b \Omega^2 \frac{1}{L} b_1^+ b_2^+ a_\omega \frac{1}{\sqrt{\mathcal{N}_\theta \omega}} = \tag{3.84}$$

$$= \left(\Omega^2(\pm\infty) - \Omega^2(\mp\infty)\right) \frac{1}{2L} \frac{1}{\sqrt{R\omega\phi_0^2}} a_\omega b_1^+ b_2^+\,,$$

where we used that the kinetic term for the Goldstone mode is normalized canonically:

$$H \supset \int dx\, \phi_b^2 \Theta_0^2(x) \dot{\zeta}^2(t) = \omega \hat{a}_\omega^\dagger \hat{a}_\omega\,. \tag{3.85}$$

Therefore, we can obtain the interaction Hamiltonian for the modes under consideration. In the regime $1/m_\psi \ll R$, when expressed in terms of the properly normalized mode operators, it reads:

$$\hat{H}_{\theta\to\psi} \;=\; \sum_{\omega_1,\omega_2} \frac{1}{2L\sqrt{\omega\mathcal{N}_\theta}}\, \hat{b}_1^\dagger \hat{b}_2^\dagger \hat{a}_\omega\,. \tag{3.86}$$

In the regime $1/m_\psi \geq R$, it receives a correction by a factor of $m_\psi R$. We have all the ingredients to evaluate the matrix element between the initial state $|i\rangle = |N_G\rangle$ and the

final state $|f\rangle = |N_G - 1\rangle \times |1_b, 1_{b'}\rangle$:

$$\langle f| \hat{H}_{\theta\to\psi} |i\rangle \sim \sqrt{N_G} \frac{1}{L\sqrt{\omega R \phi_0^2}} \sim \frac{1}{L}\,, \tag{3.87}$$

where we used that the Goldstone occupation number is $N_G = R\omega\phi_0^2$. Again, in the $1/m_\psi \geq R$ regime, we get an additional $m_\psi R$ factor. The decay rate can be obtained by integrating the squared amplitude over the phase space. Recalling that $1/L \sim dp_i$, and integrating in $\int dp_1\, dp_2\, \delta(\omega - \sum_i \omega_i)$ lead us to the total rate

$$\Gamma \sim \begin{cases} \omega & 1/m_\psi \ll R \\ \omega R^2 m_\psi^2 & 1/m_\psi \geq R\,, \end{cases} \tag{3.88}$$

The rate matches completely with the previous sections.

3.4 Understanding the spectrum

The similarity between the radiation spectrum of saturated bubbles and black holes is striking, as they both radiate with a rate and a typical energy set by the inverse size of the system:

$$\Gamma \sim \frac{1}{R}\,, \quad E \sim \frac{1}{R}\,. \tag{3.89}$$

However, there are also important differences in the characteristics of the spectrum. In particular, while in the case of a black hole, the production of particles with energy $E \gg 1/R$ is exponentially suppressed but not zero, in the case of a saturated stationary bubble, particles of energy $E > 1/R$ are not radiated at all. This discrepancy can naturally be understood in terms of charge conservation.

Quantum mechanically, as we argued in section 2.1.4, a black hole is a multi-graviton state with a particle distribution peaked around the frequency $1/R$. Higher frequencies $E \gg 1/R$ are also present in exponentially suppressed numbers $\sim e^{-ER}$. The exponential tail of the black hole spectrum emerges, quantum mechanically, from two contributions. The first is the decay of highly energetic gravitons, which is exponentially suppressed since their number is. The second is a $N \to 2$ type of rescattering of $\Delta N \sim ER$ of the main constituents with energy $1/R$ into a few energetic quanta of energy $E \gg 1/R$. These rates, for reasons analogous to the ones discussed in section 2.2.1, are exponentially suppressed as e^{-ER} [13, 82, 90]. In the saturated bubble case, however, neither of these processes can happen. On one hand, the Goldstones are all at the frequency $\omega \sim 1/R$, therefore the decay channel analogous to the black hole one is not available. The second type of process is forbidden by charge conservation. Since Goldstones are charged particles, the rescattering of $\Delta N = ER \gg 1$ of them into few energetic particles would force these particles to have a charge ΔN. Such particles, of course, do not exist in the theory, therefore the process is strictly impossible.

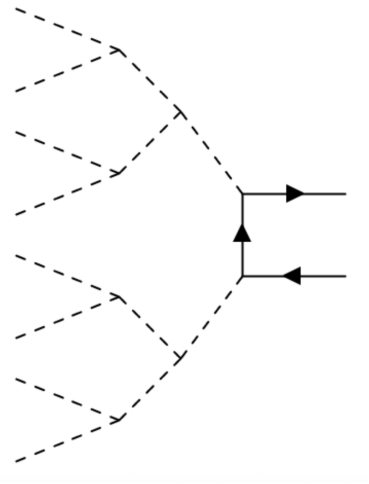

Figure 3.7: A would be $N \to 2$ process depicting the annihilation of N Goldstones into a pair of highly energetic fermions. Processes of this kind are forbidden by charge conservation.

Of course, this does not forbid other types of $1/N$ corrections when we depart from the semiclassical limit (3.46). For example, since for finite-N the bubble has a finite mass, the spectrum will be corrected due to a non-zero recoil, or the bubble can radiate higher frequency modes when excited [82]. All in all, we have identified the similarities between the radiation of the bubble and a black holes, as well as its own peculiarities.

3.5 Time-scale of information retrieval

In this final section, we discuss the time-scale of the information retrieval for the saturated bubble. It turns out that also in this regard the behaviour is analogous to the black hole case of section 2.1. The question of the retrieval of information has already been investigated for the $3+1$ dimensional version of this system and other saturons in [17, 19, 20, 102]. Here, we report the conclusions. For our bubble, the information is encoded in the $SU(N)$ quantum numbers of the Goldstones. On general grounds, the retrieval time requires the resolution of the memory modes, and therefore it is equivalent to the time-scale (3.44) associated to the inverse gaps of the memory modes themselves (3.43), since this is the minimal time required to resolve modes with a gap (3.43).

Let us show this explicitly by analyzing the possible ways to extract information from a saturated bubble [17].

The first approach is the so-called passive approach, where we wait for the result of the decay of the bubble, and we analyze its content. Notice, that it is extremely important to keep in mind that, since everything is made by quantum fields, the detector itself is a quantum object subject to the same rules and unitarity constraints as any other system.

To analyze the information content of the radiation, a detector needs to interact with the individual flavour of the emitted spectrum. Let us assume that the detector has capacity

$N_{\rm det}$. Such a capacity is bounded by unitarity to be $N_{\rm det} \leq N$. Since for a saturated bubble the emitted radiation has a frequency $\omega \sim 1/R$ and it interacts via the coupling constant $\tilde{\alpha} \sim 1/N \sim 1/S$, the interaction rate for resolving a quantum of the radiation in a detector is,

$$\Gamma_{\rm det} \sim \frac{1}{R}\frac{1}{N^2} N_{\rm det}\,. \tag{3.90}$$

Therefore, even for a detector of maximal capacity, the minimum retrieval time for beginning to extract the information of a single quantum is

$$t \gtrsim \frac{1}{\Gamma_{\rm det}} \sim S\,R\,. \tag{3.91}$$

This rate is completely analogous to Page's time [66] that sets the information retrieval scale for a black hole, discussed in section 2.1 [17, 19–21].

Moreover, the scaling of the retrieval time clarifies that the information extraction is encoded in $1/N$ effects, which disappear in the semiclassical limit. This is in accordance with the picture of the black hole N-portrait [13–15, 64].

We now move to the active approach to information retrieval. Here, we shall imagine that we probe the nature of the saturated bubble by scattering on it quanta sensitive to its flavour content [17]. For example, we could consider massive quanta of the adjoint field or the massless fermion species that are coupled to it. Let us consider a quantum of the fermionic field of energy $\sim 1/R$. Its scattering rate on the bubble is of order one, since the suppression by the coupling $1/N$ is compensated by the occupation number of Goldstones $N_G \sim N$. However, this scattering sees the bubble as a rigid object, and is insensitive to the bubble's $SU(N)$-flavor content. This is similar to a meson-baryon scattering in large-N QCD. If we want to resolve the flavor quantum numbers, we need to pay an additional $1/N$ price, leading to the rate (3.90), amounting to the time-scale (3.91).

Notice that this analysis is valid in the initial phase of the evaporation, before the memory burden takes place [25, 26]. Once the bubble enters the memory-burden phase, new effects invisible to the semiclassical description kick in, and the emission is further suppressed. Therefore, the active retrieval of information becomes the most effective way of reading the information. However, as explained in [27], the retrieval rate becomes sensitive to the particularities of the system and can be different for black holes and other saturons.

To conclude, we have shown how the timescale of extraction of the information content of a saturated bubble is infinite in the semiclassical large-N limit, and becomes finite, albeit $1/N$ suppressed, once we consider a fully quantum treatment. The information retrieval scale (3.91) is equivalent to the black holes' Page time. This underlines the universality of this behaviour, and connects it to the general phenomenon of saturation.

3.6 Conclusions

In this chapter, we have investigated a controllable example of a saturon in a renormalizable theory in $1+1$ dimensions. This saturon is a thick-wall bubble of a vacuum with a broken $SU(N)$ symmetry with large-N, in the symmetric vacuum.

We have shown that, consistently with the generic phenomenon of saturation discussed in section 2.2, a saturon bubble saturates both the coupling bound (2.32) and the area law (2.33) at the same time, thanks to the emergence of a large number of gapless Goldstone modes. These bounds are all different forms of the same physical law, and set the maximally allowed entropy for any state in a consistent QFT [16–18]. Consistently, the bubble under study becomes a saturon when the theory hits the unitarity limit.

Then, we have focused on the evaporation properties of the saturated bubble by coupling it to a massless fermionic field. Thanks to the controlled setting, we were able to calculate the dominant radiation rate both semiclassically in the large-N limit and quantum mechanically. Semiclassically, the evaporation rate is obtained from the explicit computation of the Bogoliubov coefficients of the fermionic field at asymptotic times. Quantum mechanically, we resolved the bubble in terms of its quantum constituents, and we calculated the rate of the dominant decay process that leads to evaporation, in terms of the decay of the constituent Goldstones. The latter approach has been taken for other saturated systems in [17, 19–21]. In this work, thanks to the simplicity of the model, we can derive the decay more explicitly, and we manage to show the full agreement of the two approaches.

Our results have two main implications. First, it allowed us to confirm the identical physics between black holes and generic saturated states. In particular, we obtained that the bubble radiates at a rate given by equation (3.89), where both the rate and the typical energy of the radiated particles are set by the inverse size $1/R$ of the system. This parallels the Hawking radiation for black holes, and further establishes the understanding of black holes as belonging to the universality class of saturons.

Second, the matching of the semiclassical and the fully quantum corpuscular approach offers strong support for the quantum description of a black hole given by the black hole N-portrait [13], discussed in section 2.1.4, as well as for the generic understanding of the quantum nature of classical profiles as multiparticle states [20, 23, 28, 29, 40, 64, 83, 84, 103].

Finally, the model allows us to understand very clearly the processes of information storage and retrieval. In particular, it makes the semiclassical limit and the quantum timescale of information very transparent. Information is stored in $1/N$-gapless Goldstones, whose coupling is also controlled by $1/N$. Therefore, information cannot be retrieved semiclassically, while quantum mechanically the retrieval rate is given by equation (3.91), in line with the results obtained in other saturated systems [17, 19–21]. Again, this is in complete correspondence with Page's time [66] discussed in section 2.1.3. To conclude, the identical physics between the saturated bubble and a black hole in all the relevant aspects confirms the universality of the physics of saturons and supports the picture of a black hole as a saturated state.

Chapter 4

Quantum dynamics of a relativistic $U(1)$ superfluid

In this chapter, we move away from the phenomenon of saturation, to discuss the connection between the classical and quantum dynamics in a different setting, along the lines of [3]. Of course, at a fundamental level classical dynamics should emerge from the quantum Hilbert space obtained by quantizing around a well-defined vacuum, for a given set of states in an appropriate regime of parameter space. The quantum dynamics of the states should also automatically take care of deviations from classicality. First, in the introduction, we briefly expose the general framework of the background field method [28, 29]. This approach allows us to analyze the dynamics of quantum states in a controlled semiclassical approximation, where one can clearly understand how the dynamics of the "classical" one-point function of a highly occupied coherent state receives quantum corrections from higher-order correlation functions in a controlled manner. We also briefly discuss the role of coherent states as good quantum field theoretic states to obtain an approximately classical dynamics, as well as the importance of dressing in order to properly define a quantum state that really tracks the classical motion in the most accurate way [30,31,104]. We show how, generically, genuinely quantum contributions necessarily spoil classicality for long enough times, at a quantum timescale set by the so-called quantum-break-time [22–24, 63, 105]. This has clear connections to black hole physics, since such generic corrections clearly show how the Hawking self-similar evaporation picture needs to receive $1/N$ modifications at finite quantum coupling [13, 15, 59, 67]. Beyond black holes, the concept of quantum break time has also been extremely relevant for cosmic inflation [64, 103, 106, 107], and de Sitter states in quantum gravity [13, 14, 22, 23, 64, 103, 108]. Then, we move to the main focus of this chapter, based on [3]. Here, we study the stability of a fully quantum, homogeneous superfluid state in a $U(1)$ theory with quartic interactions. We show how, with an appropriate definition of the state, the symmetries of the theory can preserve the stability of such a state, in such a way that it retains full coherence at all orders in perturbation theory. We clarify the great specificity of the state under consideration, and why all the right ingredients need to come into place in order to ensure coherence. Finally, we study the spectrum of the theory at one-loop order, and we show that as expected from

Goldstone's theorem [109,110], it admits a gapless Goldstone mode. Thus, we demonstrate the importance of a consistent loop expansion to preserve the gaplessless, clarifying how some truncations in the Hartree approximation can lead to the spurious gap that sometimes appears in the literature [111–114].

4.1 Introduction

4.1.1 States and classicality

Let us begin by discussing the concept of classicality in quantum field theories in general terms. In a quantum field theory, a generic configuration is described by a quantum state, which we shall generically denote by $|\Psi\rangle$. Such a state generates an infinite set of correlation functions, the n-point functions, of the quantum field operators, which we shall collectively name $\hat{\phi}(x,t)$, e.g.

$$\begin{aligned}
&\langle\Psi|\hat{\phi}(x)|\Psi\rangle\,,\\
&\langle\Psi|\hat{\phi}(x)\hat{\phi}(y)|\Psi\rangle\,,\\
&\langle\Psi|\hat{\phi}(x)\hat{\phi}(y)\hat{\phi}(z)|\Psi\rangle\,,\\
&\dots
\end{aligned}$$

and similar correlators involving the conjugate momenta.

These can be associated, with some limitations, with all the moments of the probability distribution for the associated observables. For example, the one-point function gives the expectation value of the field operator on a given state.

On the other hand, in a classical theory, a state is described by a single c-number field configuration (and its time derivative), which we shall denote by $\Phi(x,t)$.

Clearly, the two sets of initial data for solving the initial value problem look very different from each other. In particular, the quantum state in principle provides infinitely more information in terms of the whole set of correlation functions.

Therefore, it is a meaningful question to ask under which conditions the full quantum dynamics can be reduced to its classical counterpart, and to which extent such an approximation is justified. In general, classicality emerges in the limit of large occupation numbers, or equivalently large field values. In such a regime, one can hope that, approximately, the dynamics of the one-point function capture the leading contribution to the time evolution. In particular, one can define the classical profile as the one-point function of a relevant operator[1] $\langle\Psi|\hat{\phi}(x,t)|\Psi\rangle \equiv \Phi(x,t)$. Classicality emerges if, on the relevant scales of the problem under consideration, the higher-order correlation functions are dominated

[1]We remark that classicality can in general also be measured by a different matrix element of the field operator, beyond the expectation value, as understood for example in [64]. Nevertheless, in the subsequent discussion we shall assume the classicality is measured by the one-point function. This is the case, e.g., for (dressed) coherent states, which are the main focus of this chapter.

by their disconnected contributions, i.e.

$$\langle\Psi|\hat{\phi}(x)\hat{\phi}(y)|\Psi\rangle \simeq \langle\Psi|\hat{\phi}(x)|\Psi\rangle\langle\Psi|\hat{\phi}(y)|\Psi\rangle\,,$$
$$\langle\Psi|\hat{\phi}(x)\hat{\phi}(x)\hat{\phi}(z)|\Psi\rangle \simeq \langle\Psi|\hat{\phi}(x)|\Psi\rangle\langle\Psi|\hat{\phi}(y)|\Psi\rangle\langle\Psi|\hat{\phi}(z)|\Psi\rangle\,,$$
$$\dots$$

This entails that, approximately, the one-point function alone is sufficient to capture the full dynamics. It is important to keep in mind the limitations of such statements. First, they are scale-dependent, due to the fact that at sufficiently short scales the connected contribution will always dominate. This indicates the unavoidable breakdown of classicality at short-enough distances, where quantum fluctuations will inevitably dominate over the background. Furthermore, even if the system is initially prepared in a state with such classical features, the maintenance of classicality in time is connected to the preservation of the above-mentioned relations under the Hamiltonian flow. This is by no means guaranteed, and on the contrary, it can only hold in very specific instances.

The prototypical example of "classical" states are coherent states [4, 5, 115][2], which we shall now discuss, together with their limitations. Let us set ourselves, for the moment, in Schrodinger picture.

Both in non-interacting theories, or alternatively as asymptotic states of an interacting theory, their construction is carried on straightforwardly by using the field displacement operator on the vacuum. In an exemplar scalar theory, a coherent state is defined by

$$|\Psi\rangle = e^{-\mathrm{i}\int d^3x\left(\phi_{\rm cl}(x)\hat{\Pi}(x)-\Pi_{\rm cl}(x)\hat{\phi}(x)\right)}|0\rangle\,. \tag{4.1}$$

Notice that the field displacement operator is a unitary operator that implements a translation in field space. This is analogous, for example, to the form of the operator that implements a translation in quantum mechanics. One can easily check that the initial expectation value of canonical variables is indeed given by $\phi_{\rm cl}$ and $\Pi_{\rm cl}$. Also, if we study its dynamics, in a free theory it trivially follows from the commutation relations with the Hamiltonian that its evolution preserves coherence, namely that it can be obtained by replacing in the displacement operator the classical profiles by the time-dependent solution to the classical equation of motion with the corresponding initial conditions.

The story however changes once we turn on interactions [28, 29, 31]. First, in an interacting theory we shall be inclined to construct coherent states starting from the full vacuum:

$$|\Psi\rangle = e^{-\mathrm{i}\int d^3x\left(\phi_{\rm cl}(x)\hat{\Pi}(x)-\Pi_{\rm cl}(x)\hat{\phi}(x)\right)}|\Omega\rangle\,. \tag{4.2}$$

This corresponds to the initial conditions

$$\langle C|\hat{\phi}|C\rangle(t=0) = \phi_{\rm cl}(x)\,, \tag{4.3}$$
$$\langle C|\hat{\Pi}|C\rangle(t=0) = \Pi_{\rm cl}(x)\,. \tag{4.4}$$

[2] See also [116, 117].

The two-point functions are determined by

$$\langle C|\hat{\phi}(x,0)\hat{\phi}(y,0)|C\rangle = \phi_{\rm cl}(x)\phi_{\rm cl}(y) + \langle\Omega|\hat{\phi}(x,0)\hat{\phi}(y,0)|\Omega\rangle\,, \tag{4.5}$$

$$\langle C|\hat{\Pi}(x,0)\hat{\Pi}(y,0)|C\rangle = \Pi_{\rm cl}(x)\Pi_{\rm cl}(y) + \langle\Omega|\hat{\Pi}(x,0)\hat{\Pi}(y,0)|\Omega\rangle\,, \tag{4.6}$$

and higher n-point functions follow similarly. More importantly, it turns out that the vacuum 2-point function contribution in the correlator above, results in an infinite average energy density of the configuration under consideration [29], even after renormalization. This can be intuitively understood from the fact that a coherent state shifts the one-point function, but, modulo the classical contribution, leaves the higher-order correlation function as the ones set in the vacuum. Therefore, in general the fluctuations around the one-point function do not minimize the energy around the one-point function, effectively leading to the equivalent of highly excited states around the given expectation value. To fix this, one needs to upgrade the definition of coherent states to a more general class of dressed coherent states, order by order in perturbation theory. In particular, the vacuum of the theory $|\Omega\rangle$ must undergo a background-dependent squeezing to ensure one-loop consistency at one loop. At higher loops, even non-Gaussian modifications are required [31]. In the proceedings of the chapter, we shall see how in our scenario one can encode all the dressing consistently by considering as an initial state the ground state of the Hamiltonian for fluctuation fields around the given background, similarly to what was discussed for the kink state in chapter 1. Of course, generically, such a Hamiltonian will be time-dependent, and this definition holds only at the initial moment in time.

4.1.2 Time-evolution and the background field method

We can use coherent states to show at a first glance how the quantum dynamics in general departs from its classical counterpart. This has been discussed, for example, in [28,29,64]. Even if, as discussed above, coherent states exhibit some shortcomings, it is a good place to start in order to investigate this class of purely quantum effects. Then, we will move to the more efficient approach of the background field method, which offers more flexibility in practical uses.

To study the departure from classicality of a coherent state, one can directly analyze its time evolution:

$$|\Psi\rangle(t) = e^{-{\rm i}\hat{H}t}e^{-{\rm i}\int d^3x\left(\phi_{\rm cl}(x,0)\hat{\pi}(x)-\pi_{\rm cl}(x,0)\hat{\phi}(x)\right)}|\Omega\rangle\,, \tag{4.7}$$

and compare it with a state following a "purely classical" evolution, defined as:

$$|\Psi_{\rm cl}\rangle(t) = e^{-{\rm i}\int d^3x\left(\phi_{\rm cl}(x,t)\hat{\pi}(x)-\pi_{\rm cl}(x,t)\hat{\phi}(x)\right)}|\Omega\rangle\,. \tag{4.8}$$

This allows us to directly assess the departure from classicality, for example from the overlap among the states, which can be expanded as a time series:

$$|\langle\Psi_{\rm cl}|\Psi\rangle|^2(t) = 1 - \sum_n \alpha_n t^n\,. \tag{4.9}$$

The overlap is not one except for a free theory. The so-called quantum break time timescale [22–24, 118], where the quantum dynamics departs significantly from classicality, emerges as the time scale at which the time-dependent contribution dominates the overlap. This has been investigated, for example, in [28, 29]. However, the implementation of this approach can be challenging for physically interesting cases. Instead, it is generically convenient to think about the state in terms of its correlation functions. As we have already pointed out, the two descriptions are equivalent. As a result, instead of equation (4.7), we can analyze the coupled infinite-dimensional system of equations of motion for correlation functions. The choice of a classical state is then encoded in the initial conditions for the full tower of correlation functions. This approach goes under the name of *background field method*. As we shall see, this approach becomes significantly more practical than the full quantum evolution of the state when there is a certain hierarchy among the correlation functions, as it is the case for "classical" states. In such a setting, at a desirable order of the loop expansion the system of equations simplifies to the point that effectively only a finite number of correlators are sourcing each other.

We shall now briefly exemplify this method in the easy example of a real scalar field with quartic interactions. From now on, we will work in Heisenberg's picture. Then, the full quantum dynamics is governed by Heisenberg's equation of motion, which for the quartic theory at hand is

$$\left(-\Box + m^2\right)\hat{\phi} + \frac{\lambda}{3!}\hat{\phi}^3 = 0\,. \tag{4.10}$$

The next step is to consider as the background the one-point function of the field operator on a given state, $\Phi \equiv \langle\Psi|\hat{\phi}(x,t)|\Psi\rangle$. Notice that this is not just a classical background, and its dynamics can differ significantly. We also define an operator which characterizes fluctuations around the one-point function, $\hat{\psi} \equiv \hat{\phi} - \Phi$. Such an operator has by definition zero expectation value on the chosen state $|\Psi\rangle$. We can obtain an equation of motion for the one-point function by substituting this decomposition in equation (4.10) and taking the expectation value:

$$\left(-\Box + m^2 + \frac{\lambda}{2}\langle\Psi|\hat{\psi}^2(x,t)|\Psi\rangle\right)\Phi(x,t) + \frac{\lambda}{3!}\,\Phi^3(x,t) + \frac{\lambda}{3!}\langle\Psi|\hat{\psi}^3(x,t)|\Psi\rangle = 0\,. \tag{4.11}$$

This equation has important differences from the equation of motion for a classical configuration, as it contains quantum corrections to the dynamics of the background sourced by higher-order correlation functions. These higher correlation functions, as we shall see shortly, themselves satisfy their own equations of motion, creating an infinite tower of coupled differential equations. However, in a semiclassical limit, we have a hierarchy where the one-point function remains finite in the $\hbar \to 0$ limit, while each n-point function carries with it greater powers of $\hbar$ the higher n is. Therefore, if, for example, we are interested in leading order quantum corrections to the classical dynamics, we can ignore the last term of equation (4.11), since it becomes relevant at 2-loops. In other words, at one-loop, the above equation requires only the knowledge of the two-point function. Let us now obtain

the equation that governs the dynamics of the two-point function. By plugging the decomposition $\hat{\psi} \equiv \hat{\phi} - \Phi$ into equation (4.10), subtracting the equation of motion for the one-point function, multiplying by a power of $\psi(x', t')$, and finally taking the expectation value over $|\Psi\rangle$, one obtains:

$$0 = \left(-\Box^{(x,t)} + m^2 + \frac{\lambda}{2}\,\Phi^2(x,t) \right) \langle \Psi | \hat{\psi}(x,t)\hat{\psi}(x',t') | \Psi \rangle + \frac{\lambda}{2}\,\Phi(x,t) \langle \Psi | \hat{\psi}^2(x,t)\hat{\psi}(x',t') | \Psi \rangle + \frac{\lambda}{3!} \langle \Psi | \hat{\psi}^3(x,t)\hat{\psi}(x',t') | \Psi \rangle \,. \tag{4.12}$$

This equation is in turn sourced by higher correlators, whose equations of motion can be obtained in a similar way.

Let us now explain how quantum corrections can be incorporated iteratively in the $\hbar$ expansion. For example, to find the one-loop corrected Φ from equation (4.11), we shall solve equation (4.12) at the tree level, which corresponds to the first line with Φ replaced by the classical background. On the other hand, to obtain the one-loop corrected two-point function we need to evaluate equation (4.12) using the one-loop corrected background field Φ. Also, at the same time the second line of equation (4.12) gives additional one-loop corrections sourced from higher order correlators at tree-level. This procedure can be iterated at any loop order.

Finally, let us clarify once more the role of the choice of a state in the above construction. The initial quantum state of the system provides initial conditions for all correlation functions which can then be used to solve the coupled system of equations (4.11), (4.12) and similar ones for higher order correlators. Moreover, for a state with a macroscopic one-point function, the results at a given order in loop expansion simplify to the point that only a finite number of correlators affect each other. This is the reason why the background field method is so practical.

Let us observe that in the background field method one could also specify the state using the fluctuation field $\hat{\psi}$ order-by-order in perturbation theory and piece-wise in terms of their correlation functions. However, since fluctuations live on a time-dependent background, in general the Hamiltonian which governs the evolution of $\hat{\psi}$ is also time dependent. Therefore, no absolute notion of a vacuum exists, and one needs to resort to the instantaneous vacuum at a given time. In practice, one should keep in mind that these approaches are equivalent to each other, and to the choice of a given initial state. Its identification in terms of the original degree of freedom $\hat{\phi}$ or of the fluctuation $\hat{\psi}$ depends on the problem at hand.

Before proceeding to the superfluid system which will be central in this chapter, let us make a short remark on black hole physics. In this picture, a purely self-similar Hawking evaporation would correspond to truncating the dynamics of the one-point function at one loop, where the two-point function for the fluctuation field in the black hole background would encode Hawking's radiation. Then, this approach clarifies explicitly the necessity of $1/N \sim \alpha_{\rm gr}$ corrections to the quantum dynamics of black holes: they are the quantum corrections coming from higher order correlation functions, which necessarily spoil the exactness of the semiclassical dynamics.

After this short remark, we now move to the superfluid state that shall be the main focus for the rest of this chapter. In the next section, before diving into the core of the work, we shall give a short summary of the main points of our analysis.

4.1.3 Summary of the chapter

The analysis of this chapter will be focused on a homogeneous condensate of an interacting $U(1)$ invariant complex scalar field with quartic interactions, hereafter called a superfluid state. As discussed in the previous section, one could provide the fundamental description for such a state by a coherent state, suitably adjusted by squeezing. In general, because coherent states are not Hamiltonian eigenstates, they evolve in time. As shown in the introduction, while coherence remains intact in a free theory, in nonlinear theories it is typically lost due to quantum effects. In this chapter, we shall show that there is a proper definition of the homogeneous superfluid state under study, such that complete coherence is maintained order by order in perturbation theory.

The theory is defined by the following Lagrangian of a complex scalar with quartic interactions:

$$\mathcal{L} = \partial_\mu \Phi^\dagger \partial^\mu \Phi - m^2 |\Phi|^2 - \lambda |\Phi|^4 \,, \tag{4.13}$$

Its equations admit a stable, spatially uniform superfluid for $\lambda > 0$ and $m^2 > 0$,

$$\Phi = \frac{1}{\sqrt{2}} v e^{\mathrm{i}\mu t} \,, \qquad \text{with} \qquad \mu^2 = m^2 + \lambda v^2 \,. \tag{4.14}$$

The classical superfluid can be characterized by its VEV v, or equivalently by its chemical potential μ. The solution spontaneously breaks at the same time the global $U(1)$ symmetry responsible for number conservation and spacetime symmetries, through its explicit time dependence and nonzero energy and charge densities. The charge density reads $n = \mu v^2$. Let us remark that the classical relation between μ and v given by equation (4.14) shall receive quantum corrections. Therefore, for the time being, we will keep the quantum versions of these parameters in equation (4.15) as free independent variables.

In general, a superfluid state shall be considered as an appropriately dressed coherent state of the form:

$$|\Psi\rangle_{\mathrm{SF}} = e^{-\mathrm{i}v \int d^3x \left(\hat{\Pi} + \mathrm{i}\mu\hat{\Phi} + h.c.\right)} |S\rangle \,, \tag{4.15}$$

where $|S\rangle$ is an appropriately dressed state in which canonical degrees of freedom have vanishing expectation values. For example, in a perturbative analysis as discussed in the introduction, at one loop $|S\rangle$ has to be chosen as a nontrivially squeezed vacuum, and not merely as the vacuum of (4.16). Generically, a state of the form (4.15) will undergo a time evolution which approximately tracks the classical solution (4.14), but with nontrivial quantum corrections. We shall show, however, that we can choose an appropriate state

such that the only impact of quantum effects is to correct the classical relation between μ and v given in equation (4.14), but that beyond this retains coherence at all orders.

Another approach could be that of applying the background field method outlined above, and defining a superfluid state (4.15) as a sort of a vacuum for fluctuations around the classical background (4.14). We should note, however, that a decomposition of the form $\hat{\Phi} \equiv ve^{i\mu t} + \hat{\psi}$ leads to explicit time-dependencies in the Hamiltonian that governs the evolution of $\hat{\psi}$. Our approach is somehow a unification of both approaches, where on one hand our state is easily understood as a vacuum of fluctuations, albeit around a quantum corrected one-point function, and on the other hand can be clearly connected to a specific state written in terms of the fundamental degrees of freedom of the theory.

We shall obtain our explicit definition of a stable superfluid state going through a procedure that bears substantial similarities with the definition of a kink state discussed in section 1.1.3. First, let us consider the Hamiltonian of the theory:

$$\hat{H} = \int d^3x \left(|\hat{\Pi}|^2 + |\vec{\nabla}\hat{\Phi}|^2 + m^2|\hat{\Phi}|^2 + \lambda|\hat{\Phi}|^4 \right) . \tag{4.16}$$

The stable superfluid state is characterized most easily after we perform the following canonical transformation, corresponding to the time-dependent change of variables generated by the $U(1)$ charge $\hat{Q}$ in the fundamental theory, with a "speed" controlled by the parameter μ, yet to be specified. Notice that at this stage we have not yet introduced any background.

$$\hat{\Phi} = \hat{U}\hat{\varphi}\hat{U}^\dagger , \qquad \hat{\Pi} = \hat{U}\hat{\Pi}_\varphi\hat{U}^\dagger , \qquad \text{with} \qquad \hat{U} \equiv e^{\mathrm{i}\mu t\hat{Q}} . \tag{4.17}$$

As we shall show in the following sections, by a trivial analysis of the time-dependent canonical transformation above, the new variables $\hat{\varphi}$ and $\hat{\Pi}_\varphi$ are governed by the Hamiltonian

$$\hat{H}' = \hat{H} - \mu\hat{Q} = \int d^3x \left(|\hat{\Pi}_\varphi - \mathrm{i}\mu\hat{\varphi}^\dagger|^2 + |\vec{\nabla}\hat{\varphi}|^2 + \left(m^2 - \mu^2\right)|\hat{\varphi}|^2 + \lambda|\hat{\varphi}|^4 \right) . \tag{4.18}$$

This Hamiltonian is both time-independent and bounded below. Let us remark that these are extremely peculiar properties that do not usually hold for generic time-dependent field redefinitions.

Consequently, the Hamiltonian (4.18) has a well-defined vacuum state $|v\rangle$. It is easy to see that it spontaneously breaks the $U(1)$ symmetry, and carries a nonzero charge density. With a usual choice of the phase, the vacuum expectation value can be pointed to the real direction in the field space

$$\langle v|\hat{\varphi}|v\rangle = \frac{1}{\sqrt{2}}v , \tag{4.19}$$

Notice that the vacuum expectation value v is in one-to-one correspondence with μ. Let us also remark that we can of course rewrite the Hamiltonian (4.18) also in terms of fluctuations around its VEV, by another trivial, time-independent field reparametrization.

Classically, they are connected exactly by equation (4.14). However, quantum mechanically corrections emerge, analogously to the case of spontaneous symmetry breaking in the vacuum, where the effective potential receives Coleman-Weinberg corrections that modify the vacuum expectation value.

In the following sections, we shall review the known fact that, as expected from the properties of the Hamiltonian (4.18), the kinetic matrix for perturbations around $|v\rangle$ can be diagonalized with time-independent wavefunction coefficients. To show the connection with the background field method, we shall also explicitly construct $|v\rangle$ from the vacuum of the (Lorentz-violating) free theory of superfluid perturbations.

Let us remark that the state $|v\rangle$ is only a vacuum for $\hat{H}'$, not for $\hat{H}$. As we shall show in later sections explicitly, it is a suitably dressed coherent state. This had better be the case, if we hope to reproduce classical evolution given in equation (4.14). The (non-trivial) time evolution of $|v\rangle$ can be easily described explicitly, given the relation between $\hat{H}$ and $\hat{H}'$, and reads:

$$e^{-\mathrm{i}\hat{H}t}|v\rangle = e^{-\mathrm{i}E_\mu t}e^{-\mathrm{i}\mu t\hat{Q}}|v\rangle\,, \tag{4.20}$$

where E_μ is the background energy, which is infinite in the infinite volume limit. In other words, there exists a one-parameter family of coherent states parameterized by μ, corresponding to a different $U(1)$ charge density, whose time evolution is purely generated by the symmetry operator. In [119], such states were named symmetry probing states. Therefore, in particular, our superfluid state remains coherent at all orders, and follows a "classical" time evolution, albeit with quantum-corrected relations between v and μ. It also follows from the transformation properties of the original fields under the $U(1)$ symmetry that the time-evolution of equal-time correlators is a simple phase rotation which goes as

$$\langle v|\prod_{i=0}^{N_1}\hat{\Phi}(x_i,t)\prod_{j=0}^{N_2}\hat{\Phi}^\dagger(x_j,t)\ldots|v\rangle = e^{i(N_1-N_2)\mu t}\langle v|\prod_{i=0}^{N_1}\hat{\Phi}(x_i,0)\prod_{j=0}^{N_2}\hat{\Phi}^\dagger(x_j,0)\ldots|v\rangle\,. \tag{4.21}$$

To summarize, we have shown that, thanks to charge conservation, a non-excited superfluid state, which can be thought of as the vacuum for perturbations around the superfluid background, maintains its coherence eternally. This can also be understood in terms of constituent particles, as the superfluid is a condensate of zero-momentum fundamental particles of mass m. In this language, it is clear how stability comes from charge conservation: such particles cannot annihilate, and thanks to homogeneity there are no rescattering processes that are kinematically allowed. Notice that, in the real scalar field case, quantum depletion was instead allowed since in that case there are no constraints on $4 \to 2$ processes coming from charge conservation [29].

In the remainder of the chapter, we shall analyze the state using the background field method, confirming its stability perturbatively and giving its explicit construction. This approach allows us to compute the one-loop quantum correction to the chemical potential. Then, we shall clarify how the specific choice of dressing that comes from its definition in terms of the vacuum of the Hamiltonian $\hat{H}'$ is key in ensuring stability, by studying an explicit counterexample. Finally, still applying the background field method, we shall

analyze the spectrum of the fluctuations of the superfluid state at one-loop. We show that a proper account of the quantum corrections indeed confirms the existence of a gapless mode as expected from Goldstone's theorem [109, 110].

4.2 From the semiclassical to the quantum description of superfluids

In this section, we first review the classical and semiclassical description of superfluids, and then we move on to the quantum description.

4.2.1 Classical and semiclassical superfluids

As shown in the introduction, homogeneous classical superfluids are described by solutions of the form

$$\Phi_{\rm SF}(t) = \frac{v}{\sqrt{2}} e^{{\rm i}\mu_{\rm c} t} \ , \tag{4.22}$$

with

$$\mu_{\rm c}^2 = m^2 + \lambda v^2 \ , \tag{4.23}$$

where the chemical potential $\mu_{\rm c}$ sets the energy required to add a particle to the system. As discussed above, superfluid solutions break both $U(1)$ and time-translational invariance, even though they preserve the combination generated by $H' = H - \mu N$.

In a semiclassical approach, one can study the fluctuations around a superfluid by expanding the original field as:

$$\Phi(x) = \frac{1}{\sqrt{2}} \Big\{ v + h_c(x) + {\rm i}\pi_c(x) \Big\} e^{{\rm i}\mu_{\rm c} t} \, , \tag{4.24}$$

and quantizing the fluctuations around their vacuum. This analysis only holds in the semiclassical limit, which is a large occupation number limit where the coupling is sent to zero, keeping the collective coupling constant:

$$\lambda \to 0, \qquad (v/\mu_c)^2 \to \infty, \qquad \frac{\lambda v^2}{\mu_c^2} \to \text{const} \ . \tag{4.25}$$

In the same limit, $n_{\rm SF}$ is divergent. Physically, this implies that h_c and π_c can be meaningfully interpreted as genuine fluctuations around the classical solution only when the number density of superfluid constituents becomes infinite. Beyond this limit, as we shall show shortly, the fields $h_c(x)$ and $\pi_c(x)$ defined above do not represent proper quantum fluctuations, as they develop tadpoles. Therefore, their expectation values do not vanish on the vacuum state describing the unperturbed superfluid, and this requires an update of the background.

With the assumption above, starting from the original theory and plugging the field redefinition into equation (4.13), we can obtain the Hamiltonian for the fluctuation fields:

$$\mathcal{H} = \frac{1}{2}\left\{(\Pi_c^h + \mu_c\pi_c)^2 + \partial_i h_c \partial^i h_c + (\Pi_c^\pi - \mu_{\rm cl} h_c)^2 + \partial_i \pi_c \partial^i \pi_c\right\} + \frac{\lambda}{4}\left(h_c^2 + \pi_c^2 + 2v h_c\right)^2 , \tag{4.26}$$

written in terms of the canonical momenta

$$\Pi_c^\pi = \dot{\pi}_c + \mu_{\rm c} h_c, \qquad \Pi_c^h = \dot{h}_c - \mu_{\rm c}\pi_c. \tag{4.27}$$

Since the resulting Hamiltonian is time independent, the theory of fluctuations can be quantized by the standard procedure around the vacuum of the fluctuation fields $|\Omega^s_{h,\pi}\rangle$ (see, for example, [120,121]). Therefore, $|\Omega^s_{h,\pi}\rangle$ represents the unexcited superfluid state in this approximation.

To obtain the spectrum of the fluctuations, we solve the linearized theory [122] and get the following dispersion relations

$$(\omega^2_\pm)_c = k^2 + \lambda v^2 + 2\mu_{\rm c}^2 \pm \sqrt{4k^2\mu_{\rm c}^2 + (\lambda v^2 + 2\mu_{\rm c}^2)^2}\ . \tag{4.28}$$

Here, we just report the result, not to repeat ourselves. We shall give more details once we move to the analogous spectrum of the quantum superfluid.

As expected, since the configuration (4.22) spontaneously breaks the $U(1)$ symmetry, the theory admits a gapless mode [109,110] given by the negative branch of the dispersion relation (4.28).

This gapless mode in the non-relativistic limit has the dispersion relation of a sound wave:

$$\omega_- \simeq c_s k \qquad \text{with} \qquad c_s^2 = \frac{\lambda v^2}{2\mu_c^2}. \tag{4.29}$$

This corresponds to the phonon, which is the only low-energy degree of freedom of the superfluid. The parameter c_s reduces to the sound speed of the superfluid in the non-relativistic limit. By comparing with (4.25), we see that the sound speed remains finite in the semiclassical limit.

Beyond the semiclassical limit, the superfluid background receives quantum corrections. In the semiclassical expansions, they are captured by tadpoles in the fluctuation fields: the condition $\langle h_c(x)\rangle = \langle \pi_c(x)\rangle = 0$ cannot be consistently maintained beyond the tree level. In perturbation theory, this is seen by considering loop corrections, at finite λ to the one-point function of the fluctuation fields.

For example, one can show that the cubic vertex $h\pi^2$ in the Hamiltonian (4.26) induces the following one-loop correction to the expectation value of the radial fluctuation

$$\langle h(x)\rangle \supset -\lambda^2 v^2\, {\rm Im}\int_{-\infty_-}^{t} d^4z\, \langle \pi^2_{c,0}(z)\rangle \langle h_{c,0}(z) h_{c,0}(x)\rangle\ , \tag{4.30}$$

where the expression has been evaluated using the in-in formalism in the interaction picture [46,123,124] as discussed in appendix A, and $h_{c,0}(x)$ and $\pi_{c,0}(x)$ are the fluctuation fields of the quadratic theory. We shall give more details on this approach in section 4.2.3.

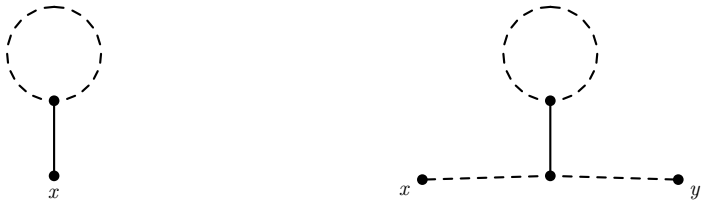

Figure 4.1: Example of tadpole diagrams. The first corresponds to a correction to the one-point function of the fluctuation field h. The second is a reducible diagram that appears in the computation of loop corrections to the $\langle\pi(x)\pi(y)\rangle$ correlation function. Diagrams of this type signal an incorrect choice of background and can be consistently reabsorbed into a shift from the classical solution to the quantum-corrected one.

Notice the appearance of an additional quantum coupling λ next to the classical collective coupling λv^2. The above correction is pictured as a tadpole diagram, represented by the left panel of Fig. 4.1, and signals that the expansion is organized around the incorrect background. Tadpole diagrams play a significant role in quantum field theory. On one hand, they encode information about the physical quantum-corrected background, as exemplified by the case of a real scalar condensate [29]. On the other hand, they also affect the dynamics of the fluctuations. For instance, tadpole contributions are crucial for ensuring that the Goldstone mode remains gapless beyond tree level, in agreement with non-perturbative results [109, 110]. In order to give a proper analysis of the superfluid beyond the semiclassical approximation, it is therefore convenient to apply the background field method consistently [29, 30], treating the superfluid solution as a one-point function over a properly defined state from the beginning. In the next section, we discuss the correct procedure to go beyond the semiclassical limit.

4.2.2 Quantum superfluids and the background field method

Quantum mechanically, an (unperturbed) superfluid is a state in the Hilbert space, which we shall denote by $|v\rangle$. As discussed in the introduction, at every time it defines both a one-point function and all the higher correlators. Let us first keep $|v\rangle$ fairly generic, by fixing only its one-point function at the initial time. Then, we shall obtain the relevant equations that shall describe the full dynamics. Finally, we clarify how the specific choice of state described in the introduction, namely the vacuum for the Hamiltonian of the fluctuations around the one-point function, correctly initializes time-independent correlation functions for the fluctuation fields, thereby providing a stable superfluid state.

To begin, we perform the following reparameterization of the scalar field

$$\Phi(x) = \frac{1}{\sqrt{2}}\left(v + h(x) + \mathrm{i}\pi(x)\right) e^{\mathrm{i}\mu t}. \tag{4.31}$$

where we shall call $h(x)$ and $\pi(x)$ radial and angular fluctuation fields respectively. The quantities v and μ are real parameters. We impose our condition on the one-point function

by taking the expectation value of the above relation over the state $|v\rangle$ and imposing:

$$\langle h(x)\rangle = \langle \pi(x)\rangle = 0 \qquad \Longrightarrow \qquad \langle \Phi(x)\rangle = \frac{v}{\sqrt{2}} e^{\mathrm{i}\mu t}, \tag{4.32}$$

This guarantees that the full dynamics of the one-point function is encoded in the parameters v and μ, while h and π are proper fluctuations [29,125], with vanishing tadpoles in the fully quantum theory. Also, the condition (4.32) fixes the initial condition for the one-point function of the field operator and its conjugate momentum at the time of definition of the state, with the first set by v and the second by μ. Let us remark that, in general, v and μ are time-dependent parameters, whose dynamics is specified by the equation of motion for the one-point function. However, we shall demonstrate that for a superfluid, they can be chosen to be time-independent. We will proceed as follows: at this stage, we assume that both v and μ are time-independent, as we are interested in a stable quantum superfluid configuration. Then, we will show that this assumption is consistent with the full quantum equations of motion, provided the state $|v\rangle$ is appropriately defined as in section 4.1.3. In other words, there exists a state for which a constant amplitude and chemical potential solve the full quantum Heisenberg equations of motion. In section 4.5, we will show that for different choices of the superfluid state, the time-independence property does not hold and one is forced to allow for a time dependence of the parameters.

Also, let us point out that unlike in the classical case where their relation is fixed by the classical equations of motion, v and μ are a priori independent, and they shall be connected with the quantum equation of motion for the one-point function.

Let us now determine the relation between the amplitude and the chemical potential in the full quantum theory. We apply the same approach discussed in section 4.1.2. The equations of motion for the field operator $\Phi(x)$ in the Heisenberg picture are:

$$\Box\Phi + m^2\Phi + 2\lambda|\Phi^2|\Phi = 0\,. \tag{4.33}$$

We shall substitute the field redefinition (4.31) in the above equation, still assuming that v and μ are time-independent functions. This leads to a set of two equations for the real and imaginary parts respectively:

$$\Box h + \left(-\mu^2 + m^2 + 3\lambda v^2\right) h - 2\mu\dot{\pi} + \left(m^2 + \lambda v^2 - \mu^2\right) v + \lambda v(3h^2 + \pi^2) + \lambda\left(h^3 + h\pi^2\right) = 0 \tag{4.34}$$

$$\Box\pi + \left(-\mu^2 + m^2 + \lambda v^2\right)\pi + 2\mu\dot{h} + \lambda\left(\pi^3 + h^2\pi + 2vh\pi\right) = 0\,. \tag{4.35}$$

To obtain the equations for the one-point function, we consider the expectation value of equation (4.34) and equation (4.35) over $|v\rangle$, and use the tadpole conditions:

$$\mu^2 = m^2 + \lambda v^2 + 3\lambda\langle h^2\rangle + \lambda\langle\pi^2\rangle + \frac{\lambda}{v}\langle h^3\rangle + \frac{\lambda}{v}\langle h\pi^2\rangle\,, \tag{4.36}$$

$$\lambda\left[\langle h\pi\rangle + \frac{1}{2v}\langle\pi h^2 + \pi^3\rangle\right] = 0. \tag{4.37}$$

As in section 4.1.2, this equation receives contributions from the equations for higher-order correlation functions. We kept the factor of λ explicit in equation (4.37) to make the loop expansion around the semiclassical limit (4.25) clearer. However, we shall drop it from now on.

Equation (4.36) gives us the quantum relation between v and μ for a stationary superfluid. It is the non-perturbative definition of the quantum chemical potential, and defines the quantum background that resums all tadpole diagrams that were emerging when expanding around the classical solution in the previous section. Notice that in the classical limit it reduces to the classical relation between the amplitude and the chemical potential. equation (4.37) is an identity that in the classical limit is trivial. We shall prove that it also vanished for a stationary superfluid. In section 4.5, we shall clarify its connection to the stability of the solution.

We remark again that the equations above have been obtained by assuming the time independence of μ and v. It remains to be proven that the above relations, coupled to the equations for the dynamics of the higher-order correlation functions, can indeed be satisfied by a constant μ and constant v provided that the state $|v\rangle$ is chosen appropriately. In particular, we have to understand the dynamics of the n-point functions of the fluctuations on the state $|v\rangle$, and show that there is a choice that makes all the correlators that enter in (4.36) time-independent. Notice that *only a specific choice* of the initial conditions for fluctuations guarantees this property, as we show in section 4.5.2.

The dynamics of the fluctuation fields is governed by a second set of equations, which in turn determines also the behavior of the correlation fluctuations in the fluctuation fields. These are obtained by plugging the relation back into equations (4.34) and (4.35), and read

$$(\Box + M_h^2)h + 2\mu\dot{\pi} + \lambda v(3h^2 - 3\langle h^2\rangle + \pi^2 - \langle\pi^2\rangle) + \lambda\left(h^3 - \langle h^3\rangle + h\pi^2 - \langle h\pi^2\rangle\right) = 0\ , \tag{4.38}$$

$$(\Box + M_\pi^2)\pi + 2\mu\dot{h} + \lambda\left(\pi^3 + h^2\pi + 2vh\pi\right) = 0\ . \tag{4.39}$$

Here, we defined

$$M_h^2 = 2\lambda v^2 - 3\lambda\langle h^2\rangle - \lambda\langle\pi^2\rangle - \frac{\lambda}{v}\langle h\pi^2\rangle - \frac{\lambda}{v}\langle\pi^3\rangle\,, \tag{4.40}$$

$$M_\pi^2 = -\lambda\langle\pi^2\rangle - 3\lambda\langle h^2\rangle - \frac{\lambda}{v}\langle\pi^3\rangle - \frac{\lambda}{v}\langle h\pi^2\rangle\,. \tag{4.41}$$

Before proceeding, some comments are due. First, we point out that these equations are coupled to the one that governs the one-point function (4.36), since the definition of the parameter μ needs also expectation values of the fluctuation field, whose dynamics in turn depend on μ. In a generic case, where both the equation for fluctuations and for the background are dynamical equations, it is possible (although technically difficult) to solve this system perturbatively, as shown for a real scalar field in [29, 30]. However, thanks to the time independence of the superfluid ansatz, in our case the situation is considerably simpler, as equation (4.36) is non-dynamical, and simply defines the chemical potential as a function of the amplitude. To sum up, the system of equations (4.36)–(4.39) fully encodes

the quantum dynamics of the background and its fluctuations, under the assumption of a constant amplitude and chemical potential.

Second, the operatorial equations of motion here depend explicitly on the expectation value of the operators themselves in the quantum state of the system. These additional terms are important, for example, in guaranteeing the tadpole condition $\langle h(x)\rangle = \langle \pi(x)\rangle = 0$ and making the formalism we defined self-consistent. They also source physical quantum effects. Third, notice that naively the angular mode seems to acquire a mass gap from the quantum contributions at one-loop. This might suggest that the would-be Goldstone boson becomes massive. However, we shall show in section 4.6 that this apparent gap is exactly canceled in the equation for the two-point function by non-linear interactions contributing at the same order, thereby guaranteeing the gaplessness of the Goldstone mode. Finally, in the classical limit, all contributions from correlation functions at time coincidence vanish, since (after proper renormalization) they carry contributions proportional to the coupling constant. Therefore, one recovers the treatment of the previous section.

To obtain a system of equations for correlation functions, we can take two approaches. First, as discussed in the introduction, we can multiply equations (4.38) and (4.39) by arbitrary products of $\pi(y_i)$ and $h(y_j)$, and then take the expectation value in the state $|v\rangle$. The result is an infinite, coupled hierarchy of ordinary differential equations for correlation functions, commonly referred to as the Schwinger–Dyson equations. We provide an example in section 4.6, where we study the two-point functions of the fluctuations to demonstrate the one-loop gaplessless of the angular mode. Alternatively, we can study the quantum theory of the fluctuation fields around the one-point function, and evaluate correlation functions perturbatively order by order on a given state. This is the approach that we shall use, as the choice of our superfluid state makes it particularly natural.

Indeed, as discussed in the introduction, we define our stable superfluid state as the vacuum state for the Hamiltonian that governs the dynamics of the fluctuation fields. This is a very natural definition, as the ground state for fluctuation fields is the state that minimizes the energy given the chosen one-point functions. In the next section, we discuss the quantum dynamics of the fluctuations, and we show how to evaluate perturbatively general correlation functions. Then, we proceed to prove the stability of our superfluid state using the background field method, in accordance with what we have discussed in section 4.1.2.

4.2.3 The dynamics of fluctuation fields and the interaction picture

To discuss the dynamics of the fluctuations, let us start by obtaining their Hamiltonian.

We begin by inserting the field redefinition (4.31) into the fundamental Lagrangian (4.13), from which we calculate the canonical momenta

$$\Pi^h = \dot{h} - \mu\pi, \qquad \Pi^\pi = \dot{\pi} + \mu h \ . \tag{4.42}$$

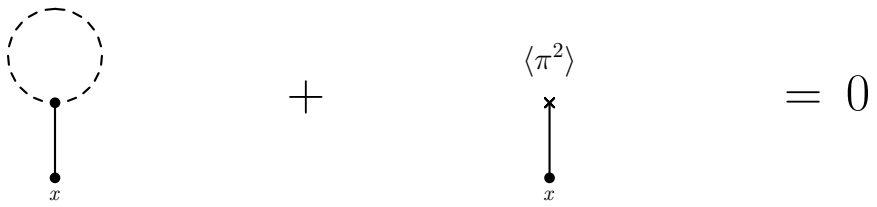

Figure 4.2: In the background field method, tadpoles in the interacting Hamiltonian are cancelled by those arising from nonlinear interaction terms. For instance, in the figure above, the vertex $h\langle\pi^2\rangle$ cancels the tadpole diagram that is generated by the cubic vertex $h\pi^2$.

We then impose the canonical equal-time commutation relations,

$$[h(\vec{x},0),\Pi^h(\vec{y},0)] = [\pi(\vec{x},0),\Pi^\pi(\vec{y},0)] = \mathrm{i}\delta(\vec{x}-\vec{y}) \ , \tag{4.43}$$

with all other commutators vanishing. Finally, we derive the full Hamiltonian $\mathcal{H} = \mathcal{H}_0 + \mathcal{H}_{\rm int}$, where

$$\mathcal{H}_0 = \frac{1}{2}\left\{(\Pi^\pi - \mu h)^2 + \partial_i\pi\partial^i\pi + (\Pi^h + \mu\pi)^2 + \partial_i h\partial^i h + 2\lambda v^2 h^2\right\} \ , \tag{4.44}$$

$$\mathcal{H}_{\rm int} = \frac{\lambda}{4}(\pi^2 + h^2 + 4hv)\left(h^2 - 3\langle h^2\rangle + \pi^2 - \langle\pi^2\rangle\right) . \tag{4.45}$$

The procedure is analogous to the one carried on in section 4.2.1; however, here we are expanding around the quantum one-point function. Notice that the Hamiltonian coincides with equation (4.18), when expanded in fluctuations around the one-point function, and is time-independent and bounded below.

Several points about the Hamiltonian are worth emphasizing. First, the terms proportional to μ^2 in the interaction Hamiltonian (4.45) have been removed by using the background equation (4.36). Second, notice that the interaction Hamiltonian $\mathcal{H}_{\rm int}$ still contains tadpole terms. However, these cancel precisely against tadpole diagrams generated by cubic and higher-order vertices, as displayed in Fig. 4.2. This is the same pattern that removes the apparent Goldstone mass. As we shall discuss in section 4.6.5, even if the quadratic terms in π within $\mathcal{H}_{\rm int}$ suggest a gap, loop corrections from higher-order interactions cancel this artifact once the expansion is treated consistently. Finally, we split the Hamiltonian into a free and an interacting part. One may object that we could express the chemical potential μ that appears in the free Hamiltonian (4.44) through μ_c and expectation values of fluctuations, and then move those expectation-value terms into $\mathcal{H}_{\rm int}$. However, this rearrangement obscures the physics, because it is μ, and not μ_c, that represents the renormalized, physical parameter of the superfluid. The same logic applies to the linear and quadratic pieces in $\mathcal{H}_{\rm int}$: while they could be absorbed into $\mathcal{H}_0$, their role in canceling tadpoles together with non-linear vertices is clearest if they remain within the interaction sector.

The Hamiltonian can be quantized perturbatively. Let us start by analyzing the free part. We shall denote by $\pi_0(x)$ and $h_0(x)$ the fields evolving with the free equations of motion. This notation will be useful once we introduce the interaction picture.

In the quadratic Hamiltonian (4.44), the radial and angular fields are kinetically mixed. Therefore, we cannot directly expand $h_0(x)$ and $\pi_0(x)$ in ladder operators. Instead, in order to identify the two independent degrees of freedom, we shall diagonalize the quadratic kinetic operator. Then, we obtain two degrees of freedom described by a mixing of $h_0(x)$ and $\pi_0(x)$, with a dispersion relation analogous to (4.28), albeit with $\mu_{\rm cl}$ replaced by μ. We shall now describe the quantization following [120, 121], where one can find all the necessary details. We introduce the ladder operators for the diagonal modes, defined as $a_\alpha(k)$ with $\alpha = \pm$, and impose that they satisfy the following commutation relations

$$[a_\alpha(k), a^\dagger_\beta(k')] = (2\pi)^3 \delta_{\alpha\beta} \delta^{(3)}(k-k') \ . \tag{4.46}$$

The ladder operators above are connected to the free radial and angular quantum fields by the following expansion:

$$\phi^a_0(x) = \sum_{\alpha=+,-} \int \frac{d^3k}{(2\pi)^3\sqrt{2\omega_\alpha}} \left(a_\alpha Z^a_\alpha e^{-{\rm i}\omega_\alpha t + {\rm i}k\cdot x} + {\rm h.c.} \right) , \tag{4.47}$$

$$\Pi^a_0(x) = \sum_{\alpha=+,-} \int \frac{d^3k}{(2\pi)^3\sqrt{2\omega_\alpha}} \left(\left(-{\rm i}\omega_\alpha Z^a_\alpha + \mu \epsilon_{\alpha\beta} Z^a_\beta \right) a_\alpha e^{-{\rm i}\omega_\alpha t + {\rm i}\vec{k}\cdot x} + {\rm h.c.} \right) , \tag{4.48}$$

with $\phi^1 = \pi$ and $\phi^2 = h$. The wavefunction coefficients required for the compatibility of the commutator (4.46) with the canonical commutation relations read

$$Z^\pi_\pm(k) = (-{\rm i})^{\frac{1}{2}\pm\frac{1}{2}} \sqrt{\frac{1}{2} \pm \frac{2\mu^2 - \lambda v^2}{2\sqrt{4k^2\mu^2 + (\lambda v^2 + 2\mu^2)^2}}} \ , \tag{4.49}$$

$$Z^h_\pm(k) = (-{\rm i})^{\frac{1}{2}\mp\frac{1}{2}} \sqrt{\frac{1}{2} \pm \frac{2\mu^2 + \lambda v^2}{2\sqrt{4k^2\mu^2 + (\lambda v^2 + 2\mu^2)^2}}} \ . \tag{4.50}$$

The non-trivial wavefunction coefficients Z^a_α appear because of the kinetic mixing.

The free vacuum of $\mathcal{H}_0$, $|0_{h,\pi}\rangle$ is, as always, the state annihilated by all the $a_\alpha(k)$, for every $\vec{k}$.

In the last part of this section, we introduce the interaction picture for the fluctuations, as in [120, 121]. The interaction picture fields evolve only under the time evolution set by H_0. These are related to the Heisenberg picture fields by

$$\pi(x) = U^\dagger(t, t_*)\pi_0(x)U(t, t_*), \qquad h(x) = U^\dagger(t, t_*)h_0(x)U(t, t_*) \, . \tag{4.51}$$

Here, t_* is the standard fiducial time at which the interaction and Heisenberg picture coincide. The operator $U(t_1, t_2)$ is the interaction picture evolution operator, determined as

$$U(t_1, t_2) = \mathcal{T} \exp\left\{ -{\rm i} \int_{t_2}^{t_1} d^4z \, \mathcal{H}_{\rm I}(z) \right\} \ , \tag{4.52}$$

where $\mathcal{H}_{\rm I}(z) = \mathcal{H}_{\rm int}[h_0(z), \pi_0(z)]$ and with $d^4z = dz^0 d^3z$.

The interaction picture formalism allows for an easy perturbative computation of (equal-time) correlation functions. A generic, time-dependent correlator of Heisenberg operators on a state $|v\rangle$ can be expressed as:

$$\langle v|\mathcal{O}[h,\pi]|v\rangle = \langle v|U^\dagger(t,t_*)\mathcal{O}[h_0,\pi_0]\ U(t,t_*)|v\rangle\,. \tag{4.53}$$

Of course, this requires an explicit form for the state $|v\rangle$. In the next section, we apply the interaction picture to discuss how our choice of the superfluid state as the ground state of $\mathcal{H}$ translates into appropriate, time-independent correlators.

4.3 The stable superfluid state

In this section, we present the explicit expression for the stable superfluid state and discuss its various descriptions in different languages.

The equations that we have derived up to now are valid with the only assumption that the state $|v\rangle$ is characterized by a constant radial amplitude and a time-independent chemical potential. Such a state is uniquely identified with the interacting vacuum of the fluctuation Hamiltonian (the sum of equations (4.44) and (4.45)), $|v\rangle \equiv |\Omega_{h,\pi}\rangle$.

The interacting vacuum can be written in terms of the interaction-picture evolution of the free vacuum $|0_{h,\pi}\rangle$, namely the ground state of the quadratic Hamiltonian (4.44), as [3]:

$$|v\rangle \equiv |\Omega_{h,\pi}\rangle = U(t_*, -\infty_-)|0_{h,\pi}\rangle, \tag{4.54}$$

with $\infty_\pm = \infty(1 \pm \mathrm{i}\epsilon)$.

Next, we prove that the correlation functions on the state in question have the following properties:

(i) Equal time correlation functions of the fluctuation fields $h(x)$ and $\pi(x)$ in their interacting vacuum are time-independent.

(ii) All the correlation functions containing an odd power of $\pi(x)$ vanish.

These two properties are sufficient to show, respectively, that the equations for the background equation (4.36) and (4.37) are satisfied. Therefore, they guarantee that the state $|v\rangle$ describes a stable superfluid.

The property (i) is trivially satisfied given the definition of the superfluid state and the time independence of the full Hamiltonian density governing the fluctuation theory. To see it explicitly in interaction picture, let us write a generic expectation value involving the fluctuation fields, as in equation (4.53), in the form

$$\langle v|\mathcal{O}[h,\pi]|v\rangle = \langle 0_{h,\pi}|U^\dagger(t,-\infty_-)\mathcal{O}[h_0,\pi_0]\ U(t,-\infty_-)|0_{h,\pi}\rangle\,. \tag{4.55}$$

[3] This last identity is the standard projection of the interacting vacuum on the free vacuum (see chapter 4.2 of [123]).

The expression above is a standard in-in correlator evaluated on a stable vacuum. Its time independence holds under two conditions: that the mode wavefunctions of the quadratic theory do not depend on time, and similarly that the couplings appearing in the interaction Hamiltonian are also time-independent. The first condition is trivial. The second condition requires more care because, in the background-field method, the interaction coefficients are themselves functions of equal-time correlators. Therefore, one could imagine that there's a circularity in assuming them to be time independent. However, everything is clarified by the structure of the loop expansion: at each order, the interaction coefficients are fixed entirely by correlators computed at lower orders. Consequently, by induction, if tree-level correlators are time independent, no spurious time dependence appears at any finite order in perturbation theory.

Next, we consider property (ii). Such a property is similar in spirit to what happens in the case of spontaneous symmetry breaking (SSB) in a vacuum. There, the underlying $\mathbb{Z}_2$ symmetry of the π-sector guarantees that all correlators involving an odd number of Goldstone fluctuations vanish. For a superfluid, however, due to the kinetic mixing between radial and angular modes such a symmetry is broken. For example, one can check that the mixed correlator $\langle h(x)\pi(y)\rangle$ doesn't vanish for $t_x \neq t_y$.

However, we can prove that all correlators of the type considered vanish at equal times. This is guaranteed by a symmetry of the fluctuation Hamiltonian, which reflects the CT symmetry of a stable superfluid. In terms of the π field, it reads:

$$\pi \to -\pi, \qquad t \to -t. \tag{4.56}$$

It is easy to check that the kinetic mixing term is invariant under the transformation above. Obviously, the vacuum of $\mathcal{H}$, $|v\rangle = |\Omega_{h,\pi}\rangle$ is also invariant under this symmetry.

As a result, equal-time correlators obey

$$\langle v|h^m(x,t),\pi^n(\vec{x},t)|v\rangle = (-1)^n\langle v|h^m(x,-t),\pi^n(\vec{x},-t)|v\rangle = (-1)^n\langle v|h^m(x,t),\pi^n(\vec{x},t)|v\rangle, \tag{4.57}$$

where in the last step we used the time-independence of equal-time correlators, as established in (i). If n is odd, equation (4.57) implies that correlation functions involving an odd number of π vanish when evaluated at the same time.

Thus, we have proven that the vacuum state for the fluctuation fields around the one-point function (4.32), namely, the state which minimizes the energy of fluctuations around such a background, indeed describes a stable homogeneous superfluid.

4.3.1 Defining the superfluid state without the fluctuation fields

In this paragraph, we clarify the meaning of the state discussed above in terms of the fundamental field of the theory. First, we show how to reconstruct it in terms of its correlation functions. Then, we give an explicit expression in terms of an appropriately dressed coherent state, which can be obtained by acting on the vacuum of the theory with specific operators built out of the original field operator and its conjugate momentum.

In the previous section, we performed a field reparametrization to define the quantized fluctuation fields $h(x)$ and $\pi(x)$, and we defined the superfluid state starting from their dynamics. On the other hand, clearly one should also be allowed to first quantize the theory in terms of the fundamental field $\Phi(x)$, and then directly select the state representing a given configuration, such as the superfluid state above. Let us first clarify the connection between the two approaches in terms of the correlation functions of the superfluid state. In order to do so, we demonstrate how to define the stable superfluid state directly in terms of $\Phi(x)$, without reference to the Hilbert space of $h(x)$ and $\pi(x)$.

We shall characterize the state by providing all the correlation functions of the field operator and its conjugate momentum at the time of its definition $t = 0$. Here, we obtain them from the definition given above. Clearly, one is free to take them as a definition of the state, and use the fluctuation fields just as auxiliary tools to obtain the proper set of initial conditions at initial time.

First, we determine the one-point functions of the field operator and its conjugate momentum in the superfluid state $|v\rangle$. These follow directly from its definition:

$$\langle v|\Phi(\vec{x},0)|v\rangle = \langle v|\Phi^\dagger(\vec{x},0)|v\rangle = \frac{v}{\sqrt{2}}, \qquad \langle v|\Pi(\vec{x},0)|v\rangle = -\langle v|\Pi^\dagger(\vec{x},0)|v\rangle = -\mathrm{i}\mu\frac{v}{\sqrt{2}}. \tag{4.58}$$

In order to obtain a coherent dynamics, the chemical potential μ must be related to v through equation (4.36). This requires higher correlation functions of the fluctuation fields, which are ultimately only c-number functions of the parameters m, λ, and v and can be taken as given as part of the initial conditions for the quantum state.

Next, we describe the higher correlators. We concentrate on the two-point function; the rest follows analogously. To characterize the higher-order correlation functions of the original field $\Phi(x)$, we rewrite it by the transformation (4.31). Since we know the correlation functions in terms of fluctuations, this allows us to reconstruct the correlators that we desire to obtain. For example, the two-point function is characterized by

$$\langle v|\Phi(\vec{x},0)\Phi^\dagger(\vec{y},0)|v\rangle = \frac{v^2}{2} + \frac{1}{2}\left\{\langle\Omega_{h,\pi}|h(\vec{x},0)h(\vec{y},0)|\Omega_{h,\pi}\rangle + \langle\Omega_{h,\pi}|\pi(\vec{x},0)\pi(\vec{y},0)|\Omega_{h,\pi}\rangle\right\}, \tag{4.59}$$

$$\langle v|\Phi(\vec{x},0)\Phi(\vec{y},0)|v\rangle = \frac{1}{2}\Big(v^2 + \langle\Omega_{h,\pi}|h(\vec{x},0)h(\vec{y},0)|\Omega_{h,\pi}\rangle - \langle\Omega_{h,\pi}|\pi(\vec{x},0)\pi(\vec{y},0)|\Omega_{h,\pi}\Big). \tag{4.60}$$

Similar conditions apply to the conjugate momenta and to the complex conjugates of the expressions above. We have used once more that the correlators with an odd number of π fields vanish at equal times. The extension to higher-order correlators follows straightforwardly.

As a consistency check, let us show that in the limit of $v \to 0$, where the superfluid disappears, the state $|v\rangle = |\Omega_{h,\pi}\rangle$ reduces to the fundamental vacuum of the theory. We

exemplify it by considering the tree-level two-point function:

$$\lim_{v\to 0}\langle v|\Phi(\vec{x},0)\Phi^\dagger(\vec{y},0)|v\rangle = \frac{1}{2}\int \frac{d^3k}{2\omega_k(2\pi)^3}\Big(\underbrace{1}_{h}+\underbrace{1}_{\pi}\Big)e^{i\vec{k}\cdot(\vec{x}-\vec{y})} = \int \frac{d^3k}{(2\pi)^3 2\omega_k}e^{i\vec{k}\cdot(\vec{x}-\vec{y})}, \tag{4.61}$$

$$\lim_{v\to 0}\langle v|\Phi(\vec{x},0)\Phi(\vec{y},0)|v\rangle = \frac{1}{2}\int \frac{d^3k}{2\omega_k(2\pi)^3}\Big(\underbrace{1}_{h}-\underbrace{1}_{\pi}\Big)e^{i\vec{k}\cdot(\vec{x}-\vec{y})} = 0, \tag{4.62}$$

where $\omega_k^2 = k^2 + m^2$ is the standard vacuum dispersion relation.

With this correlation functions at initial time as the set of initial conditions, the Heisenberg equation for $\Phi(x)$, as given by equation (4.33), will describe the same stationary superfluid configuration previously characterized using the fluctuation fields. This gives an equivalent way of characterizing the superfluid, in terms of correlators of the fundamental field and conjugate momenta.

4.3.2 The superfluid as a dressed coherent state

After having described the superfluid state from its correlation functions, we can give an explicit formula to express it as a state built of the perturbative free vacuum of the full theory. Of course, if needed, it can also be connected to the full vacuum through the Gell-Mann Low formula. This approach, for instance, is particularly useful when constructing a coherent state in an interacting quantum field theory, as demonstrated in [28, 29]. In this case, the corresponding operator is simply an exponential, with an exponent that is linear in the field content. In contrast, if the exponent is quadratic in the field content, it generates a squeezed state [31].

To obtain the superfluid state explicitly, it is enough to connect the free vacuum for the fluctuation fields h and π, with the free vacuum of the original field Φ. In particular, $|0_{h,\pi}\rangle$ is a squeezed coherent state on top of the free vacuum $|0\rangle$, defined in terms of the free Hamiltonian of Φ and $\Phi^\dagger$. A squeezed coherent state is obtained by acting on $|0\rangle$ by operators of the form $\hat{f}$ and $\hat{S}$

$$|C\rangle = e^{-if[\Phi_i]}\, e^{-iS[\Phi_i]}|0\rangle, \tag{4.63}$$

where,

$$\hat{f} = \int d^3x \left\{\Pi_i^{\rm cl}(\vec{x})\,\hat{\Phi}_i(\vec{x}) - \hat{\Pi}_i(\vec{x})\,\Phi_i^{\rm cl}(\vec{x})\right\}, \tag{4.64}$$

$$\hat{S} = \int d^3x\, d^3y \begin{pmatrix}\hat{\Pi}_i(\vec{x}) & \hat{\Phi}_i(\vec{x})\end{pmatrix}\begin{pmatrix}\Delta_{11}^{ij}(\vec{x}-\vec{y}) & \Delta_{12}^{ij}(\vec{x}-\vec{y}) \\ \Delta_{12}^{ij*}(\vec{x}-\vec{y}) & \Delta_{22}^{ij}(\vec{x}-\vec{y})\end{pmatrix}\begin{pmatrix}\hat{\Pi}_j(\vec{y}) \\ \hat{\Phi}_j(\vec{y})\end{pmatrix}, \tag{4.65}$$

and we are using the real basis

$$\Phi = \frac{1}{\sqrt{2}}\left(\Phi_1 + i\Phi_2\right). \tag{4.66}$$

The operator $\hat{f}$, called the displacement operator, generates a pure coherent state and shifts the one-point function of the field and its canonical momentum to the profiles $\Phi^{\rm cl}$ and $\Pi^{\rm cl}$. The operator $\hat{S}$, the squeezing operator, is more easily understood in terms of ladder operators:

$$S = \int \frac{d^3k}{2(2\pi)^3} \sum_{i,j=1,2} \left(\alpha_{ij} a^i_{\vec{k}} \, a^j_{-\vec{k}} + \text{h.c.} \right) \tag{4.67}$$

and generates the Bogoliubov transformation that correctly diagonalizes the quadratic Hamiltonian for fluctuations around the new background. All in all, it holds that

$$\langle C|\mathcal{O}[\Phi_i, \Pi_i]|C\rangle = \langle 0|\mathcal{O}[\Phi_i^{\rm cl} + e^{{\rm i}\hat{S}} \hat{\Phi}_i e^{-{\rm i}\hat{S}}, \Pi_i^{\rm cl} + e^{{\rm i}\hat{S}} \hat{\Pi}_i e^{-{\rm i}\hat{S}}]|0\rangle, \tag{4.68}$$

Therefore, imposing

$$\Phi_1^{\rm cl} = v, \quad \Phi_2^{\rm cl} = 0, \qquad \Pi_1^{\rm cl} = 0, \quad \Pi_2^{\rm cl} = \mu v \ . \tag{4.69}$$

gives the correct expectation value. The action of $e^{{\rm i}\hat{S}}$ with appropriately chosen coefficients takes care of the Bogoliubov transformation. For more details, one can refer, for example, to [31], where they consider a real scalar field.

All the above implies that the interacting vacuum for fluctuations can be written as

$$\begin{aligned} |v\rangle \equiv & \mathcal{T} \exp\left\{ -{\rm i} \int_{-\infty_-}^{0} d^4z \, \mathcal{H}_{\rm I}[h_0(z), \pi_0(z)] \right\} |0_{h,\pi}\rangle \\ = & \mathcal{T} \exp\left\{ -{\rm i} \int_{-\infty_-}^{0} d^4z \, \mathcal{H}_{\rm I}[h_0[\Phi(z), \Phi^\dagger(z)], \pi_0[\Phi(z), \Phi^\dagger(z)]] \right\} \exp\left\{ {\rm i}\hat{f}[\Phi, \Phi^\dagger] \right\} \exp\left\{ {\rm i}\hat{S}[\Phi, \Phi^\dagger] \right\} |0\rangle. \end{aligned} \tag{4.70}$$

It is important to remark that the stationary superfluid state is intrinsically a non-Gaussian state. In section 4.5.2, we shall show that neglecting these non-Gaussianities and representing the superfluid state merely as a squeezed coherent state leads to a configuration unstable at the quantum level.

4.3.3 The superfluid state as the ground state of $\hat{H} - \mu\hat{N}$

Finally, let us further clarify the dynamics of our stable superfluid state. We have already discussed in the introduction how, although it is not an eigenstate of the Hamiltonian, its evolution is nevertheless trivial in the sense that the time dependence of all correlation functions of the field operator $\Phi(x,t)$ (and conjugate momentum) simply reduces to an overall oscillating phase.

The essence of this phenomenon is that the superfluid state satisfies the relation

$$\left(\hat{H} - \mu \hat{Q} \right) |c\rangle = 0 \, . \tag{4.71}$$

Thus, while it is not an eigenstate of the Hamiltonian, it is an eigenstate of the modified operator $\hat{H} - \mu\hat{Q}$. In [119], these states have been referred to as spontaneous symmetry

probing (SSP) states. For states satisfying this identity, the dynamics is controlled by the generator of the symmetry Q. Therefore, this leads to a preservation of coherence, since the only effect of the time evolution is a motion along the orbits of the symmetry under consideration.

We now expand on the procedure followed in the introduction to further clarify the nature of $|v\rangle$.

As discussed in the previous section, $|v\rangle$ is the state that minimizes the Hamiltonian for fluctuations, obtained from the Lagrangian (4.13) after performing the field redefinition (4.31). This field redefinition is implemented by a canonical transformation, which we decompose into two steps:

$$\Phi(x,t) = e^{\mathrm{i}\mu t\hat{Q}}\Phi'(x,t)e^{-\mathrm{i}\mu t\hat{Q}} = e^{\mathrm{i}\mu t}\Phi'(x,t)\,, \tag{4.72}$$

$$\Phi'(t) = v + h + \mathrm{i}\pi\ . \tag{4.73}$$

Here, $\hat{Q}$ is the charge associated with the $U(1)$ symmetry. A similar relation applies to the conjugate momentum. For a time-dependent canonical transformation implemented on the field content by a unitary operator of the form

$$\Phi \to \Phi' = e^{\mathrm{i}\alpha(t)\hat{T}}\Phi e^{-\mathrm{i}\alpha(t)\hat{T}}, \tag{4.74}$$

the Hamiltonian transforms as [4]

$$H[\Phi] \to \tilde{H}[\Phi'] = H[\Phi'] - \partial_t(\alpha(t)T[\Phi'])\,. \tag{4.75}$$

If we now consider the case in (4.72), the modified Hamiltonian that controls the evolution of Φ' is:

$$\tilde{H} = H[\Phi'] - \mu Q[\Phi']. \tag{4.76}$$

After a second, time-independent shift to the fluctuations around the v.e.v given by equation (4.73), this Hamiltonian coincides with equations (4.44)-(4.45). Therefore, the state $|v\rangle$ indeed is the ground state of the Hamiltonian (4.44)-(4.45), and satisfies the relation (4.71).

Let us point out that, from the general behaviour of correlation functions given in equation (4.21), it follows in particular that the one-point function tracks the classical behaviour:

$$\langle v(t)|\phi(x)|v(t)\rangle = \frac{iv}{\sqrt{2}}e^{i\mu t}. \tag{4.77}$$

To sum up, in this section we showed how the superfluid state can be described from the various possible perspectives, and we made explicit the connection between its stability and its peculiar properties under the $U(1)$ symmetry of the theory. In the next section, we shall use the power of the background field method to compute one-loop corrections to the chemical potential.

[4] This can be proven by substituting the field redefinition in the Heisenberg equation of motion, $\dot{\Phi} = i[H,\Phi]$. Then, one obtains that the new field variables and respective conjugate momenta evolve according to the modified Hamiltonian (4.75).

4.4 The renormalized one-loop chemical potential

In this section, we study the equations (4.36) and (4.37), that define the relations between v and μ, at one-loop order. In particular, we compute the one-loop corrections to the classical relation (4.23). We show that the divergences that appear can be renormalized just with the counterterms needed for the standard renormalization for processes around the vacuum. This is similar to what happens for the one-loop correction to the kink mass discussed in section 1.1.3, and it is an important consistency check of the validity of our definition. In general, it happens that coherent states without appropriate dressings develop physical infinities that cannot be cured by renormalization [29, 31, 104], we show that our definition gives rise to a physical state where all the quantities of interest are finite.

The one-loop corrections to the chemical potential appear as expectation values of powers of the fluctuation fields. In particular, we shall evaluate the correlation functions appearing in equation (4.36) at coincidence. To this end, we use the identity given in equation (4.55), and we expand the Dyson operator in powers of the interaction Hamiltonian. The in-in version of the S-matrix computation is discussed in [124], and reviewed in Appendix A. For correlation functions of Hermitian operators at time coincidence, one obtains:

$$\langle v|\mathcal{O}(x)|v\rangle = \langle \mathcal{O}_0(x)\rangle - 2\,\mathrm{Im}\int_{-\infty_-}^{t} d^4z_1\,\langle \mathcal{H}_I(z_1)\mathcal{O}_0(x)\rangle + \int_{-\infty_+}^{t} d^4z_1\int_{-\infty_-}^{t} d^4z_2\,\langle \mathcal{H}_I(z_1)\mathcal{O}_0(x)\mathcal{H}_I(z_2)\rangle$$
$$- 2\,\mathrm{Re}\int_{-\infty_+}^{t} d^4z_2\int_{-\infty_+}^{t_1} d^4z_1\,\langle \mathcal{H}_I(z_1)\mathcal{H}_I(z_2)\mathcal{O}_0(x)\rangle + \dots\,, \tag{4.78}$$

where $\mathcal{O}_0(x) = \mathcal{O}[h_0(x), \pi_0(x)]$, and all expectation values of the right-hand side of (4.78) are taken over the free vacuum. The interaction Hamiltonian is given by (4.45). Here, we report it split into cubic and quartic terms

$$\mathcal{H}_{\mathrm{I}}^{(3)} = \lambda v\left(h^3 - 3\langle h^2\rangle h\right) + \lambda v(h\pi^2 - \langle\pi^2\rangle h) \tag{4.79}$$

$$\mathcal{H}_{\mathrm{I}}^{(4)} = \frac{\lambda}{4}\left(h^2+\pi^2 - 3\langle h^2\rangle - \langle\pi^2\rangle\right)\left(\pi^2+h^2\right). \tag{4.80}$$

Therefore, we apply equation (4.78) to evaluate the equation for the chemical potential in equation (4.36). Perturbatively, at a generic order, the correlators in (4.78) can be calculated by rewriting them as products of two-point functions at tree level, using Wick theorem. The latter are quickly obtained from the modes decomposition provided in section 4.2.3.

Notice that there are two parameters controlling the interactions. One is the classical collective coupling λv^2, the other is the true quantum coupling λ. In the classical limit, only the first survives. Instead, the quantum perturbative expansion is organized in powers of λ alone. For example, two insertions of the cubic vertex $\mathcal{H}_{\mathrm{I}}^{(3)}$ shall contribute with a weight of order $\lambda\,(\lambda v^2)$, which is the same loop (or equivalently, λ) order of one insertion of the quartic vertex $\mathcal{H}_{\mathrm{I}}^{(4)}$, similarly to what happens in perturbation theory around the vacuum.

At one loop, we just need the first term of (4.78), which singles out the quadratic correlators. The two-point functions at coincidence read:

$$\langle h_0^2(x)\rangle = \int \frac{d^3k}{(2\pi)^3 2}\left(\frac{|Z_+^h|^2}{\omega_+}+\frac{|Z_-^h|^2}{\omega_-}\right), \quad \langle \pi_0^2(x)\rangle = \int \frac{d^3k}{(2\pi)^3 2}\left(\frac{|Z_+^\pi|^2}{\omega_+}+\frac{|Z_-^\pi|^2}{\omega_-}\right). \tag{4.81}$$

One obtains the following one-loop chemical potential:

$$\mu^2_{\text{1-loop}} = m^2_{\text{ph}} + \lambda_{\text{ph}} v^2 \left\{1 + \frac{3\lambda_{\text{ph}}}{4\pi^2}\left[1 + f(c_s)\right]\right\}, \tag{4.82}$$

with

$$f(c_s) = -\frac{c_s^2}{3} - \frac{(1-c_s^2)}{3}\sqrt{1+\frac{1}{c_s^2}} + \left(1+\frac{1}{3c_s^2}\right)\log\left(\frac{c_s+\sqrt{1+c_s^2}}{\sqrt{1-2c_s^2}}\right), \tag{4.83}$$

and where the non-relativistic adiabatic sound speed c_s is given by equation (4.29).

The expression (4.82), has been made finite by the renormalization of the mass and the coupling, as

$$m^2_{\text{ph}} = m^2 + \frac{\lambda}{2\pi^2}\left\{\Lambda^2 + \frac{m^2}{2} - m^2\log\left(\frac{2\Lambda}{m}\right)\right\}, \qquad \lambda_{\text{ph}} = \lambda - \frac{5\lambda^2}{4\pi^2}\log\left(\frac{2\Lambda}{m}\right), \tag{4.84}$$

with Λ an ultraviolet regulator.

Notice that all the divergences can be cured by the same counterterms that are needed to renormalize the theory in the vacuum and no additional infinities appear. Let us stress again that not all states have their dynamics regularized by the same counterterms used in the vacuum theory. As shown in [29, 31, 104], discrepancies in this direction often hint at issues with the chosen configuration, such as a divergent energy density of the system. Let us also remark that the one-loop chemical potential is time-independent as expected, and that in the semiclassical limit (4.25), the one-loop correction vanishes, recovering the classical relation (4.23) for the relativistic chemical potential as a function of v.

The procedure to obtain the chemical potential can be systematically extended at arbitrary loop orders. For example, the chemical potential at two-loops can be obtained from equation (4.36) by evaluating at one-loop quadratic correlation functions $\langle h^2\rangle$ and $\langle \pi^2\rangle$, and at tree-level the correlation functions $\langle h^3\rangle$ and $\langle h\pi^2\rangle$.

To conclude, we point out that our result matches with the analog derivation performed in [126], where the authors evaluated the one-loop corrections to the effective potential in a general $U(1)$-invariant theory, and found that field-independent prescriptions are enough to make the effective potential finite.

4.5 Two-loops (in-)stability

In this section, we clarify the importance of choosing our specific superfluid state in order to guarantee stability at all orders. In particular, we show that not all states whose one-point

function reproduces the classical behaviour (4.22) at early times remain stable quantum mechanically. On the contrary, the precise highly non-Gaussian structure of the interacting vacuum in equation (4.54) is pivotal in ensuring stationarity.

To prove our point, first we analyze the conditions for a stationary superfluid (4.36) and (4.37) explicitly at two-loop level in perturbation theory, for the stable superfluid state $|v\rangle$. Even if the stability is clear and already proven at all orders, we shall analyze it in a perturbative approach to point out what can (and indeed, will) go wrong for different choices of the superfluid state. Then, we examine what happens when the interacting (non-Gaussian) vacuum is replaced with a Gaussian state, such as a squeezed coherent state. We show that such a state, even if it looks semiclassically stable, develops instabilities starting at two-loop order. In particular, the one-point function of the field operator begins to deviate from the stationary profile (4.32). Thus, we prove that in interacting field theories undressed coherent states are not optimal in tracking the classical dynamics, and should be replaced by properly dressed states. Also, we clarify how our formalism can be applied to non-equilibrium situations where there is a non-trivial quantum dynamics.

It goes without saying that, for a general time-dependent classical profile, even the optimal choice for a quantum state, represented by the instantaneous ground state of the Hamiltonian for fluctuations around the one-point function, shall deviate from the classical dynamics due to quantum effects sourced by higher-order correlation functions. Full stability can only be obtained under very specific circumstances, as the one under consideration in this chapter.

4.5.1 Explicit check of the two-loop stability

The explicit perturbative evaluation of the two-loop contributions to the chemical potential is quite cumbersome and not instructive. However, it is straightforward to show for the very definition of the superfluid state $|v\rangle$ that the resulting correlation functions are time-independent. The key element to this fact is that the definition of the superfluid as the interacting vacuum (4.55) extends the time integration in the Dyson series (4.78) all the way to $-\infty$, thus mimicking a vacuum process.

We shall demonstrate it, without loss of generality, by considering the cubic correlator $\langle h^3\rangle$:

$$\langle h^3\rangle \sim \sum_{\alpha,\beta,\gamma=\pm}\int d^3k_1 d^3k_2 \int_{-\infty_-}^{t} dt_z f_{\alpha\beta\gamma}(k_1,k_2) e^{-\mathrm{i}(\omega_\alpha(k_1)+\omega_\beta(k_2)+\omega_\gamma(k_1+k_2))(t_z-t)} \tag{4.85}$$

$$\sim \sum_{\alpha,\beta,\gamma=\pm}\int d^3k_1 d^3k_2 \int_{-(\infty+t)+(\mathrm{i}\epsilon)\infty}^{0} d\tilde{t}\, f_{\alpha\beta\gamma}(k_1,k_2) e^{-\mathrm{i}(\omega_\alpha(k_1)+\omega_\beta(k_2)+\omega_\gamma(k_1+k_2))\tilde{t}}, \tag{4.86}$$

where we introduced the shifted integration variable $\tilde{t} = t_i - t$. Also, $f_{\alpha\beta\gamma}$ are the time-independent functions of the spatial momenta k_1 and k_2 that emerge from the Wick contractions. The time-independence of $f_{\alpha\beta\gamma}(k_1,k_2)$ follows from the time-independence of

both the wavefunction coefficients of the quadratic theory and the coefficients in the interaction Hamiltonian. We see that, after performing the shift in the time integration variable, the contribution from the lower limit is exponentially suppressed by the imaginary time rotation at infinity, and therefore vanishes. Consequently, the correlation function is time independent.

This is general: for an arbitrary correlation function, integrands will only depend on time differences of the form $t_i - t$, where t_i are internal times. By redefining the time integration variables, the explicit dependence on the external time t can always be completely shifted to the lower integration limits. Since the time contour begins at $-\infty_\pm$, shifting the contour by a finite and real amount does not affect the damping behavior and these contributions vanish, making the correlator time-independent. This confirms, for example, that quantum corrections to the chemical potential remain time-independent.

To ensure stability, we should also examine equation (4.37), and show that the correlators identically vanish. Again, this has already been proven in section 4.3 thanks to the CT symmetry. However, we shall obtain the same result perturbatively. This will be important when moving to an unstable superfluid state. Let us then consider equation (4.37) at order $\hbar^2$. First, we consider the one-loop dynamics. At one-loop, the relevant corrections are obtained by evaluating the quadratic correlation function at the leading order in the interaction Hamiltonian. Therefore, we reduce to consider the free two-point function $\langle \pi_0(x) h_0(x) \rangle$. Since the free two-point functions are the building blocks of the perturbative expansion and we shall need them in the next section, we report them here:

$$\langle \pi_0(x)\pi_0(y)\rangle = \int \frac{d^3k}{(2\pi)^3 2}\left(\frac{|Z^\pi_+|^2}{\omega_+}e^{-\mathrm{i}\omega_+(t-t')} + \frac{|Z^\pi_-|^2}{\omega_-}e^{-\mathrm{i}\omega_-(t-t')}\right)e^{\mathrm{i}\vec{k}\cdot(\vec{x}-\vec{y})}\ , \tag{4.87}$$

$$\langle h_0(x)h_0(y)\rangle = \int \frac{d^3k}{(2\pi)^3 2}\left(\frac{|Z^h_+|^2}{\omega_+}e^{-\mathrm{i}\omega_+(t-t')} + \frac{|Z^h_-|^2}{\omega_-}e^{-\mathrm{i}\omega_-(t-t')}\right)e^{\mathrm{i}\vec{k}\cdot(\vec{x}-\vec{y})}\ , \tag{4.88}$$

$$\langle h_0(x)\pi_0(y)\rangle = -\langle \pi_0(y)h_0(x)\rangle = \int \frac{d^3k}{(2\pi)^3 2}\frac{(Z^\pi_+)^* Z^h_+}{\omega_+}\left(e^{-\mathrm{i}\omega_+(t-t')} - e^{-\mathrm{i}\omega_-(t-t')}\right)e^{\mathrm{i}\vec{k}\cdot(\vec{x}-\vec{y})}. \tag{4.89}$$

Going back to what is of interest now, we notice that in equation (4.89), when $t = t'$, the off-diagonal correlation function vanishes. Therefore, equation (4.37) is satisfied at order $\hbar$.

At two loops, we need to consider both the cubic and the quadratic correlation functions. We start with the cubic correlation functions. Their first-order correction is determined by the first term of equation (4.78)

$$\langle \pi h^2 + \pi^3\rangle = -2\lambda v\ \mathrm{Im}\int_{\infty_-}^{t} d^4z\ \Big\langle \Big(h_0^3(z) - 3\langle h_0^2\rangle h_0(z) + h_0(z)\pi_0^2(z) - 2\langle \pi_0^2\rangle h_0(z)\Big) \times (\pi_0(x)h_0^2(x) + \pi_0^3(x))\Big\rangle. \tag{4.90}$$

Let us argue why the correlator vanishes. First, we notice that the fact that since equation (4.90) contains an odd number of π fields, after expanding in Wick contractions,

we will always obtain at least one off-diagonal term as $\langle h_0(z), \pi_0(x)\rangle$. Such terms carry an overall factor of i, since the product $Z_+^\pi Z_+^h$ is purely imaginary. This is different from diagonal contractions, which are proportional to squared norms of the Z-factors. Then one needs to evaluate the time integral after plugging equation (4.87)-(4.89) into (4.90). Then, the integral produces two contributions. The one at $t = -\infty$ again vanishes. We remain with the one from the upper limit of the integration, which gives a factor $\mathrm{i}/(\omega_1 + \omega_2 + \omega_3)$, where $\omega_i = \omega(k_i)$ denote the frequencies associated with internal momenta k_i. At equal times, the oscillatory terms become unity. Therefore, by the previous observations, the integral is real. Since we have to take the imaginary part, the entire term vanishes.

Observe that this cancellation does not hold for correlators with an even number of π fields, where some contractions can be fully real, nor for correlators that are not at time coincidence, where the oscillatory prefactors no longer trivialize.

Finally, we consider the one-loop corrections to the quadratic correlation function $\langle h\pi\rangle$. They are generated by contractions with a single insertion of the quartic vertex $\mathcal{H}_I^{(4)}$, or by two insertions of the cubic vertex $\mathcal{H}_I^{(3)}$. However, they both vanish by arguments along the lines of the ones that we gave for cubic correlation functions.

For example, the contribution from the last integral of equation (4.78) vanishes, since the integral is purely imaginary due to the additional time integration, that generates an additional power of i compared to the previous order. The third term of equation (4.78) also vanishes, since it can be written as

$$\int_{-\infty}^{t} d^4z_1 \int_{-\infty}^{t} d^4z_2 \langle \mathcal{H}_I(z_1) h_0(x)\pi_0(x))\mathcal{H}_I(z_2)\rangle \\ = 2\mathrm{Re}\int_{-\infty}^{t} d^4z_1 \int_{-\infty}^{t_1} d^4z_2 \langle \mathcal{H}_I(z_1) h_0(x)\pi_0(x))\mathcal{H}_I(z_2)\rangle\,, \tag{4.91}$$

and then we can apply the argument above.

This completes the check that correlation functions entering equation (4.37) vanish individually up to order $\hbar^2$. Notice that the definition of $|v\rangle$ was instrumental for the perturbative realization of stability. In the next paragraph, we explicitly show that with a different choice stability is not guaranteed.

4.5.2 Beyond equilibrium: Gaussian states and unstable superfluids

At this point, it is clear that the choice of the superfluid state as the interacting vacuum for fluctuations provides a state which is stable in its quantum dynamics. In particular, correlation functions of the fluctuation fields are time-independent, self-consistently with the properties of the background. However, not all states whose classical dynamics reproduce the classical solution (4.22) retain this property once quantum corrections are taken into account. In particular, different states could share the same (semi)-classical limit, but could have a completely different quantum evolution. In this paragraph, we analyze a particular example, namely the Gaussian coherent state which corresponds to the free

vacuum for fluctuations:

$$|\tilde{v}\rangle = |0_{h,\pi}\rangle = e^{-\mathrm{i}f} e^{-\mathrm{i}S} |0\rangle \,. \tag{4.92}$$

As we discussed in section 4.3.2, this state can be seen as a squeezed coherent state built on top of the free vacuum of the theory. At the initial time, it has the correct one and two-point functions to look like a good candidate for a superfluid. However, we shall show that while such a state approximates well a stable superfluid configuration up to order $\hbar$, it nevertheless fails to fully track the classical evolution in the quantum theory. This is to be expected: in [31], the authors pointed out that states as the one above develop pathologies starting from two-loop corrections to the background in interacting theories, such as a divergent energy density of the system. This can be taken as a signal that the full dynamics shouldn't be the optimal one once quantum corrections are taken into account. In this sense, one can understand the divergences above as a signal that the state chosen is not properly minimizing the fluctuations on top of the background, and consequently it induces a nontrivial time evolution. Again, while in our case an optimal choice for fluctuations ensures full stability, for a generic background a deviation from the classical dynamics is unavoidable, and an optimal choice can only avoid spurious, additional effects beyond the quantum effects intrinsic in the given background.

Since we expect the state $|\tilde{v}\rangle$ to develop quantum time-dependencies in its one-point function, we generalize from the beginning the framework of the previous section to more general time-dependent configurations. Therefore, we parametrize the field as:

$$\Phi(x) = \frac{1}{\sqrt{2}} \left(v(t) + h(x) + \mathrm{i}\pi(x)\right) e^{\mathrm{i}\mu(t)t}. \tag{4.93}$$

As in the stationary case, we impose tadpole conditions on $h(x)$ and $\pi(x)$:

$$\langle\tilde{v}|h(x)|\tilde{v}\rangle = \langle\tilde{v}|\pi(x)|\tilde{v}\rangle = 0 \qquad \Longrightarrow \qquad \langle\tilde{v}|\Phi(x)|\tilde{v}\rangle = \frac{1}{\sqrt{2}} v(t) e^{\mathrm{i}\mu(t)t}. \tag{4.94}$$

At the classical level (so ignoring fluctuation fields), this configuration describes a general time-dependent configuration with a net charge density

$$n_{\mathrm{cl}}(t) = v_{\mathrm{cl}}^2(t) \frac{d}{dt}(\mu_{\mathrm{cl}} t) \,. \tag{4.95}$$

Classically, the quantity above is conserved on-shell. In particular, the imaginary part of the classical equation of motion yields precisely the constraint $\dot{n}_{\mathrm{cl}} = 0$.

Now we move on to the quantum theory. By the same procedure described in the section 4.2.2, we take the expectation value of the Heisenberg equations on the state $|\tilde{v}\rangle$. This leads to the equations analogous to equation (4.36) and equation (4.37):

$$(\mu + \dot{\mu}t)^2 - \frac{\ddot{v}}{v} = m^2 + \lambda v^2 + 3\lambda\langle h^2\rangle + \lambda\langle\pi^2\rangle + \frac{\lambda}{v}\langle h^3\rangle + \frac{\lambda}{v}\langle h\pi^2\rangle \,, \tag{4.96}$$

$$\frac{\partial}{\partial t} n(t) + 2\lambda v^2 \langle h\pi\rangle + \lambda v \langle \pi h^2 + \pi^3\rangle = 0 \,. \tag{4.97}$$

Notice that these equations allow for a coupled time evolution of the one-point functions and the higher correlation functions, consistently with the fact that for a general state the classical profile can be imposed only at the initial time, and it is the quantum dynamics that controls its evolution.

Equation (4.96) generalizes the radial equation (4.36) by introducing an additional term which takes into account a time variation of the amplitude. However, the most interesting generalization is provided by equation (4.97), which now contains an additional contribution proportional to the time derivative of $n(t) = v^2(t)\frac{d}{dt}(\mu t)$.

Let us comment on equation (4.97). We shall call the quantity $n(t) = v^2(t)\frac{d}{dt}(\mu t)$ the *background charge density*, and the associated charge Q the *background charge*. Notice that, since we are in a translational invariant setting, the two are related at all times simply by multiplication by a volume factor, and we shall use them interchangeably. This quantity is the quantum equivalent of the classical charge, since it has the same functional form but depends on the quantum one-point function of the field operator. As such, it represents (in expectation value) the charge stored in the background. However, once quantum corrections are included, the background charge is generally no longer conserved on its own: its time evolution is coupled to higher correlation functions of the fluctuation fields, which can also store charge themselves. Let us clarify this point. In the full quantum theory, the $U(1)$ symmetry is reflected in the conservation of the charge operator at the operatorial level. Consequently, it is the expectation value of the charge operator over the full quantum state that remains conserved. We can obtain the charge operator in the field parametrization in terms of fluctuations (4.93). Therefore, the quantum conservation of the charge leads to the following identity [5]:

$$\partial_t \langle \hat{Q} \rangle = \dot{Q} + \dot{Q}_{\text{fluct}} = 0, \tag{4.98}$$

with

$$Q_{\text{fluct}} = \int \mathrm{d}^3x \, \left(\langle \Pi^\pi(x) h(x) \rangle - \langle \Pi^h(x) \pi(x) \rangle \right) . \tag{4.99}$$

We shall call Q_{fluct} the *fluctuation charge*.

Equation (4.98) offers a clear picture of the physics of a quantum superfluid. On one hand, we have the background charge, which corresponds to the charge stored in the condensate and represents the number density of particles at zero momentum. On the other hand, there is the fluctuation charge, which is the charge carried by excitations propagating on top of the condensate in the form of Φ-particles with finite momentum. In a stable superfluid, the fluctuation charge needs to remain zero at all times, and the background charge is conserved in its own. That held, for the state $|v\rangle$, thanks to the discrete symmetry in the π field discussed in section 4.3, which guaranteed the vanishing of the fluctuation charge.

However, as we see from equations (4.97) and (4.98), the separate conservation of background and fluctuation charges is not guaranteed in general. In a more general superfluid

[5] Here, we restrict to states that do not break rotations and spatial translations. Therefore $\partial_i \langle Q \rangle = 0$.

state, the fluctuations evolve in time coupled to the background, leading to a charge exchange between the condensate and its excitations. In such cases, the background charge itself evolves to guaranteed total charge conservation, and this leads to a departure of the quantum dynamics of the one-point function from its classical trajectory. An easy example to build intuition can be obtained by introducing, let us say, a non-trivial fluctuation mode $a_{\pm}(k)$ on top of the vacuum. This can lead to a rescattering with the zero-momentum particles in the condensate, which implies a transfer of momentum to the background. Consequently, the configuration of the zero-momentum component gets modified itself, leading to a joint non-trivial time-evolution.

Now, we show that the free vacuum for fluctuations $|0_{h,\pi}\rangle$ has a non-trivial quantum dynamics. To this end, we compute the correlators over $|\tilde{v}\rangle$ in equations (4.96) and (4.97). If we apply the interaction picture as in equation (4.53) to $|\tilde{v}\rangle$, (we set the reference time to zero, $t_* = 0$), we get from the Dyson series:

$$\langle\tilde{v}|\mathcal{O}(x)|\tilde{v}\rangle = \langle 0_{h,\pi}|U^{\dagger}(0,t)\mathcal{O}_0(x)\ U(0,t)|0_{h,\pi}\rangle \simeq \langle\mathcal{O}_0(x)\rangle - 2\,\mathrm{Im}\int_0^t d^4z_1\,\langle\mathcal{H}_I(z_1)\mathcal{O}_0(x)\rangle + \dots\,. \tag{4.100}$$

The crucial point to observe is that, compared to the correlators over $|v\rangle$, here the early-time boundary of the evolution operator is $t_z = 0$, instead of $t_z = -\infty_-$. This difference originates from the missing non-Gaussian dressing and shall be instrumental for generating a quantum instability. Another fundamental point is that, comparing the perturbative expansion over the two states, namely equations (4.100) and (4.78) respectively, their leading quantum contribution is identical, and differences only emerge at order $\hbar^2$ or higher. Therefore, both classically and semiclassically, these states may seem equivalent in describing a good superfluid. The instability of the Gaussian state $|\tilde{v}\rangle$ is a genuinely quantum phenomenon, which is manifest only when we consider loop corrections to quadratic correlation functions or tree-level contributions to cubic and higher-order correlators.

Notice that one could understand this phenomenon with a parallelism to what would happen if, in the standard perturbative analysis of vacuum processes, one were to forget to properly connect the free vacuum to the full one at the appropriate order in perturbation theory.

Of course, at higher orders, the interaction picture decomposition and the equations for the fluctuations should be modified to include the explicit time dependence of $\mu(t)$ and $v(t)$, since, for example, the true mode expansion now is in terms of a time-dependent background. However, since the leading order effects arise at $\hbar^2$, these modifications shall enter in higher order effects, which we are not considering here. At higher loops, they should be taken into account, and they lead to a further complication of the dynamics.

Let us now proceed to show explicitly that the fluctuation charge does not vanish, and that it indeed acquires a time dependence. Therefore, we consider the leading quantum correction to the cubic correlators in equation (4.97). Using equation (4.100), we obtain

schematically:

$$\begin{aligned}\langle\tilde{v}|\langle\pi h^2+\pi^3\rangle|\tilde{v}\rangle &= -2\,\mathrm{Im}\int_0^t d^4z\,\langle\mathcal{H}_{\mathrm{I}}^{(3)}(z)(\pi_0(x)h_0^2(x)+\pi_0^3(x))\rangle \\ &= \sum_{\alpha,\beta,\gamma=\pm}\int d^3k_1 d^3k_2\, g_{\alpha\beta\gamma}(k_1,k_2)\sin[(\omega_\alpha(k_1)+\omega_\beta(k_2)+\omega_\gamma(k_1+k_2))t]\,.\end{aligned} \tag{4.101}$$

Here, we have captured in the functions $g_{\alpha\beta\gamma}(k_1,k_2)$ the momentum dependence of the field decompositions, analogously to equation (4.86). Such functions are just appropriate combinations of the wave-function coefficients and the frequencies associated with the mode expansion. Also, we performed the integral over the internal time, where the crucial difference compared to the stable superfluid arises. Since the integration starts at $t_z = 0$, in this case we cannot shift the time integration variable as before to remove the explicit time dependence, which instead remains as in the second line of (4.101). Therefore the cubic correlator at equal time $|\tilde{v}\rangle$ responsible for the fluctuation charge is both nonzero for $t > 0$ and explicitly time-dependent.

Observe that, exactly at $t = 0$, the correlator still vanishes. This is also immediate from the fact that $|\tilde{v}\rangle$ is a Gaussian state at $t = 0$. Therefore, at that time, all the connected higher-order correlators are null. Nevertheless, the quantum dynamics forces it to evolve in time into something non-trivial at later times.

To sum up, we have shown that beyond the leading order, the time-derivative of the background charge for the state $|\tilde{v}\rangle$ is non-zero, indicating a transfer of the charge density from the one-point function to higher-order correlation functions, and therefore departure from the classical dynamics.

Obviously, a complete proof would require the full evaluation of the integral above to check the final result explicitly. However, luckily, this has already been investigated numerically in [127, 128], where the authors studied the dynamics of a superfluid in a complex scalar field in 1+1 dimensions, initialized precisely on the state $|\tilde{v}\rangle$. There, it has been shown that a Gaussian superfluid departs from the classical dynamics exactly at the two-loop order discussed above [6].

The stability of $|v\rangle$ can be understood, as we discussed, in a particle language. The state $|v\rangle$ is a condensate of fundamental charged particles at zero momentum. If we minimize fluctuations, no number-changing process can take place due to charge conservation, and no rescattering among the constituents can happen for kinematic reasons (see also [73] for similar scenarios). On the other hand, in the state $|\tilde{v}\rangle$ fluctuations are not fully controlled, and this effectively populates the state with some particle content on top of the condensate. This, in turn, leads to a non-trivial dynamics.

Therefore, we clarified the importance of taming the fluctuations around the background in order to maximize the stability of a superfluid state quantum mechanically. In the next

[6] As previously discussed, this approach breaks down beyond the leading order due to its failure to regularize key observables. Nonetheless, it remains informative for probing certain aspects of the background evolution, as discussed in [29] in the case of a real scalar condensate.

section, we shall finally analyze the proper spectrum of modes on the stable superfluid state.

4.6 One-loop gaplessness of the Goldstone

We conclude the chapter by studying the spectrum of fluctuations around the superfluid, and in particular we check that the one-loop spectrum of perturbations exhibits a gapless Goldstone mode. Indeed, it has been proven that even for non-Lorentz invariant configurations, the Goldstone theorem [109] continues to hold nonperturbatively [110].

However, some doubt arose that this feature could be lost in perturbation theory, the so-called Hohenberg-Martin dilemma. Indeed, several perturbative computations suggested that the Goldstone acquires a gap once loop corrections are included. These analyses are typically performed in the two-particle-irreducible (2PI) formalism [129, 130], using the Hartree approximation (see e.g. [131]). Although most of these studies are in a finite temperature setting, their gap persists even in the zero-temperature limit [111–113], the case under consideration in this chapter. Within the 2PI formalism, several prescriptions have been advanced to eliminate the emergent gap. These proposals rely on ad-hoc modifications of the generating functional [114, 132, 133] and, as a consequence, they abandon self-consistency.

Here, we show that, in a consistent loop expansion, gaplessness is preserved also order by order in perturbation theory, in agreement with the non-perturbative result. Therefore, we give a perturbative check of the validity of the Goldstone theorem beyond the semiclassical limit (4.25), where loop corrections cannot be neglected anymore. We show that, to preserve the gaplessness, it is crucial to properly take into account all the vacuum polarization diagrams at a given order, including the one emerging from nonlinear terms [7].

Additionally, in the process, we shall also confirm that all the one-loop corrected two-point correlation functions are finite when the renormalization conditions (4.84) are applied.

4.6.1 Equations of motion for quadratic correlation functions

Our strategy to verify the gaplessness of the Goldstone mode is to show that the one-loop propagator exhibits a simple pole at zero momentum, namely, that the correlation function scales as $\vec{q}^{-1}$ in momentum space for $\vec{q} \to 0$. Since Lorentz boosts are spontaneously broken, we shall work in the $(\vec{q}, t)$ representation of the correlators, taking the Fourier transform. For convenience, we drop the vector symbol on momenta in the leftover of this section.

[7] An additional issue arises when using the 2PI formalism: specifically, unlike the standard 1PI effective action, the 2PI generating functional loses its $U(1)$ invariance when truncated at a given loop order. Consequently, spurious contributions to the Goldstone mass may still appear, even when cubic vertices are included [114].

Also, we introduce the following notation for the (spatial) momentum representation of correlators:

$$\langle \mathcal{O}(x,y)\rangle_q = \int d^3\vec{r}\,\langle \mathcal{O}(x,y)\rangle e^{-\mathrm{i}\vec{q}\cdot(\vec{x}-\vec{y})}. \tag{4.102}$$

The subscript q indicates that the Fourier-transformed correlation function is a function of the external momentum q. The coordinates x and y are intended to include also the time component, which is not Fourier-transformed.

Let us start by considering the operatorial equations of motion (4.34) and (4.35). From them, we can obtain the associated equations for the quadratic correlation functions by multiplying by $h(y)$ and $\pi(y)$, and taking the expectation value over the stable superfluid state $|v\rangle$. This leads to four coupled equations of motion. The diagonal ones read:

$$\begin{aligned}\Big\{\Box_x - 3\lambda\langle h^2\rangle - \lambda\langle\pi^2\rangle\Big\}\langle\pi(y)\pi(x)\rangle + 2\mu\partial_t\langle\pi(y)h(x)\rangle + 2\lambda v\langle\pi(y)\pi(x)h(x)\rangle + \\ + \lambda v\langle\pi(y)\pi(x)^2\rangle + \lambda\langle\pi(y)\pi(x)^3\rangle + \lambda\langle\pi(y)\pi(x)h(x)^2\rangle + \ldots = 0,\end{aligned} \tag{4.103}$$

and

$$\begin{aligned}\Big\{\Box_x + 2\lambda v^2 - 3\lambda\langle h^2\rangle - \lambda\langle\pi^2\rangle\Big\}\langle h(y)h(x)\rangle - 2\mu\partial_t\langle h(y)\pi(x)\rangle + 3\lambda v\langle h(y)h(x)^2\rangle + \\ + \lambda v\langle h(y)\pi(x)^2\rangle + \lambda\langle h(y)h(x)^3\rangle + \lambda\langle h(y)h(x)\pi(x)^2\rangle + \ldots = 0.\end{aligned} \tag{4.104}$$

Here, we truncated the equations at the quartic order in fluctuations, since higher-order terms carry additional powers of $\hbar$ and contribute only at higher loops. We can obtain the two off-diagonal equations by replacing

$$h(y) \to \pi(y) \quad \text{and} \quad \pi(y) \to h(y) \tag{4.105}$$

in the first and second equation respectively.

Then, we move in momentum space. Also, we perform the Wick contractions on the quartic terms. This reduces them to the products of the two-point function on the free vacuum, times other two-point functions on the free vacuum at coincidence. However, even if the contraction of quartic diagrams yields the correlator $\langle\pi_0(y),\pi_0(x)\rangle$, we promoted it back to the full interacting correlator $\langle\pi(y),\pi(x)\rangle$. They begin to deviate from each other only at higher loop orders, so the substitution is consistent. We shall see that, expressed this way, the quartic correlators make the emergence of an effective Goldstone gap more explicit. All together, we obtain:

$$\Big\{\partial_t^2 + q^2 + 2\lambda\langle\pi_0^2\rangle - 2\lambda\langle h_0^2\rangle\Big\}\langle\pi(y)\pi(x)\rangle_q + 2\mu\partial_t\langle\pi(y)h(x)\rangle_q + 2\lambda v\langle\pi(y)\pi(x)h(x)\rangle_q = 0, \tag{4.106}$$

$$\Big\{\partial_t^2 + q^2 + 2\lambda v^2\Big\}\langle h(y)h(x)\rangle'_q - 2\mu\partial_t\langle h(y)\pi(x)\rangle_q + \lambda v\left(3\langle h(y)h(x)^2\rangle_q + \langle h(y)\pi(x)^2\rangle_q\right) = 0\,. \tag{4.107}$$

We also write the equations for the non-diagonal correlation functions, which read

$$\left\{\partial_t^2 + q^2 + 2\lambda\langle\pi_0^2\rangle - 2\lambda\langle h_0^2\rangle\right\}\langle h(y)\pi(x)\rangle_q + 2\mu\partial_t\langle h(y)h(x)\rangle_q + 2\lambda v\langle h(y)\pi(x)h(x)\rangle_q = 0, \tag{4.108}$$

$$\left\{\partial_t^2 + q^2 + 2\lambda v^2\right\}\langle\pi(y)h(x)\rangle_q - 2\mu\partial_t\langle\pi(y)\pi(x)\rangle_q + \lambda v\left(3\langle\pi(y)h(x)^2\rangle_q + \langle\pi(y)\pi(x)^2\rangle_q\right) = 0, \tag{4.109}$$

We now have all the ingredients to move on to evaluating the equations above perturbatively at one-loop.

4.6.2 Quartic correlation functions and the anomalous average

To begin, we consider the correlation function $\langle\pi_0^2 - h_0^2\rangle$, which enters in equations (4.106) and (4.108).

We evaluate it by performing the Wick contractions and using the ladder expansion for the radial and angular fields:

$$\begin{aligned}\langle\pi_0^2 - h_0^2\rangle =& \int \frac{d^3k}{(2\pi)^3 2}\left(\frac{|Z_+^\pi|^2 - |Z_+^h|^2}{\omega_+} + \frac{|Z_-^\pi|^2 - |Z_-^h|^2}{\omega_-}\right)\\ =& \frac{\mu^2 c_s^2}{2\pi^2}\left\{c_s^2\left(1 - \sqrt{1 + c_s^{-2}}\right) + \log\left(\frac{2\Lambda}{\mu}\right) - \log\left(\sqrt{1 + c_s^2} + c_s\right)\right\}\,.\end{aligned} \tag{4.110}$$

The result is logarithmically divergent, as can be seen by employing cutoff regularization and introducing the UV regulator Λ. However, we observe that the result vanishes for $v = 0$. This is consistent with the fact that in the absence of a superfluid, the correlator reduces to

$$\langle 0_{h,\pi}|\pi_0^2(x,t) - h_0^2(x,t)|0_{h,\pi}\rangle \sim e^{-2\mathrm{i}\mu t}\langle 0|\Phi(x,t)\Phi(x,t)|0\rangle\,, \tag{4.111}$$

which is zero by charge conservation.

If we neglect the cubic correlation functions from the system of equations (4.111), it seems that this term introduces a logarithmically divergent gap in the Goldstone dispersion relation. As an aside, notice that in the non-relativistic limit of the theory, the analogue of the term above is called the anomalous average, and generates the gap of the Goldstone in the Hartree approximation [112].

Moreover, this (spurious) gap is physically divergent, and contrary to what happened, for example, to the one-loop corrections to the chemical potential, it cannot be renormalized by the counterterms of the theory.

These two problems are two faces of the same coin, and arise because it is not consistent to neglect contributions of the same order coming from the cubic correlators. We now proceed to show that, when everything is properly taken into account, at the same time the divergence is cured and the gaplessness of the Goldstone is restored.

4.6.3 Evaluating the cubic correlation functions in the diagonal equations of motion

We now turn to the perturbative evaluation of the cubic correlation functions that appear in the equations of motion (4.106) [8]. The nontrivial superfluid background makes these contributions impossible to evaluate analytically for all momenta. However, we studied them in a series expansion for small external momenta q. The first order of this expansion is proportional to the zero momentum limit of the tree-level massless two-point function $\langle\pi(y)\pi(x)\rangle_q$, which diverges as q^{-1}. In addition, there are finite time-dependent contributions which we denote by ellipses:

$$\lim_{q/\mu\to 0}\langle\pi(y)\pi(x)h(x)\rangle_q = \delta m_\pi^2\langle\pi(y)\pi(x)\rangle_q + \dots\,. \tag{4.112}$$

The coefficient δm_π^2 is given by the following expression

$$\begin{aligned}\delta m_\pi^2 =& -\lambda v\sum_{\beta=\pm}\int\frac{d^3k}{2(2\pi)^3}\left\{\frac{|Z_\beta^h|^2|Z_\beta^\pi|^2}{\omega_\beta^3} + \frac{|Z_+^h|^2|Z_-^\pi|^2+|Z_-^h|^2|Z_+^\pi|^2}{\omega_-\omega_+(\omega_-+\omega_+)} + \frac{|Z_\beta^h|^2|Z_\beta^\pi|^2(\omega_+-\omega_-)^2}{2\omega_\beta^2\omega_+\omega_-(\omega_-+\omega_+)}\right\}\\ =& -\frac{1}{v}\langle\pi_0^2-h_0^2\rangle\,,\end{aligned} \tag{4.113}$$

and exactly reproduces the anomalous average, with the opposite sign. Also, the residual terms that go to a constant in the $q\to 0$ limit are UV-finite. Therefore, the only UV-divergent contribution of the cubic correlation functions in equation (4.106) is enclosed in δm_π^2.

The details of the computation are given in Appendix B. To keep the expression above readable, we suppressed the $\vec{k}$-dependence in $\omega_\pm$ and in the wavefunction factors $Z_\alpha^{h,\pi}$ that enter (4.113). We checked the equality in the last line by explicitly evaluating the integral. In section 4.6.5, we show that the finite terms do not change the Goldstone dispersion relation in the small momentum limit.

Thus, we showed that, as announced, the cubic correlation functions exactly cancel the spurious mass term in equation (4.108), and at the same time they cure the unphysical divergence. This is the most important step in proving the gaplessness of the Goldstone.

We now move on to evaluate also the cubic correlators in the equation of motion for $\langle h(y)h(x)\rangle$, equation (4.108).

This amounts to computing the quantity $\langle 3h(y)h(x)^2+h(y)\pi(x)^2\rangle$. Again, we extract the zero momentum limit (see Appendix B for details):

$$\langle 3h(y)h(x)^2+h(y)\pi(x)^2\rangle_q = \left(\delta m_h^2\right)_\infty\langle h_0(y)h_0(x)\rangle_q + \dots\,, \tag{4.114}$$

with

$$\left(\delta m_h^2\right)_\infty = -\frac{5\lambda v}{2\pi^2}\log\left(\frac{2\Lambda}{m_h}\right)\,. \tag{4.115}$$

[8] These are the terms that would be missed in the Hartree approximation in the 2PI analysis, where in the effective action the setting sun diagram is neglected.

In this case, there are no terms that scale as q^{-1}, and the $q \to 0$ gives a finite contribution, proportional to $\langle h_0(y)h_0(x)\rangle_q$.

Similarly to the case above, the other contributions in the ellipses are UV-finite, and the UV-divergence is fully captured by (4.115). However, differently from the anomalous average, this divergence can be renormalized by a shift of the coupling constant, coming from the vacuum counterterm (4.84).

4.6.4 Evaluating the cubic correlation functions in the off-diagonal equations of motion

Last, we consider the cubic correlation functions of the non-diagonal equations (4.108) and (4.109). As above, we extract the leading low-q behavior. Again, it turns out that the remaining terms are UV-finite and the UV-divergences are completely encoded in the leading terms.

The low-momentum limit of the cubic correlation function in equation (4.108), reads

$$\lim_{q/\mu\to 0}\langle h(y)\pi(x)h(x)\rangle_q = \delta m_\pi^2\langle h_y\pi_x\rangle_q + \dots . \tag{4.116}$$

This cancels the anomalous average also in equation (4.108), and removes the unphysical UV-divergence.

For the cubic correlators of equation (4.109) we find

$$3\langle\pi(y)h(x)^2\rangle_q + \langle\pi(y)\pi(x)^2\rangle_q = \left(\delta m_h^2\right)_\infty \langle\pi_0(y)h_0(x)\rangle_q + \dots , \tag{4.117}$$

with $(\delta m_h^2)_\infty$ given by equation (4.115). As above, this UV-divergence can be renormalized by the coupling constant renormalization.

4.6.5 One-loop finiteness of the spectrum and gaplessness of the Goldstone

Now that we have calculated all the necessary ingredients, we can write the complete system of equations for the two-point functions, in the zero momentum limit. We shall write it in the following matrix form:

$$\begin{pmatrix} \partial_t^2 & 2\mathrm{i}\mu\partial_t \\ -2\mathrm{i}\mu\partial_t & \partial_t^2 + 2\lambda_{\mathrm{ph}}v^2 \end{pmatrix} \langle \boldsymbol{G}\rangle_q = \boldsymbol{J}_q(t-t'), \tag{4.118}$$

where the matrix

$$\langle \boldsymbol{G}\rangle_q = \begin{pmatrix} \langle\pi(y)\pi(x)\rangle_q & \langle h(y)\pi(x)\rangle_q \\ \langle\pi(y)h(x)\rangle_q & \langle h(y)h(x)\rangle_q \end{pmatrix} \tag{4.119}$$

is the matrix of the four two-point functions built from the radial and angular fields.

The matrix $\boldsymbol{J}_q$ is a matrix that encodes the contributions that are finite (but nonzero) in the limit $q \to 0$. For example, it contains the finite terms of equation (4.112). We kept

the momentum q since we want to confirm that we are taking the limit precisely; however, the expression above shall be intended for $q \to 0$.

This matrix can be parametrized as follows:

$$J_q^{ab} = \sum_{\alpha=\pm} \sigma_\alpha^{ab} e^{-\mathrm{i}\omega_\alpha (t'-t)}. \tag{4.120}$$

The precise form for the coefficients σ_α^{ab} is not known. However, we will show that we can constrain them by symmetry considerations.

Let us remark that the system above is UV-finite: the anomalous average, and the associated unphysical UV-divergence, canceled exactly. The divergent contribution in $\langle \pi(y) h(x) \rangle$ and $\langle h(y) h(x) \rangle$, has been absorbed by the renormalization of the coupling constant, (4.84), which replaced λ by λ_{ph}.

Also, the Goldstone gap multiplying the $\langle \pi(x)\pi(y) \rangle$ canceled exactly together with the anomalous average. Therefore, it is almost proven that the $\langle \pi(x)\pi(y) \rangle$ correlator has a pole at zero momentum, and consequently that the Goldstone remains massless.

However, one could wonder if the finite terms that survive at zero momentum could conspire to spoil the result. We argue that this is impossible.

First we show that for the $\langle \pi(x)\pi(y) \rangle$ correlator, the only possible low-momentum modifications come from σ_-^{11}. In order to do so, we solve for $\langle \pi(x)\pi(y) \rangle$ with a convolution. We obtain that:

$$\begin{aligned}\langle \pi(x)\pi(y) \rangle_{\mathrm{q}} =& \langle \pi_0(x)\pi_0(x) \rangle_q + \sum_{\alpha=\pm} \int_{-\infty_-}^{t} dt_z \left\{ \sigma_\alpha^{11} \langle [\pi_0(y), \pi_0(z)] \rangle_q + \sigma_\alpha^{21} \langle [h_0(y), \pi_0(z)] \rangle_q \right\} e^{-\mathrm{i}\omega_\alpha (t'-t_z)} \\ =& \frac{1}{2(2\pi)^3} \frac{|Z_-^\pi|^2}{\omega_-} \left(1 - \frac{\sigma_-^{11}}{2\omega_-} e^{-\mathrm{i}\omega_- (t'-t)} + \dots \right) e^{-\mathrm{i}\omega_- (t'-t)} + \dots . \end{aligned} \tag{4.121}$$

In the last line, we singled out the only term that scales as q^{-2}, namely, the one originating from σ_-^{11}. This is due to the appearance of two ω_- factors.

While this may seem an awkward contribution, this term is not associated with the appearance of a gap. Indeed, the emergence of a mass gap from the expansion around a massless theory arises from contributions that scale as q^{-3}. This is exactly the behavior we would obtain if the anomalous average were retained. For example, perturbing a massless theory by treating the mass of the scalar field as a perturbation, we would find the following expansion of the propagator

$$\langle \phi(\vec{x}, 0) \phi(\vec{y}, 0) \rangle = \int \frac{d^3 q}{2q} \left(1 + \frac{m^2}{q^2} + \dots \right) e^{\mathrm{i}\vec{q}\cdot(\vec{x}-\vec{y})} \sim \int \frac{d^3 q}{2\sqrt{q^2 + m^2}} e^{\mathrm{i}\vec{q}\cdot(\vec{x}-\vec{y})} . \tag{4.122}$$

On the contrary, if nonzero, this term could be interpreted as a q-dependent correction to the leading phonon dispersion relation, which lies beyond the approximation employed here. A precise derivation of this contribution is left to future work.

This concludes this section and verifies that the existence of a gapless Goldstone mode is not spoiled by one-loop corrections.

4.7 Conclusions

In this chapter, we have investigated the quantum dynamics of a relativistic homogeneous superfluid in a $U(1)$-invariant theory. In general, the understanding of the interplay between a classical solution and its quantum mechanical counterpart in regimes where classical non-linearities play a substantial role is of great interest for many physical systems, from black holes to de Sitter space, to cosmological scenarios [13, 22, 24, 82]. The study of prototypical systems such as our superfluid state, beyond its intrinsic interest, is therefore important to firmly establish the basics for a thorough analysis of more complicated settings.

On general grounds, quantum field theories enter a classical regime in the limit of high occupation number of constituents [4–6, 134], and the quantum state associated with a classical profile is a highly occupied coherent state. Semiclassically, nonlinearities are controlled by a collective coupling that remains finite in the infinite occupation limit. In interacting theories, purely quantum processes mediated by the quantum coupling in the form of rescattering of the constituents give rise to deviations from classicality and cause a loss of coherence of the classical state and deviations from the classical dynamics [23, 30].

However, there might be some situations where specific properties of the theory and the state at hand can prevent such deviations. In this chapter, we proved that the superfluid under consideration falls within these exceptions. Thanks to the special role of the $U(1)$ symmetry, we proved that there exists a well-defined superfluid state which retains coherence at all orders in perturbation theory. Such a state requires an appropriate and specific non-Gaussian dressing, which is naturally interpreted as originating from the minimization of the energy of fluctuations around its one-point function. To ensure stability, it is crucial that the state is invariant under a combination of time translations and $U(1)$ rotations. We showed that the aforementioned state is free from spurious divergences at one loop by calculating the one-loop corrections to its chemical potential. This further supports its physicality.

Subsequently, we clarified the role of non-Gaussianities in enforcing stability, comparing the quantum dynamics of the stable superfluid state with the one of a Gaussian coherent state. We showed that the Gaussian state loses coherence and develops non-trivial quantum deviations from classicality.

Finally, we analyzed the spectrum of the fluctuations on top of the stable superfluid state at one-loop order. We showed that the equations for the two-point functions are made finite after renormalization, without the need for additional counterterms besides the vacuum ones. More importantly, we clarified the role of nonlinearities in preserving the gaplessness of the Goldstone mode of the broken $U(1)$ symmetry, which we showed explicitly.

To conclude, the existence of a quantum-mechanically stable superfluid state clarifies the possibility of the preservation of classicality under quantum corrections, and at the same time helps to understand what the restrictive conditions are to make such a phenomenon possible.

Appendix A

The in-in formalism in the interaction picture

In this appendix, we derive the formulas (4.78) and (B.1) used to calculate the correlators of Hermitian operators perturbatively in interaction picture. Hermiticity is a natural assumption for the in-in formalism, since expectation values of observable quantities are real. Also, this is all we need for the relevant correlators of chapter 4.

Let us start with equation (4.78). We shall follow [124] (see also [135]). The starting point is (4.55), which combines the standard interaction picture formula for operators (4.53) with the definition of the state as the interaction vacuum (4.54), to express a general correlator in the following form:

$$\langle v|\mathcal{O}[h,\pi]|v\rangle = \langle 0_{h,\pi}|U^\dagger(t,-\infty_-)\mathcal{O}[h_0,\pi_0]\; U(t,-\infty_-)|0_{h,\pi}\rangle\,. \tag{A.1}$$

Then, one calculates the correlator by expanding the evolution operator U in the Dyson series of $\mathcal{H}_I$, starting from the usual definition:

$$U(t,-\infty_-) = T e^{-\mathrm{i}\int_{-\infty}^{t}\mathcal{H}_I(t)dt}\,. \tag{A.2}$$

Notice that, compared to the usual in-out expansion, in (A.1) both the evolution operators from the left and from the right are going from $-\infty$ to the given time t. This requires care in the expansion. The hermiticity of $\mathcal{H}_I$ and $\mathcal{O}$ implies that $(\mathcal{H}_I\mathcal{O})^\dagger = \mathcal{O}\mathcal{H}_I$. Therefore, at zero and first order, we obtain:

$$\langle\mathcal{O}(x)\rangle = \langle\mathcal{O}_0(x)\rangle - 2\,\mathrm{Im}\int_{-\infty_-}^{t} d^4z_1\,\langle\mathcal{H}_I(z_1)\mathcal{O}_0(x)\rangle\,.$$

The second-order contribution, again using the hermiticity of the operators, can be written as:

$$\begin{aligned}\langle\mathcal{O}(x)\rangle^{(2)} = &+\int_{-\infty_+}^{t} d^4z_1\int_{-\infty_-}^{t} d^4z_2\,\langle\mathcal{H}_I(z_1)\mathcal{O}_0(x)\mathcal{H}_I(z_2)\rangle\\ &-2\,\mathrm{Re}\int_{-\infty_+}^{t} d^4z_2\int_{-\infty_+}^{t_1} d^4z_1\,\langle\mathcal{H}_I(z_1)\mathcal{H}_I(z_2)\mathcal{O}_0(x)\rangle\,.\end{aligned} \tag{A.3}$$

Then, we move to equation (B.1), for two-point functions of Hermitian operators at different times. Let us denote the two operators as $\mathcal{O}(y)$ and $\mathcal{W}(x)$, consistently with the notation used in Appendix B, with $x = (\vec{x}, t)$ and $y = (\vec{y}, t')$. The procedure hardly bears any difference from the previous analysis. We express the original correlator in interaction picture, to obtain:

$$\langle v|\mathcal{O}(y)\mathcal{W}(x)|v\rangle = \langle 0_{h,\pi}|U^\dagger(t,-\infty_-)\mathcal{O}_0(y)U(t,t')\mathcal{W}_0(x)U(t',-\infty_-)|0_{h,\pi}\rangle\,. \tag{A.4}$$

Then, we expand at first order, where $U(t_1,t_2) \sim 1 - \mathrm{i}\int_{t_2}^{t_1}\mathcal{H}_I$. Again, we use the hermiticity of $\mathcal{O}$, $\mathcal{W}$ and $\mathcal{H}_I$ to extract imaginary parts. It is straightforward to obtain

$$\begin{aligned}\langle \mathcal{O}(y)\ \mathcal{W}(x)\rangle =& \langle \mathcal{O}_0(y)\ \mathcal{W}_0(x)\rangle - 2\,\mathrm{Im}\int_{-\infty_-}^{t} d^4z\,\langle \mathcal{H}_{\mathrm{I}}(z)\mathcal{O}_0(y)\mathcal{W}_0(x)\rangle \\ &- \mathrm{i}\int_t^{t'} d^4z\Big(\langle \mathcal{O}_0(y)\mathcal{H}_{\mathrm{I}}(z)\mathcal{W}_0(x)\rangle - \langle \mathcal{H}_{\mathrm{I}}(z)\mathcal{O}_0(y)\mathcal{W}_0(x)\rangle\Big)\,,\end{aligned} \tag{A.5}$$

which is equation (B.1).

Appendix B

Evaluating the cubic correlation functions

This appendix provides details on the procedure adopted to evaluate cubic correlation functions of section 4.6. In particular, we extend the Dyson series for the in-in formalism of section 4.4 to the case where operators are not necessarily at time coincidence. Let us consider two generic local operators $\mathcal{O}$ and $\mathcal{W}$, functions of space-time coordinates $x = (\vec{x}, t)$ and $y = (\vec{y}, t')$. The in-in correlator on the interacting vacuum for hermitian operators can be expanded perturbatively as follows, as discussed in appendix A:

$$\begin{aligned}\langle \mathcal{O}(y)\ \mathcal{W}(x)\rangle =& \langle \mathcal{O}_0(y)\ \mathcal{W}_0(x)\rangle - 2\,\mathrm{Im}\int_{-\infty_-}^{t} d^4z\,\langle \mathcal{H}_{\rm I}(z)\mathcal{O}_0(y)\mathcal{W}_0(x)\rangle \\ &- \mathrm{i}\int_t^{t'} d^4z\Big(\langle \mathcal{O}_0(y)\mathcal{H}_{\rm I}(z)\mathcal{W}_0(x)\rangle - \langle \mathcal{H}_{\rm I}(z)\mathcal{O}_0(y)\mathcal{W}_0(x)\rangle\Big). \end{aligned} \tag{B.1}$$

Following the notation in the chapter 4, we are denoting the fields in interaction pictures with a null subscript. Also, by convention, we intend all the expectation values of interacting fields as taken over the free vacuum $|0_{h,\pi}\rangle$, while the ones involving full Heisenberg fields are evaluated on $|v\rangle$.

Moreover, in what follows we shall denote the tree-level quadratic correlation functions provided by the expressions (4.87)-(4.89) as:

$$G_{\pi\pi}(x_i - x_j) = \langle \pi_0(x_i)\pi_0(x_j)\rangle \qquad G_{\pi h}(x_i - x_j) = \langle h_0(x_i)\pi_0(x_j)\rangle \tag{B.2}$$

$$G_{\pi h}(x_i - x_j) = \langle \pi_0(x_i)h_0(x_j)\rangle \qquad G_{hh}(x_i - x_j) = \langle h_0(x_i)h_0(x_j)\rangle\,. \tag{B.3}$$

First, we calculate the correlation function $\langle \pi(y)\pi(x)h(x)\rangle$. This is the relevant correlator for the equation (4.103), for the $\langle \pi\pi\rangle$ two-point function. At one loop, it reads:

$$\begin{aligned}\langle \pi(x)\pi(x)h(x)\rangle =& -\mathrm{i}\int_t^{t'} d^4z\,\Big\{\langle \pi_0(y)\mathcal{H}_I^{(3)}(z)\ \pi_0(x)h_0(x)\rangle - \langle \mathcal{H}_I^{(3)}(z)\ \pi_0(y)\pi_0(x)h_0(x)\rangle\Big\} \\ &- 2\mathrm{Im}\int_{-\infty_-}^{t} d^4z\,\langle \mathcal{H}_{\rm I}^{(3)}(z)\ \pi_0(y)\pi_0(x)h_0(x)\rangle, \end{aligned} \tag{B.4}$$

where the cubic interaction Hamiltonian is given by equation (4.79).

The expression above is simplified by performing the Wick contractions. It reduces to:

$$\begin{aligned}\langle\pi(x)\pi(x)h(x)\rangle = -4\lambda v\,\mathrm{Im}\int_{-\infty}^{t} d^4z\Big\{&G_{\pi\pi}(z-y)\Big[G_{h\pi}(z-x)G_{\pi h}(z-x)+G_{hh}(z-x)G_{\pi\pi}(z-x)\rangle\Big]\\&+G_{h\pi}(z-y)\Big[G_{\pi h}(z-x)G_{\pi\pi}(z-x)+3G_{hh}(z-x)G_{h\pi}(z-x)\Big]\Big\}\\-2\mathrm{i}\lambda v\int_{t}^{t'} dt_1\Big\{&\Big(G_{\pi\pi}(y-z)-G_{\pi\pi}(z-y)\Big)\Big[G_{h\pi}(z-x)G_{\pi h}(z-x)+G_{hh}(z-x)G_{\pi\pi}(z-x)\Big]\\&+\Big(G_{\pi h}(y-z)-G_{h\pi}(z-y)\Big)\Big[G_{\pi h}(z-x)G_{\pi\pi}(z-x)+3G_{hh}(z-x)G_{h\pi}(z-x)\Big]\Big\}\end{aligned}\,. \tag{B.5}$$

The next step is to go in momentum space, and to perform time integrals. As in the main body, we denote the external three-momentum by q. Schematically, each contraction takes the form

$$\langle\pi(y)\pi(x)h(x)\rangle_q \sim \int d^3k_1 d^3k_2\,\delta^{(3)}(q+k_1+k_2)f(q,k_1,k_2;t-t'), \tag{B.6}$$

where f is the integrand after the time integration is performed.

Then, we move on to considering the small-q regime. Consequently, we can drop the q in the delta function before integrating over one of the internal momenta. Finally, we check the low-q behavior of each contraction. We denote the terms in equation (B.5) proportional to $G_{\pi\pi}(z-y)$ and $G_{\pi h}(z-y)$ respectively A and B for convenience. The first reads:

$$\begin{aligned}A = -\lambda v\sum_{\alpha=\pm}\frac{|Z^\pi_\alpha(q)|^2}{(2\pi)^3 2\omega_\alpha(q)}e^{-\mathrm{i}\omega_\alpha(t'-t)}\int\frac{d^3k}{(2\pi)^3}\Bigg(&\frac{2|Z^h_+|^2|Z^\pi_+|^2(\omega_--\omega_+)^2}{\omega_+^2((\omega_\alpha(q)+2\omega_-)(\omega_\alpha(q)+2\omega_+)(\omega_\alpha(q)+\omega_-+\omega_+)}\\&+\frac{|Z^h_-|^2|Z^\pi_-|^2}{\omega_-^2(\omega_\alpha(q)+2\omega_-)}+\frac{|Z^h_-|^2|Z^\pi_+|^2+|Z^h_+|^2|Z^\pi_-|^2}{\omega_-^2\omega_+^2(\omega_\alpha(q)+\omega_-+\omega_+)}+\frac{|Z^h_+|^2|Z^\pi_+|^2}{\omega_+^2(\omega_\alpha(q)+2\omega_+)}\Bigg)\,,\end{aligned} \tag{B.7}$$

while the second is given by

$$\begin{aligned}B = -\lambda v\sum_{\alpha=\pm}\frac{(Z^\pi_\alpha(q))^*Z^h_\alpha(q)}{(2\pi)^3}e^{-\mathrm{i}\omega_\alpha(t'-t)}\int\frac{d^3k}{(2\pi)^3\omega_-\omega_+}\sum_{\beta=\pm}\Bigg(&\frac{|Z^\pi_\beta|^2-3|Z^h_\beta|^2}{(\omega_-(q)+2\omega_-)(\omega_+(q)+2\omega_\beta)}\\&-\frac{|Z^\pi_\beta|^2-3|Z^h_\beta|^2}{(\omega_+(q)+\omega_-+\omega_+)(\omega_-(q)+\omega_-+\omega_+)}\Bigg)(Z^h_+)^*Z^\pi_+\,.\end{aligned} \tag{B.8}$$

For simplicity, we do not explicitly write the dependence of frequencies and wavefunction coefficients on internal momenta.

The last step is to expand the integrands in a series of $\omega_+(q)$ and $\omega_-(q)$. It turns out that B approaches a constant in the limit $q\to 0$. Therefore, it only contributes to the

constant terms σ_+ in equation (4.120). In particular, at the leading order in the expansion, B approaches the correlation function $\mathrm{i}\partial_t\langle h(y)\pi(x)\rangle$, and hence provides a loop correction to the kinetic mixing.

On the other hand, A contains the terms diverging as q^{-1}. These contain a contribution that diverges as q^{-1}, in the small q-limit. We isolated them with the help of the symbolic computational software Mathematica, to obtain the expression δm_π^2 given in equation (4.113). In the last section, we were also interested in the subleading corrections that go to a constant for $q \to 0$. In particular, one can also show that the ones oscillating with frequency ω_- can be reassembled in the time derivative of the two-point correlation function of π. The other finite contributions enter the σ_+ terms. Therefore, we find

$$\lim_{q/m_h\to 0}\langle\pi(y)\pi(x)h(x)\rangle_q = (\delta m_\pi^2 + \mathrm{i}\alpha\partial_t)\langle\pi_0(y)\pi_0(x)\rangle_q - \sigma_+ e^{-\mathrm{i}\omega_+(t'-t)} \tag{B.9}$$

Second, we consider the correlation functions $\langle 3h(y)h(x)^2 + h(y)\pi(x)^2\rangle$ that enter the equation of motion for the $\langle h(x)h(y)\rangle$ correlator. With an analogous procedure, we can expand them with Wick's theorem:

$$\langle 3h(y)h(x)^2 + h(y)\pi(x)^2\rangle = \tag{B.10}$$

$$\begin{aligned}
&- 4\lambda v\,\mathrm{Im}\int_{-\infty}^{t} d^4z\Big\{G_{hh}(z-y)\Big[9G_{hh}(z-x)^2 + 3G_{h\pi}(z-x)^2 + 3G_{\pi h}(z-x)^2 + G_{h\pi}(z-x)^2\Big] \\
&\qquad + G_{\pi h}(z-y)\Big[6G_{\pi h}(z-x)G_{hh}(z-x) + 2G_{h\pi}(z-x)G_{\pi\pi}(z-x)\Big]\Big\} \\
&- 2\mathrm{i}\lambda v\int_{t}^{t'} dt_1\Big\{\Big(G_{hh}(y-z) - G_{hh}(z-y)\Big)\Big[9G_{hh}(z-x)^2 + 3G_{h\pi}(z-x)^2 + 3G_{\pi h}(z-x)^2 + G_{h\pi}(z-x)^2\Big] \\
&\qquad + \Big(G_{h\pi}(y-z) - G_{\pi h}(z-y)\Big)\Big[6G_{\pi h}(z-x)G_{hh}(z-x) + 2G_{h\pi}(z-x)G_{\pi\pi}(z-x)\Big]\Big\}.
\end{aligned} \tag{B.11}$$

Again, the expression above is evaluated by going in Fourier space and taking the zero external momentum limit. It turns out that the only terms which contain UV-divergences are the ones proportional to $G_{hh}(z-y)$ and $G_{hh}(y-z)\rangle$. Moreover, they arise from the t integration boundary. They can be extracted by expanding all the wavefunction factors and frequencies for big k, with k the residual internal momentum, and then integrating in time, to obtain the result of equation (4.115). This has also been done with the help of Mathematica. The procedure to obtain the correlator $\langle 3\pi(y)h(x)^2 + \pi(y)\pi(x)^2\rangle$ is analogous.

Bibliography

[1] P.K. Townsend, *Black holes: Lecture notes*, gr-qc/9707012.

[2] G. Contri, G. Dvali and O. Sakhelashvili, *Similarities in the evaporation of saturated solitons and black holes*, 2509.08049.

[3] L. Berezhiani, G. Cintia and G. Contri, *Coherence and Quantum Stability of Relativistic Superfluid States*, 2509.21667.

[4] R.J. Glauber, *Coherent and incoherent states of the radiation field*, *Phys. Rev.* **131** (1963) 2766.

[5] E.C.G. Sudarshan, *Equivalence of semiclassical and quantum mechanical descriptions of statistical light beams*, *Phys. Rev. Lett.* **10** (1963) 277.

[6] S. Weinberg, *The Quantum theory of fields. Vol. 1: Foundations*, Cambridge University Press (6, 2005), 10.1017/CBO9781139644167.

[7] R. Penrose, *Gravitational collapse and space-time singularities*, *Phys. Rev. Lett.* **14** (1965) 57.

[8] S.W. Hawking, *Black holes in general relativity*, *Commun. Math. Phys.* **25** (1972) 152.

[9] G. 't Hooft, *Graviton Dominance in Ultrahigh-Energy Scattering*, *Phys. Lett. B* **198** (1987) 61.

[10] G. Dvali, G.F. Giudice, C. Gomez and A. Kehagias, *UV-Completion by Classicalization*, *JHEP* **08** (2011) 108 [1010.1415].

[11] J.D. Bekenstein, *Black holes and entropy*, *Phys. Rev. D* **7** (1973) 2333.

[12] S.W. Hawking, *Particle Creation by Black Holes*, *Commun. Math. Phys.* **43** (1975) 199.

[13] G. Dvali and C. Gomez, *Black Hole's Quantum N-Portrait*, *Fortsch. Phys.* **61** (2013) 742 [1112.3359].

[14] G. Dvali and C. Gomez, *Black Holes as Critical Point of Quantum Phase Transition*, *Eur. Phys. J. C* **74** (2014) 2752 [1207.4059].

[15] G. Dvali and C. Gomez, *Black Hole's 1/N Hair*, *Phys. Lett. B* **719** (2013) 419 [1203.6575].

[16] G. Dvali, *Area Law Saturation of Entropy Bound from Perturbative Unitarity in Renormalizable Theories*, *Fortsch. Phys.* **69** (2021) 2000090 [1906.03530].

[17] G. Dvali, *Entropy Bound and Unitarity of Scattering Amplitudes*, *JHEP* **03** (2021) 126 [2003.05546].

[18] G. Dvali, *Unitarity Entropy Bound: Solitons and Instantons*, *Fortsch. Phys.* **69** (2021) 2000091 [1907.07332].

[19] G. Dvali and O. Sakhelashvili, *Black-hole-like saturons in Gross-Neveu*, *Phys. Rev. D* **105** (2022) 065014 [2111.03620].

[20] G. Dvali, O. Kaikov and J.S.V. Bermúdez, *How special are black holes? Correspondence with objects saturating unitarity bounds in generic theories*, *Phys. Rev. D* **105** (2022) 056013 [2112.00551].

[21] G. Dvali and R. Venugopalan, *Classicalization and unitarization of wee partons in QCD and gravity: The CGC-black hole correspondence*, *Phys. Rev. D* **105** (2022) 056026 [2106.11989].

[22] G. Dvali and C. Gomez, *Quantum Exclusion of Positive Cosmological Constant?*, *Annalen Phys.* **528** (2016) 68 [1412.8077].

[23] G. Dvali, C. Gomez and S. Zell, *Quantum Break-Time of de Sitter*, *JCAP* **06** (2017) 028 [1701.08776].

[24] G. Dvali and S. Zell, *Classicality and Quantum Break-Time for Cosmic Axions*, *JCAP* **07** (2018) 064 [1710.00835].

[25] G. Dvali, *A Microscopic Model of Holography: Survival by the Burden of Memory*, 1810.02336.

[26] G. Dvali, L. Eisemann, M. Michel and S. Zell, *Black hole metamorphosis and stabilization by memory burden*, *Phys. Rev. D* **102** (2020) 103523 [2006.00011].

[27] G. Dvali, J.S. Valbuena-Bermúdez and M. Zantedeschi, *Memory burden effect in black holes and solitons: Implications for PBH*, *Phys. Rev. D* **110** (2024) 056029 [2405.13117].

[28] L. Berezhiani and M. Zantedeschi, *Evolution of coherent states as quantum counterpart of classical dynamics*, *Phys. Rev. D* **104** (2021) 085007 [2011.11229].

[29] L. Berezhiani, G. Cintia and M. Zantedeschi, *Background-field method and initial-time singularity for coherent states*, *Phys. Rev. D* **105** (2022) 045003 [2108.13235].

[30] J. Baacke, K. Heitmann and C. Patzold, *On the choice of initial states in nonequilibrium dynamics*, *Phys. Rev. D* **57** (1998) 6398 [hep-th/9711144].

[31] L. Berezhiani, G. Cintia and M. Zantedeschi, *Perturbative construction of coherent states*, *Phys. Rev. D* **109** (2024) 085018 [2311.18650].

[32] D.J. Gross and A. Neveu, *Dynamical Symmetry Breaking in Asymptotically Free Field Theories*, *Phys. Rev. D* **10** (1974) 3235.

[33] T.D. Lee and G.C. Wick, *Vacuum Stability and Vacuum Excitation in a Spin 0 Field Theory*, *Phys. Rev. D* **9** (1974) 2291.

[34] S.R. Coleman, *Q-balls*, *Nucl. Phys. B* **262** (1985) 263.

[35] E.B. Bogomolny, *Stability of Classical Solutions*, *Sov. J. Nucl. Phys.* **24** (1976) 449.

[36] M.K. Prasad and C.M. Sommerfield, *An Exact Classical Solution for the 't Hooft Monopole and the Julia-Zee Dyon*, *Phys. Rev. Lett.* **35** (1975) 760.

[37] E. Witten and D.I. Olive, *Supersymmetry Algebras That Include Topological Charges*, *Phys. Lett. B* **78** (1978) 97.

[38] S. Coleman, *Aspects of Symmetry: Selected Erice Lectures*, Cambridge University Press, Cambridge, U.K. (1985), 10.1017/CBO9780511565045.

[39] E.J. Weinberg, *Classical solutions in quantum field theory: Solitons and Instantons in High Energy Physics*, Cambridge Monographs on Mathematical Physics, Cambridge University Press (9, 2012), 10.1017/CBO9781139017787.

[40] G. Dvali, C. Gomez, L. Gruending and T. Rug, *Towards a Quantum Theory of Solitons*, *Nucl. Phys. B* **901** (2015) 338 [1508.03074].

[41] H.B. Nielsen and P. Olesen, *Vortex Line Models for Dual Strings*, *Nucl. Phys. B* **61** (1973) 45.

[42] G. 't Hooft, *Magnetic Monopoles in Unified Gauge Theories*, *Nucl. Phys. B* **79** (1974) 276.

[43] A.M. Polyakov, *Particle Spectrum in Quantum Field Theory*, *JETP Lett.* **20** (1974) 194.

[44] R.F. Dashen, B. Hasslacher and A. Neveu, *Nonperturbative Methods and Extended Hadron Models in Field Theory 2. Two-Dimensional Models and Extended Hadrons*, *Phys. Rev. D* **10** (1974) 4130.

[45] R.F. Dashen, B. Hasslacher and A. Neveu, *The Particle Spectrum in Model Field Theories from Semiclassical Functional Integral Techniques*, *Phys. Rev. D* **11** (1975) 3424.

[46] S. Weinberg, *Quantum contributions to cosmological correlations*, *Phys. Rev. D* **72** (2005) 043514 [hep-th/0506236].

[47] R.F. Dashen, B. Hasslacher and A. Neveu, *Nonperturbative Methods and Extended Hadron Models in Field Theory 1. Semiclassical Functional Methods*, *Phys. Rev. D* **10** (1974) 4114.

[48] R.F. Dashen, B. Hasslacher and A. Neveu, *Semiclassical Bound States in an Asymptotically Free Theory*, *Phys. Rev. D* **12** (1975) 2443.

[49] Y. Frishman and J. Sonnenschein, *Non-Perturbative Field Theory*, Cambridge University Press (2010), 10.1017/9781009401654.

[50] G. 't Hooft, *A Planar Diagram Theory for Strong Interactions*, *Nucl. Phys. B* **72** (1974) 461.

[51] J. Hubbard, *Calculation of partition functions*, *Phys. Rev. Lett.* **3** (1959) 77.

[52] R. Friedberg, T.D. Lee and A. Sirlin, *A Class of Scalar-Field Soliton Solutions in Three Space Dimensions*, *Phys. Rev. D* **13** (1976) 2739.

[53] T.D. Lee and Y. Pang, *Nontopological solitons*, *Phys. Rept.* **221** (1992) 251.

[54] A. Kusenko, *Small Q balls*, *Phys. Lett. B* **404** (1997) 285 [hep-th/9704073].

[55] A.G. Cohen, S.R. Coleman, H. Georgi and A. Manohar, *The Evaporation of Q Balls*, *Nucl. Phys. B* **272** (1986) 301.

[56] E.T. Newman, E. Couch, K. Chinnapared, A. Exton, A. Prakash and R. Torrence, *Metric of a Rotating, Charged Mass*, *J. Math. Phys.* **6** (1965) 918.

[57] L. Smarr, *Mass formula for Kerr black holes*, *Phys. Rev. Lett.* **30** (1973) 71.

[58] G. Dvali, *S-Matrix and Anomaly of de Sitter*, *Symmetry* **13** (2020) 3 [2012.02133].

[59] G. Dvali, *Non-Thermal Corrections to Hawking Radiation Versus the Information Paradox*, *Fortsch. Phys.* **64** (2016) 106 [1509.04645].

[60] J.D. Bekenstein, *A Universal Upper Bound on the Entropy to Energy Ratio for Bounded Systems*, *Phys. Rev. D* **23** (1981) 287.

[61] P. Hayden and J. Preskill, *Black holes as mirrors: Quantum information in random subsystems*, *JHEP* **09** (2007) 120 [0708.4025].

[62] Y. Sekino and L. Susskind, *Fast Scramblers*, *JHEP* **10** (2008) 065 [0808.2096].

[63] G. Dvali, D. Flassig, C. Gomez, A. Pritzel and N. Wintergerst, *Scrambling in the Black Hole Portrait*, *Phys. Rev. D* **88** (2013) 124041 [1307.3458].

[64] G. Dvali and C. Gomez, *Quantum Compositeness of Gravity: Black Holes, AdS and Inflation*, *JCAP* **01** (2014) 023 [1312.4795].

[65] G. Veneziano, *Quantum hair and the string-black hole correspondence*, *Class. Quant. Grav.* **30** (2013) 092001 [1212.2606].

[66] D.N. Page, *Information in black hole radiation*, *Phys. Rev. Lett.* **71** (1993) 3743 [hep-th/9306083].

[67] G. Dvali and C. Gomez, *Black Hole Macro-Quantumness*, 1212.0765.

[68] G. Dvali, A. Franca, C. Gomez and N. Wintergerst, *Nambu-Goldstone Effective Theory of Information at Quantum Criticality*, *Phys. Rev. D* **92** (2015) 125002 [1507.02948].

[69] G. Dvali and M. Panchenko, *Black Hole Based Quantum Computing in Labs and in the Sky*, *Fortsch. Phys.* **64** (2016) 569 [1601.01329].

[70] G. Dvali, *Area law microstate entropy from criticality and spherical symmetry*, *Phys. Rev. D* **97** (2018) 105005 [1712.02233].

[71] R. Kanamoto, H. Saito and M. Ueda, *Quantum phase transition in one-dimensional bose-einstein condensates with attractive interactions*, *Phys. Rev. A* **67** (2003) 013608.

[72] R. Kanamoto, H. Saito and M. Ueda, *Symmetry breaking and enhanced condensate fraction in a matter-wave bright soliton*, *Phys. Rev. Lett.* **94** (2005) 090404.

[73] G. Dvali, C. Gomez and D. Lüst, *Classical Limit of Black Hole Quantum N-Portrait and BMS Symmetry*, *Phys. Lett. B* **753** (2016) 173 [1509.02114].

[74] A. Averin, G. Dvali, C. Gomez and D. Lust, *Gravitational Black Hole Hair from Event Horizon Supertranslations*, *JHEP* **06** (2016) 088 [1601.03725].

[75] G. Dvali, *A string theoretic derivation of gibbons-hawking entropy*, *Gen. Rel. Grav.* **57** (2025) 118 [2407.01510].

[76] A. Alexandre, G. Dvali and E. Koutsangelas, *New mass window for primordial black holes as dark matter from the memory burden effect*, *Phys. Rev. D* **110** (2024) 036004 [2402.14069].

[77] M. Zantedeschi and L. Visinelli, *Ultralight black holes as sources of high-energy particles*, *Phys. Dark Univ.* **49** (2025) 102034 [2410.07037].

[78] G. Dvali, M. Zantedeschi and S. Zell, *Transitioning to Memory Burden: Detectable Small Primordial Black Holes as Dark Matter*, 2503.21740.

[79] V. Thoss, A. Burkert and K. Kohri, *Breakdown of hawking evaporation opens new mass window for primordial black holes as dark matter candidate*, *Mon. Not. Roy. Astron. Soc.* **532** (2024) 451 [2402.17823].

[80] A. Dondarini, G. Marino, P. Panci and M. Zantedeschi, *The fast, the slow and the merging: probes of evaporating memory burdened PBHs*, 2506.13861.

[81] M. Ettengruber and F. Kuhnel, *Micro Black Hole Dark Matter*, 2506.14871.

[82] G. Dvali and L. Eisemann, *Perturbative understanding of nonperturbative processes and quantumization versus classicalization*, *Phys. Rev. D* **106** (2022) 125019 [2211.02618].

[83] L. Berezhiani, G. Dvali and O. Sakhelashvili, *de Sitter space as a BRST invariant coherent state of gravitons*, *Phys. Rev. D* **105** (2022) 025022 [2111.12022].

[84] L. Berezhiani, G. Dvali and O. Sakhelashvili, *Coherent states in gauge theories: Topological defects and other classical configurations*, *Phys. Rev. D* **111** (2025) 065018 [2411.11657].

[85] M.B. Voloshin, *Estimate of the onset of nonperturbative particle production at high-energy in a scalar theory*, *Phys. Lett. B* **293** (1992) 389.

[86] A.S. Gorsky and M.B. Voloshin, *Nonperturbative production of multiboson states and quantum bubbles*, *Phys. Rev. D* **48** (1993) 3843 [hep-ph/9305219].

[87] L.S. Brown, *Summing tree graphs at threshold*, *Phys. Rev. D* **46** (1992) R4125 [hep-ph/9209203].

[88] D.T. Son, *Semiclassical approach for multiparticle production in scalar theories*, *Nucl. Phys. B* **477** (1996) 378 [hep-ph/9505338].

[89] E.N. Argyres, R.H.P. Kleiss and C.G. Papadopoulos, *Amplitude estimates for multi - Higgs production at high-energies*, *Nucl. Phys. B* **391** (1993) 42.

[90] G. Dvali, C. Gomez, R.S. Isermann, D. Lüst and S. Stieberger, *Black hole formation and classicalization in ultra-Planckian 2→N scattering*, *Nucl. Phys. B* **893** (2015) 187 [1409.7405].

[91] G. Dvali and D. Pirtskhalava, *Dynamics of Unitarization by Classicalization*, *Phys. Lett. B* **699** (2011) 78 [1011.0114].

[92] G. Dvali, *Classicalization Clearly: Quantum Transition into States of Maximal Memory Storage Capacity*, 1804.06154.

[93] G. 't Hooft, *A Two-Dimensional Model for Mesons*, *Nucl. Phys. B* **75** (1974) 461.

[94] G. Veneziano, *Some Aspects of a Unified Approach to Gauge, Dual and Gribov Theories*, *Nucl. Phys. B* **117** (1976) 519.

[95] E. Witten, *Baryons in the 1/n Expansion*, *Nucl. Phys. B* **160** (1979) 57.

[96] A.V. Manohar, *Large N QCD*, in *Les Houches Summer School in Theoretical Physics, Session 68: Probing the Standard Model of Particle Interactions*, pp. 1091–1169, 2, 1998 [hep-ph/9802419].

[97] S.R. Coleman and E. Witten, *Chiral Symmetry Breakdown in Large N Chromodynamics*, *Phys. Rev. Lett.* **45** (1980) 100.

[98] E. Witten, *Current Algebra, Baryons, and Quark Confinement*, *Nucl. Phys. B* **223** (1983) 433.

[99] T.H.R. Skyrme, *A Unified Field Theory of Mesons and Baryons*, *Nucl. Phys.* **31** (1962) 556.

[100] G. Dvali and A. Vilenkin, *Solitonic D-branes and brane annihilation*, *Phys. Rev. D* **67** (2003) 046002 [hep-th/0209217].

[101] S.S. Clark, *Particle production from Q-balls*, *Nucl. Phys. B* **756** (2006) 38 [hep-ph/0510078].

[102] G. Dvali, *Bounds on quantum information storage and retrieval*, *Phil. Trans. A. Math. Phys. Eng. Sci.* **380** (2021) 20210071 [2107.10616].

[103] L. Berezhiani, *On Corpuscular Theory of Inflation*, *Eur. Phys. J. C* **77** (2017) 106 [1610.08433].

[104] J. Baacke, D. Boyanovsky and H.J. de Vega, *Initial time singularities in nonequilibrium evolution of condensates and their resolution in the linearized approximation*, *Phys. Rev. D* **63** (2001) 045023 [hep-ph/9907337].

[105] P. Ehrenfest, *Bemerkung über die angenäherte Gültigkeit der klassischen Mechanik innerhalb der Quantenmechanik*, *Z. Phys.* **45** (1927) 455.

[106] L. Berezhiani and M. Trodden, *How Likely are Constituent Quanta to Initiate Inflation?*, *Phys. Lett. B* **749** (2015) 425 [1504.01730].

[107] L. Berezhiani and M. Trodden, *A relativistic gas of inflatons as an initial state for inflation*, *Phys. Lett. B* **840** (2023) 137852 [2211.06222].

[108] L. Berezhiani, G. Dvali and O. Sakhelashvili, *Consistent Canonical Quantization of Gravity: Recovery of Classical GR from BRST-invariant Coherent States*, 2409.18777.

[109] J. Goldstone, A. Salam and S. Weinberg, *Broken Symmetries*, *Phys. Rev.* **127** (1962) 965.

[110] H.B. Nielsen and S. Chadha, *On How to Count Goldstone Bosons*, *Nucl. Phys. B* **105** (1976) 445.

[111] M.G. Alford, S. Kumar Mallavarapu, A. Schmitt and S. Stetina, *Role reversal in first and second sound in a relativistic superfluid*, *Phys. Rev. D* **89** (2014) 085005 [1310.5953].

[112] A. Sharma, J. Khoury and T. Lubensky, *The Equation of State of Dark Matter Superfluids*, *JCAP* **05** (2019) 054 [1809.08286].

[113] A. Sharma, G. Kartvelishvili and J. Khoury, *Finite temperature description of an interacting Bose gas*, *Phys. Rev. D* **106** (2022) 045025 [2204.02423].

[114] A. Pilaftsis and D. Teresi, *Symmetry Improved CJT Effective Action*, *Nucl. Phys. B* **874** (2013) 594 [1305.3221].

[115] T.W.B. Kibble, *Frequency Shift in High-Intensity Compton Scattering*, *Phys. Rev.* **138** (1965) B740.

[116] W.-M. Zhang, D.H. Feng and R. Gilmore, *Coherent States: Theory and Some Applications*, *Rev. Mod. Phys.* **62** (1990) 867.

[117] W.-M. Zhang, *Coherent states in field theory*, hep-th/9908117.

[118] G. Dvali, L. Eisemann, M. Michel and S. Zell, *Universe's Primordial Quantum Memories*, *JCAP* **03** (2019) 010 [1812.08749].

[119] A. Nicolis and F. Piazza, *Spontaneous Symmetry Probing*, *JHEP* **06** (2012) 025 [1112.5174].

[120] P. Creminelli, M. Delladio, O. Janssen, A. Longo and L. Senatore, *Non-analyticity of the S-matrix with spontaneously broken Lorentz invariance*, *JHEP* **06** (2024) 201 [2312.08441].

[121] L. Hui, I. Kourkoulou, A. Nicolis, A. Podo and S. Zhou, *S-matrix positivity without Lorentz invariance: a case study*, *JHEP* **04** (2024) 145 [2312.08440].

[122] J. Bernstein and S. Dodelson, *Relativistic bose gas*, *Phys. Rev. Lett.* **66** (1991) 683.

[123] M.E. Peskin and D.V. Schroeder, *An Introduction to quantum field theory*, Addison-Wesley, Reading, USA (1995), 10.1201/9780429503559.

[124] P. Adshead, R. Easther and E.A. Lim, *Cosmology With Many Light Scalar Fields: Stochastic Inflation and Loop Corrections*, *Phys. Rev. D* **79** (2009) 063504 [0809.4008].

[125] D. Boyanovsky, H.J. de Vega, R. Holman and M. Simionato, *Dynamical renormalization group resummation of finite temperature infrared divergences*, *Phys. Rev. D* **60** (1999) 065003 [hep-ph/9809346].

[126] A. Nicolis, A. Podo and L. Santoni, *The connection between nonzero density and spontaneous symmetry breaking for interacting scalars*, *JHEP* **09** (2023) 200 [2305.08896].

[127] A. Kovtun and M. Zantedeschi, *Breaking BEC*, *JHEP* **07** (2020) 212 [2003.10283].

[128] A. Kovtun and M. Zantedeschi, *Breaking BEC: Quantum evolution of unstable condensates*, *Phys. Rev. D* **105** (2022) 085019 [2008.02187].

[129] J.M. Cornwall, R. Jackiw and E. Tomboulis, *Effective action for composite operators*, *Phys. Rev. D* **10** (1974) 2428.

[130] J. Berges, *Introduction to nonequilibrium quantum field theory*, *AIP Conf. Proc.* **739** (2004) 3 [hep-ph/0409233].

[131] M. Bender, P.-H. Heenen and P.-G. Reinhard, *Self-consistent mean-field models for nuclear structure*, *Rev. Mod. Phys.* **75** (2003) 121.

[132] Y.B. Ivanov, F. Riek and J. Knoll, *Gapless Hartree-Fock resummation scheme for the O(N) model*, *Phys. Rev. D* **71** (2005) 105016 [hep-ph/0502146].

[133] V. Yukalov, *Representative statistical ensembles for bose systems with broken gauge symmetry*, *Annals of Physics* **323** (2008) 461.

[134] A. Duncan, *The Conceptual Framework of Quantum Field Theory*, Oxford University Press (8, 2012), 10.1093/acprof:oso/9780199573264.001.0001.

[135] Y. Donath and E. Pajer, *The in-out formalism for in-in correlators*, *JHEP* **07** (2024) 064 [2402.05999].

Acknowledgements

This is the third (and hopefully last) thesis for which I have to write the acknowledgments section. And, every time I write, I feel more and more the fundamental role of the many dear people who surrounded me, from family, to friends and colleagues, in allowing me to achieve this important step. These years have been as intense and challenging as they were rewarding, and the support that came in different forms from all of you, be it a lovely hug, an interesting scientific discussion, a much-needed laugh, all of it has been necessary in bringing me to the point where I am. This thesis is dedicated to all of you, since it would not exist without you.

First, I want to thank my advisor Gia Dvali. Already in my master thesis, I wrote how your incredible knowledge has changed how I was seeing physics, and this was only reinforced during the PhD. Thank you for always having an invaluable insight to my physics questions, and for having been a true model of scientific thinking and integrity.

Then, I want to thank Lasha. The importance of your presence in our group cannot be overestimated. You were always around to help and support me, offering guidance in moments of doubt, and many long and interesting physics discussions any time I was stepping into your office. A big thanks goes to Oto for all our many long meetings during our project together, and your humor always ready to bring a laugh.

I want to thank the many fellow students that I have met at MPP, many of whom have become not only colleagues but friends. Thank you, Emi, Anja, Manuel, Lucy, Juan, Ana, Philip, Tong, Chiara, Joachim, Leonardo, Carmine and Prisco.

Now, let me move to my faithful office mate, Maxi. The list of things in which you helped me and I should thank you for is too long[1], so let me just thank you for all our talks and moments that we shared in these years. I was very lucky to have you as a partner in crime.

In my group, I want to especially thank Giordano, the duke of Bavaria, for all his support and for his friendship (and for his blue sofa). I want to thank the group of PhD representatives who shared with me our intense year: Giorgio, Alessandro, Antonela, Daniel, Moritz and Zsofi.

I want to thank Alessandro (the one above) and Christian for all the fun together, also with Giordano, and for having managed to bring me to a gym, albeit sporadically.

Another thanks goes to Ivano for the many eternally long physics discussions, always

[1]An honorable mention goes to proof-reading my whole thesis at a level of detail which made other, more modern software-based grammar checks redundant.

challenging and stimulating. Your perspective has always been enriching and taught me a lot.

I thank Alessandro and Deniz, whose master thesis I had the honour to supervise.

I would also like to express a big thanks to Dieter Lüst, for accepting to be my second referee. Before moving out of the MPP, let me thank Frank Steffen and Giulia Zanderighi for their fundamental role as IMPRS coordinator (and lead Ringberg singer-guitarist) and spokesperson, respectively.

In these years, I was lucky to have many friends around me with whom I shared a lot of moments that will remain in my heart. I want to thank Matthias, Sara, Davide, and Carla, who have been the ever-present backbone of this journey. From laughs, to long chats about everything, coffees, trips to the mountains or to the seaside, you have been so important to me.

I want to thank Francesco, Alberto, Angelica, Gael, Caterina, Damiano, Andrea, Beatrice, Davide, Caro, and Giulio, for being such good friends, and for the many weekends and evenings spent together talking and having fun [2].

I thank my volleyball team (mit einer schwalzenterzunger schweinebraten) Picco-Rosso.

A big thanks also to the friends who were not here in Munich, but whose presence I have constantly felt in my heart. Thank you, Adriá, Laura, Isabelle, and Fulvia. I still remember the nice time together here during my master. Thank you Joan, for always being close to me despite the distance. Thank you Nico, Matte, Angelo, Tommi, Caccia, Kamil, Yas, Paolo, Matte and Andre, my oldest friends. Every time we manage to meet, it feels as if we were never apart.

I thank my family, my parents Giotti and Silvia, and my brother Paolo. It is hard to find the right words to express how important you are to me. In these years, despite the distance, I have always thought of you, and every time I was back in Milan, I truly felt at home again.

Finally, I want to thank Giulia. Your love and care are what kept me going in the toughest moments of this journey, and what filled all the others with happiness. I love you.

[2]This is a good place to advertise the next concert of Mona&co, don't miss it.